

KADIR HAS UNIVERSITY
SCHOOL OF GRADUATE STUDIES
PROGRAM OF COMPUTATIONAL BIOLOGY AND BIOINFORMATICS

**IN SILICO SCREENING OF POTENTIAL PEROXISOME
PROLIFERATOR-ACTIVATED RECEPTORS(ALPHA-
GAMMA) PPARS α/γ FOR THE TREATMENT OF
HUMAN DIABETIC MELLITIES (DM)**

FARAH ISMAEL ABDUL_JABBAR

MASTER'S THESIS

ISTANBUL, January, 20

FARAH ISMAEL ABDUL-JABBAR

M.Sc. Thesis

January, 20





**IN SILICO SCREENING OF POTENTIAL PEROXISOME
PROLIFERATOR-ACTIVATED RECEPTORS(ALPHA-
GAMMA) PPARS α/γ FOR THE TREATMENT OF
HUMAN DIABETIC MELLITIES (DM)**

FARAH ISMAEL ABDUL-JABBAR

MASTER'S THESIS

Submitted to the School of Graduate studies of Kadir Has University in partial fulfillment of the requirements for the degree of Master's in the Program of Computational Biology and Bioinformatics

ISTANBUL, January, 20

DECLARATION OF RESEARCH ETHICS

I, FARAH ISMAEL ABDUL_JABBAR, hereby declare that;

- This master's thesis is my own original work and that due references have been appropriately provided on all supporting literature and resources.
- This master's thesis contains no material that has been submitted or accepted for a degree or diploma in any other educational institution.
- I have followed “Kadir Has University Academic Ethics Principles” prepared in accordance with the “The Council of Higher Education’s Ethical Conduct Principles”

In addition, I understand that any false claim in respect of this work will result in disciplinary action in accordance with University regulations.

Furthermore, both printed and electronic copies of my work will be kept in Kadir Has Information Center under the following condition as indicated below:

- ❖ The full content of my thesis will be accessible from everywhere by all means.



FARAH ISMAEL ABDUL_JABBAR

09/01/2020

KADIR HAS UNIVERSITY
GRADUATE SCHOOL OF SCIENCE AND ENGINEERING

ACCEPTANCE AND APPROVAL

This work entitled KADIR HAS UNIVERSITY
GRADUATE SCHOOL OF SCIENCE AND ENGINEERING

This work entitled **IN SILICO SCREENING OF POTENTIAL PEROXISOM
PROLIFERATOR-ACTIVATED RECEPTORS (ALPHA-GAMMA) PPARS
 α/γ FOR THE TREATMENT OF HUMAN DIABETIC MELLITIS (DM).**

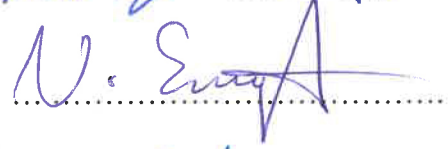
Prepared by **FARAH ISMAEL ABDUL-JABBAR** has been judged to be successful
at the defense exam held on **9 January 2020** and accepted by our jury as **MASTER'S
THESIS.**

APPROVED BY:

Prof. Dr. Kemal Yelekçi (Advisor)
Kadir Has University



Assist. Prof. Dr. Vildan Enisoğlu Atalay
Üsküdar University



Assist. Prof. Dr. Hatice Bahar Şahin
Kadir Has University



I certify that the above signatures belong to the faculty members named above.



Dean of Graduate School of Studies
DATE OF APPROVAL: 09/01/2020

Table of Contents

<i>ABSTRACT</i>	<i>vi</i>
<i>ÖZET</i>	<i>vii</i>
<i>ACKNOWLEDGEMENT</i>	<i>viii</i>
<i>LIST OF TABLES</i>	<i>x</i>
<i>LIST OF FIGURES</i>	<i>xi</i>
<i>LIST OF ABBREVIATION</i>	<i>xiii</i>
1. CONTEXT and GOALS, A BERIF DISCRITION OF METHODOLOGY	xiv
1.1 CONTEXT and GOALS	xiv
1.2 ABERIF DISCRITION OF METHODOLOGY	xvi
2. INTRODUCTION	1
2.1 Diabetes mellitus	1
2.2 Nuclear Receptor	2
2.3 Peroxisome Proliferator Activated Receptors (PPARs)	3
2.4 PPAR γ	4
2.5 PPAR α	4
2.6 Activation of peroxisome proliferator activated receptors	5
2.7 PPARS Drugs Modulators (Pharmacological role of PPARs agonists in human disease)	5
2.8 Structure of PPAR	6
2.9 Diabetes-Associated Complications	6
2.10 Computer aid drug design	7
2.10.1 Docking Studies	8
2.10.2 Pharmacophore	8
2.10.3 Virtual screening	8
2.10.5 Molecular dynamics simulations	9
3. MATERIALS AND METHODS	11
3.1 Screening and preparation the ZINC15 Chemical Library	12
3.2 Structure and superimposition of PPARα and PPARγ	13
3.3 Principles of Structure-Based Drug Design	16
3.3.1. Rationale and Target Selection	16
3.3.2 Methods of SBDD	16
3.3.3 Protein Preparation	17
3.3.4 Pharmacophore Generation	17
3.4 Ligand-Based Approach	24
3.4.1 Protein Preparation	24
3.4.2 Known Inhibitor, Molecular Docking Validation	24
3.4.3 Data sets	29

3.4.4 Pharmacophore Generation	30
3.5 Pharmacophore validation	33
3.6 Virtual Screening	38
3.7 PyRx	38
3.8 AutoDock	38
3.9 Molecular-docking approach (CDOCKER)	39
3.10 ADMET-prediction	39
3.11 Molecular dynamics simulations	39
<i>4. RESULTS AND DISCUSSION</i>	41
<i>5. Conclusion</i>	73
<i>References</i>	74



IN SILICO SCREENING OF POTENTIAL PEROXISOME PROLIFERATOR ACTIVATED RECEPTORS (ALPHA-GAMMA) PPARS α/γ FOR THE TREATMENT OF HUMAN DIABETIC MELLITIES (DM)

ABSTRACT

Diabetes mellitus (DM) means a metabolic ailment identified by hyperglycemia, obesity, hypertension, which can contribute to the metabolic disturbances on sugars, lipids, and protein. PPAR α and PPAR γ become signified the common broadly reviewed Peroxisome proliferator-activated receptor (PPAR) subtypes of Nuclear receptors because of their significant jobs in managing glucose, lipids, and cholesterol digestion. Throughout combining the lowering serum triglyceride levels benefit of PPAR α agonists (as fibrates) with the glycaemic advantages of the PPAR γ agonists (as TZD), the dual PPAR agonists approach can both improve the metabolic impacts and limit the symptoms brought about by either operator alone, and subsequently, has become a promising system for planning powerful medications against type-2 diabetes (T2DM). The result in this study, we performed computer procedures to gain one compound ZINC000002805504 with high binding score low toxicity from ZINC15 database through (CBP) models virtual screening. The compounds ZINC000002805504, ZINC000058367624 were found, which could activate PPAR α and PPAR γ receptors as the anti-diabetic. Our research has provided a design for gaining the potential of both PPAR α/γ agonists to diabetes therapy.

Keywords: Diabetes mellitus type; Docking analysis CDOCKER; Novel PPAR α/γ agonists; molecular dynamics simulations (MD); pharmacophore approach; docking; ADMET prediction.

Potansiyel PEROKSISOM PROLIFERATÖRÜ AKTİF ALICILARIN (ALPHA-GAMMA) PPARs α / γ İNSAN DIABETİK MELLİTLERİNİN (DM) TEDAVİSİ İÇİN SİLİKO EKCRANINDA

ÖZET

Diyabetes mellitus (DM), şekerler, lipitler ve protein üzerindeki metabolik rahatsızlıklara katkıda bulunabilen hiperglisemi, obezite, hipertansiyon ile tanımlanan bir metabolik hastalık anlamına gelir. PPAR α ve PPAR γ , glikoz, lipitler ve kolesterol sindirimini yönetmedeki önemli işleri nedeniyle yaygın olarak incelenen Peroksisom proliferatör ile aktive edilen Nükleer reseptörün (PPAR) alt tiplerini ifade eder. Azalan serum trigliserit seviyelerinin PPAR α agonistlerinin (fibratlar) PPAR α agonistlerinin (TZD olarak) glisemik avantajları ile yararları birleştirilirken, çift PPAR agonistleri yaklaşımı hem metabolik etkileri artırabilir hem de sadece operatörün getirdiği semptomları sınırlayabilir ve daha sonra, tip 2 diyabete (T2DM) karşı güçlü ilaçların planlanması için umut verici bir sistem haline geldi. Bu çalışmada, . Bu çalışmanın sonucunda ZINC15 veri tabanının içinde bulunan ZINC000002805504 molekülü, yüksek bağlanma skoru ve düşük toksisite değeri ile sanal tarama yöntemleri ile bulunmuştur. ZINC000002805504 ve ZINC000058367624, PPAR α ve PPAR γ reseptörleri üzerinde aktivite gösterebilecek bileşikler olarak belirlenmiştir. Çalışmamız PPAR α ve PPAR γ agonistlerinin anti-diyabetik ilaç ile tedavisi için bir potansiyel sağlamıştır.

Anahtar Kelimeler: Diabetes mellitus tipi; Yerleştirme analizi CDOCKER; Yeni PPAR α / γ agonistleri, moleküler dinamik simülasyonları (MD); farmakofor yaklaşımı; yerleştirme; ADMET tahmini.

ACKNOWLEDGEMENT

First and foremost Grateful and gratitude to God the Beneficent, the Merciful

My deepest gratitude to my parents, **Ismail Abdul Jabbar** and **Anwar Abdul Razzaq** and Sisters (Hiba & Noor) and Brothers (Fahad & Saad) and **Jamal Al Nori** and off course My sincere appreciation goes to my a supervisors (**Prof. Dr. Kemal Yelekçi**) , (Post doc. Abdullahi Ibrahim Uba) and for them guidance during my studies and the entire faculty members of the department of Bioinformatics and Computational Biology of Kadir Has University, my friends, and colleagues in the laboratory.

**This thesis is dedicated to my beloved parents, Anwar Abdul Razzaq and Ismael
Abdul Jabbar**

" الله لا يحرمني منكم "

LIST OF TABLES

Table 3. 1 PPAR (α/γ) The validation outcomes of the 13 pharmacophore models on the activity of active compounds by using "Receptor-Ligand Pharmacophore" protocol	23
Table 3. 2 The known ligand used for validation of both PPAR(α/γ) receptors.	29
Table 3. 3 This is when decoy 41 of best 13 and obtained hypothesis.....	34
Table 3. 4 HIP-HOP table decoy42 with best13 and obtain 55(active and inactive) The pharmacophore validation result Ligand-Based Approaches.....	34
Table 3. 5 Statistical parameters for generating pharmacophore models are listed as top ten pharmacophore hypotheses generated by implementation protocol for the pharmacophore validation result Ligand-Based Approaches.....	35
Table 3. 6 Positive Goodness of the Hit Results of both PPAR (α/γ) Could know the differences between each table that depend on D.	37
Table 3. 7 Negative Goodness of the Hit Results Common Feature Pharmacophore Generation of 42 as active training set 13 as selective training set and test set decoys number are 1991.	37
Table 4. 1 The compounds and properties obtained from structure-based approaches...	43
Table 4. 2 Ligand-Based approaches the resulting compounds and their properties.....	43
Table 4. 3 Structure-Based Cross-Docking between the different PDB Macromolecules.	45
Table 4. 4 The composition, energy(AutoDock and Cdocker),Fit values flow of small molecules.....	59

LIST OF FIGURES

Figure 1. 1 The flowchart of a brief illustration of research methodology for obtaining potential dual PPAR α/γ agonists.	xvi
Figure 2. 1 Types of diabetes mellitus.	2
Figure 2. 2 General structure of atomic receptors.	3
Figure 2. 3 Computer aid drug design.	7
Figure 4. 1 2D scheme Structure of the Inhibitor from the Ligand-Based approaches... ..	44
Figure 4. 2 2D Structure of the inhibitors from the structure-based approach.....	46
Figure 4. 3 10 best-fitting lead compounds that satisfied the geometric constraints of Hypo1of the ligand CHMBL326015 identified by a 3D query against the “Zinc15” Database in Biovia DS 4.5.	47
Figure 4. 4 A) 3DInteraction diagram between the amino acid residues and the binding pocket of 2PRG and ZINC000002805504. B)2D interactions.....	48
Figure 4. 5 A) 3DInteraction diagram between the amino acid residues and the binding pocket of 2PRG and ZINC000010853984. B)2D interactions.....	49
Figure 4. 6 A) 3DInteraction diagram between the amino acid residues and the binding pocket of 2PRG and ZINC000033275541. B)2D interactions.....	50
Figure 4. 7 A) 3DInteraction diagram between the amino acid residues and the binding pocket of 2PRG and ZINC000058367624. B)2D interactions.....	51
Figure 4. 8 A) 2D interactions. B) 3D Interaction diagram between the amino acid residues and the binding pocket of 1I7G and ZINC000058367624.	52
Figure 4. 9 A) 2D interactions. B) 3D Interaction diagram between the amino acid residues and the binding pocket of 1I7G and ZINC000252503037.	53
Figure 4. 10 A) 2D interactions. B) 3D Interaction diagram between the amino acid residues and the binding pocket of 1I7G and ZINC000033275541.	54
Figure 4. 11 A) 2D interactions. B) 3D Interaction diagram between the amino acid residues and the binding pocket of 1I7G and ZINC000002805504.	55
Figure 4. 12 A) 2D interactions. B) 3D Interaction diagram between the amino acid residues and the binding pocket of 1I7G and ZINC000010853984.	56

Figure 4. 13 The ligand-protein association with two-dimensional (2D) diagrams in the pocket of PPAR α and PPAR γ .	56
Figure 4. 14 (A)Interpolated charge surfaces and (B)Solvent accessibility surfaces (fa-b),the natural ligand binding layer AZ242 and BRL (green) and the PPAR α receptor pocket compound ZINC000002805504 (yellow)and PPAR γ (Red) ZINC000002805504 (green).	57
Figure 4. 15 The calculated ADMET properties for the Structure-Based inhibitors.	60
Figure 4. 16 The calculated ADMET properties for the Ligand-Based inhibitors.	61
Figure 4. 17 The graph of ADMET PSA 2D vs AlogP98 (the trust mark between 95 and 99 percent ellipses According to the BBB and HIA ligands).	61
Figure 4. 18 During simulations of 30 ns, the RMSD trajectories of PPAR α / γ -ligandcomplexes.	63
Figure 4. 19 Throughout the simulations, the RMSF maps of PPAR α / α and PPAR α / γ – ligand complexes.	64
Figure 4. 20 Throughout the 30ns simulations, the Rg-maps of PPAR α / α and PPAR α / γ .	65
Figure 4. 21 From the final frame, The MD simulation results how it looks like before and after.	67
Figure 4. 22 The MD simulation result in the entire MD simulations (NAMD)30ns. 3D Ligand-protein interaction diagrams in a pocket of PPAR α .	68
Figure 4. 23 2D-the MD simulation using (NAMD)30ns performance.	69
Figure 4. 24 From the final frame. The MD simulation results in how it looks like before and after.	70
Figure 4. 25 3D-structure The MD simulation result in the entire MD simulations (NAMD)30ns.	71
Figure 4. 26 2D-structure the MD simulation all MD simulations (NAMD)30ns result. The ligand-protein interaction diagrams in PPAR γ (2PRG) pocket.	72

LIST OF ABBREVIATION

WHOWorld Health Organization?
ADMETAbsorption, Distribution, Metabolism, Excretion and Toxicity.
CHARMMChemistry at HARvard Macromolecular Mechanics.
VMDVisual molecular dynamics.
FDAFood and Drug Administration.
IUPACThe International Union of Pure and Applied Chemistry.
PDBProtein Data Bank.
HTSHigh-Throughput Screening.
CADDComputer Aided Drug Design.
KIInhibition constant.
PDBQTProtein Data Bank Partial charge and Atom Type.
DPFDocking Parameter File.
LBDLigand-binding domain.
PPARPeroxisome proliferator-activated receptors.
TGTriacylglycerol.
TZDThiazolidinediones.
GPFGrid Parameter File.

1. CONTEXT and GOALS, A BERIF DISCRITION OF METHODOLOGY

1.1 CONTEXT and GOALS

Diabetes mellitus (DM) means a predominant ailment with hyperglycemia as the essential element. An ever-increasing number of individuals have diabetes because of an undesirable way of life (Hossain et al., 2016). These days, diabetes gets to come to the third rank, significant illness after heart and blood vessel disease, and malignant growth. For the past few years, the total number of people suffering from diabetes mellitus is rapidly increasing all the time (Liu et al., 2013). It estimated that people with diabetes would reach more than 300 million by 2030 years in the world (Darwish, Salama, Mostafa, Gomaa, & Helal, 2016). Furthermore, China has gotten probably the most nation that people with diabetes anticipated to increment to 139 million by 2035 years. Many chronic complications affect our health, for example, neurogenic malady and cerebrovascular ailment. Along these lines, improvement of the powerful remedy for diabetes medicine is exceptionally-important (Feng et al., 2019). Peroxisome proliferator-activated receptors PPARs as nuclear receptors are transcription. Generally, PPARs are PUFA (poly unsaturated fatty acids), play a part in the regulatory of fat-lipid, and blood pressure (Nevin, Peters, Carta, Fayne, & Lloyd, 2012). Three isoforms of PPARS are PPAR alpha, PPARgamma, PPAR beta/delta are distributing in various tissues. Furthermore, PPAR α remarkably represented in the fat tissue, liver, and heart (Aleshin, Strokin, Sergeeva, & Reiser, 2013). Introduce the PPARalpha-receptor for performing correct insulin opposition, furthermore reduction the incidence of diabetes by decreasing serum (TG) by Fibrates. However, the treatments (like fibrates) owned common symptoms like headaches, also vertigo. On the other side, PPAR γ presented in adipose-tissues and the immunity, when activated, to improve transcriptional gene translation and express the regulation protein. (TZDs), considering, commonly regarded as one of the most PPAR gamma-agonists that improve the sensibility (insulin) and carbohydrate metabolism inside the body (Rajapaksa, Bhatia, Wegener, Petrovsky, & Bruning, 2017). Yet there are various reverse effects, through like, weight increase, and pneumonic edema; these have consequences that can increase the probability of congestive failure. Today, multi-targets on antidiabetic sedate has been the focal point of much intrigue. These days PPAR α/γ agonists, for example, Lobeglitazone and

Saroglitazar have demonstrated as promoted, which may add to advance glucose and lipid heights and use diabetes with lower adverse effects (Jani, Kansagra, Jain, & Patel, 2013). The point of this exploration is to locate an incredible PPAR α/γ double agonist that can use diabetes. In the study, we got a likely plus different metal element of 30-million mixes via a progression of methodology incorporating virtualizing-screening by mean of CBP also docking analysis of energy by mean of CDOCKER, (ADMET) predict and (MD) simulation. All works carried out utilizing Discovery Studio4.0 and Autodock tools ADT 1.5.6 and PyRx programming individually. Chosen compounds that have fundamental biological activity as binding affinity, they were exposed to CDOCKER investigation and ADMET test. One a compound with the best-binding energy and lowest toxicity performed to MD for 30 ns.

Our specific objectives were:

1. To develop and validate a VS workflow to predict molecules that can act as PPAR α/γ inhibitors.

The predicted molecules will be used as lead compounds in drug design projects. We discover novel PPAR α/γ double agonists by methods for pharmacophore virtual screening.

2. To identify known antidiabetic activity that contain at least one molecule found to be novel PPAR α/γ inhibitor.

The utilization of the recently created VS work process to a ZINC 15 database that contains the atoms and the ID of which VS hits are available in known antidiabetic movement will enable us to accomplish this goal. A compound was acquired which would do well to superimposition with created pharmacophore model, higher dock score and lower ADMET quality.

3. To contribute to the knowledge of the in-silico screening of potential PPAR α/γ agonists.

To achieve this objective, it will be necessary to develop and validate Complexed Based Pharmacophores CBP that correlate the structures of known PPAR α/γ agonists with their binding affinities and transactivation activities. This examination gave an important methodology in building up a double novel and incredible PPAR α/γ agonist and may be a reference for the improvement of DM prescriptions and an establishment for further research.

1.2 ABERIF DISCRITION OF METHODOLOGY

On this part of section, a brief clarification on the steps which that applied on current study as in Figure 1.1 to provide a general look on the major steps. In addition to this, to comprehensive illustration of all the details are presented in chapter three.

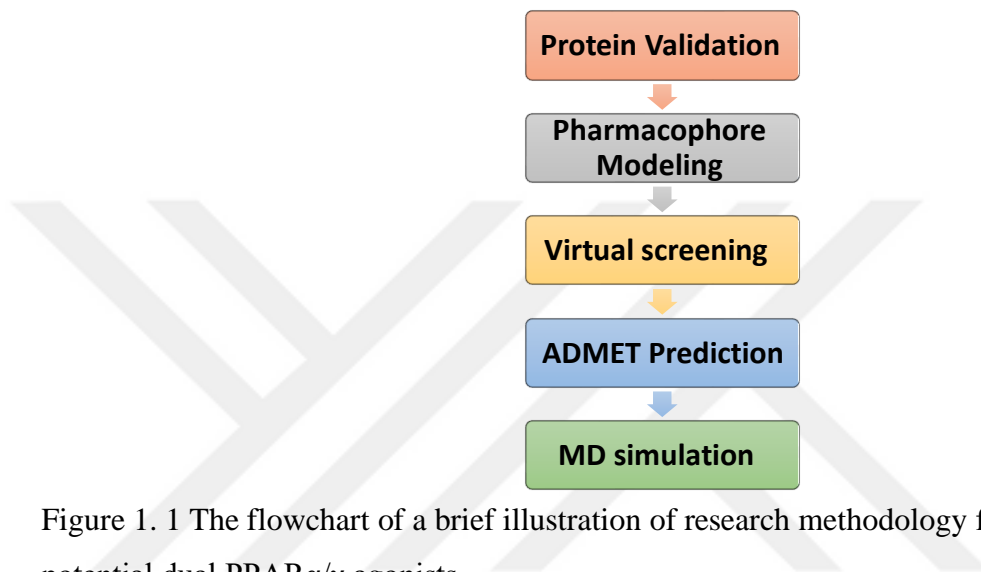


Figure 1. 1 The flowchart of a brief illustration of research methodology for obtaining potential dual PPAR α / γ agonists.

2. INTRODUCTION

2.1 Diabetes mellitus

Diabetes mellitus (DM) is a metabolically disorder that comprises a significant medical issue (Meetoo, McGovern, & Safadi, 2007; Wild, Roglic, Green, Sicree, & King, 2004). It is assessed that 246 million individuals worldwide have diabetes and that 380 million individuals have diabetes by 2025. What's more, 3.8 million individuals bite the dust every year from diabetes (International Diabetes Federation, 2011). DM is defined by unusually elevated levels of plasma glucose, known as hyperglycemia, in the fasting state or after the organization of glucose during an oral glucose resilience test. DM is brought about by a family member or supreme inadequacy in insulin emission, protection from insulin discharge, or both (DeFronzo & Abdul-Ghani, 2011; Marchetti et al., 2009). The World Health Organization perceives two particular clinical types of diabetes figure 2.1, type 1 diabetes (T1DM), and type 2 diabetes (T2DM). T1DM, additionally alluded to as the adolescent assortment of DM results from an outright insufficiency of insulin because of the annihilation of insulin delivering pancreatic β cells. T2DM is a multifactorial infection that is portrayed by insulin opposition related to hyperinsulinemia and hyperglycemia as well as atherosclerosis, hypertension, and a different lipid profile (Garten et al., 2011). T2DM represents 90-95% of the analyzed instances of DM (Bharatam, Patel, Adane, Mittal, & Sundriyal, 2007). Hereditary and ecological variables, expanded stature and weight improvement, expanded maternal age at conveyance, and presentation to some prevalent diseases have likewise connected to the danger of treating T1DM. A few hazard factors have related to T2DM, including weight, changes in diet and physical action, generation, insulin obstruction, a family ancestry of diabetes, and ethnicity (Aekplakorn et al., 2011; Viljoen & Sinclair, 2011). Changes in diet and physical movement identified with fast improvement and urbanization have prompted a sharp increment in the number of individuals creating diabetes. T1DM and T2DM require cautious observing and control. Without legitimate administration, they can prompt extremely high glucose levels, which can bring about the long term of harm to different organs and tissues. Consequences of

diabetes are cardiovascular ailment, (Holt, 2011; Voors & Van Der Horst, 2011); nephropathy (Ritz, 2011).

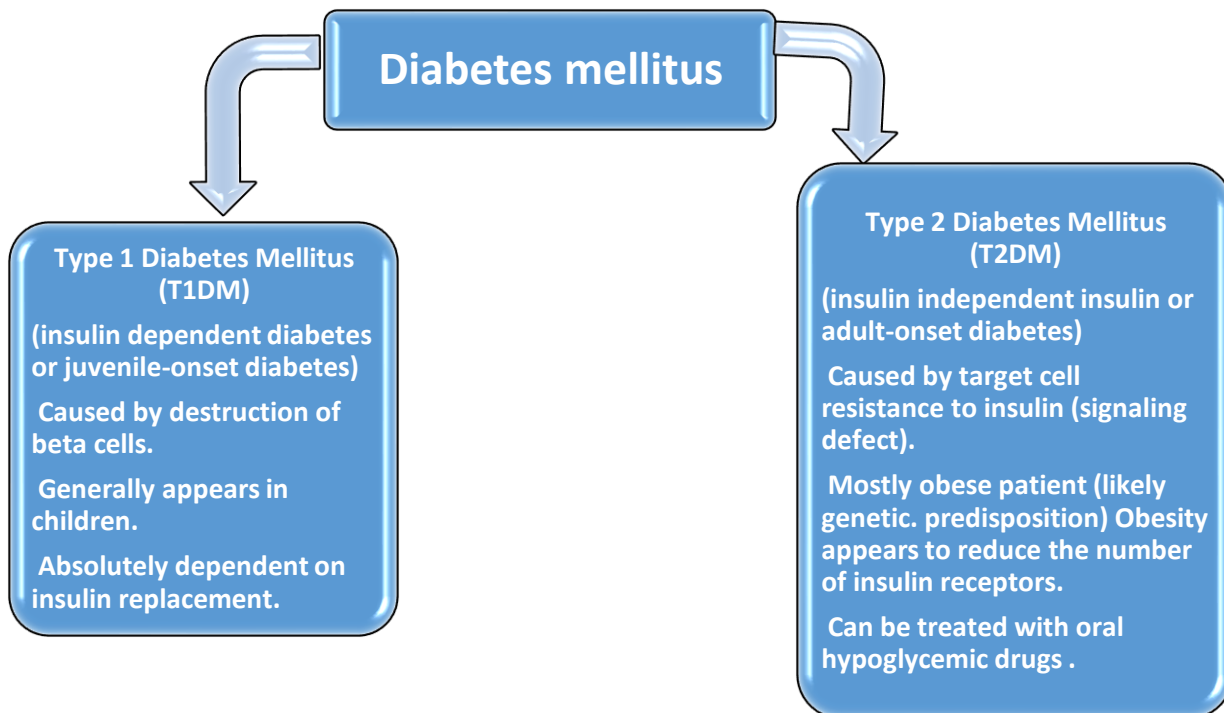


Figure 2. 1 Types of diabetes mellitus.

2.2 Nuclear Receptor

Nuclear receptors are DNA binding transcription factors with a conserved domain organization figure 2.2, whose activity is controlled by lipophilic ligands, phosphorylation, and other proteins. Most nuclear receptors, regardless of the presence of a ligand, are localized in the cell nucleus, but steroid receptors in the absence of a hormone can also be in the cytoplasm. After ligand binding, receptors of all types are redistributed within the nucleus between the nucleoplasm and chromatin. In the superfamily of nuclear receptors, two groups are most studied: steroid hormone receptors; thyroid hormone and retinoic acid receptors. Currently, the superfamily of nuclear receptors has up to 200 members, the ligands of many of them are still unknown. Known nuclear receptor ligands include hormonal compounds (e.g., 9 cis retinoic acid, testosterone, estradiol, etc.), as well as common low molecular weight metabolites (e.g., cholesterol hydroxy derivatives for liver-specific SF 128 and LXR) The discovery of orphan

receptors and their ligands has changed the idea of the signaling functions of various metabolites.

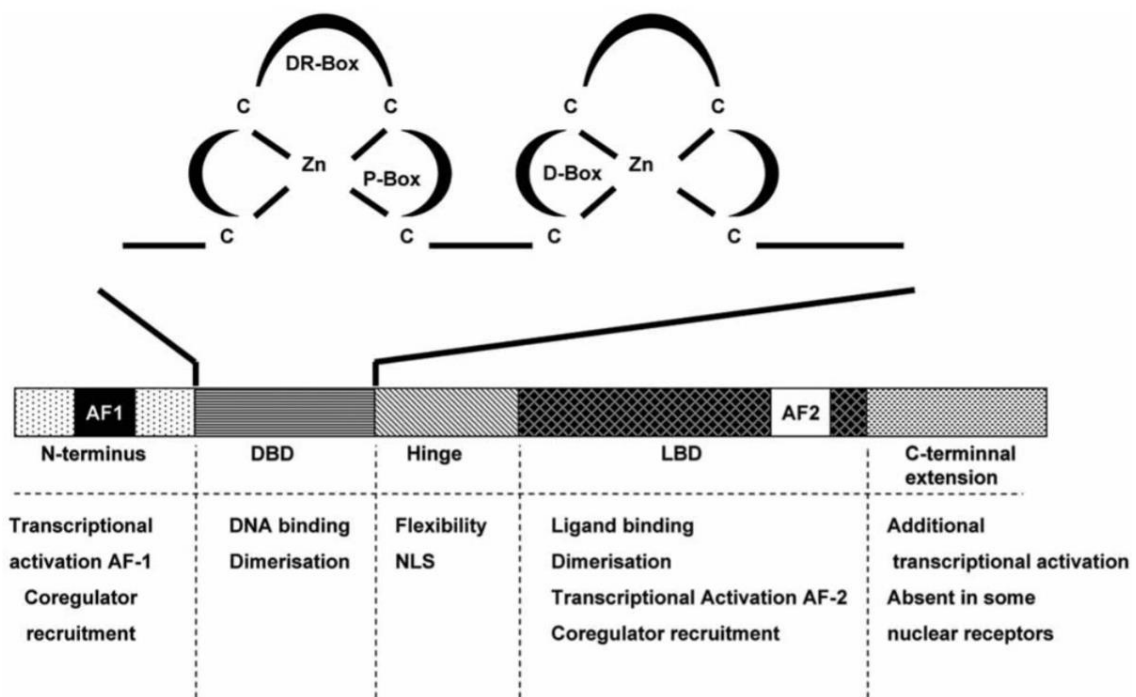


Figure 2. 2 General structure of atomic receptors. In the N end the initiation work 1 (AF 1) is demonstrated, in the ligand restricting space (LBD) the enactment work (AF 2) is appeared. A schematic portrayal of the two zinc fingers framed by the protein structure of the DNA restricting space (DBD) is appeared over the nonexclusive atomic receptor structure. Places of DR, P (known as protein themes) and Dboxes are demonstrated inside each relating peptide circle. Trademark elements of every area are recorded at the base. Adopted from(Novac & Heinzl, 2004).

2.3 Peroxisome Proliferator Activated Receptors (PPARs)

Peroxisome proliferator enacted receptors (PPARs) are individuals from the atomic receptor superfamily that direct the quality articulation of proteins associated with vitality, glucose and lipid digestion, adipocyte expansion and separation and insulin affectability (Francis, Fayard, Picard, & Auwerx, 2003). PPARs go about as cell sensors that actuate translation in light of the official of regular or manufactured ligands. Three subtypes, PPAR α , PPAR β/δ , and PPAR γ , have been distinguished. Even though the subtypes share a significant level of grouping and basic homology (Garcia Vallvé & Palau, 1998), they exhibit differences in tissue

expression and physiological function (Berger & Moller, 2002). Agonists of PPAR α and PPAR γ are currently approved for treating dyslipidemia and type 2 diabetes, respectively (Garcia Vallvé & Palau, 1998; Shearer & Billin, 2007). Moreover, Peroxisome proliferator-activated receptors (PPAR) α and β / δ control the expression of fatty acid oxidation (FA) genes, which are the source of 70-90% of ATP in the myocardium. PPAR α controls the oxidation of FA and affects myocardial energy homeostasis, mainly through the supply of circulating FA from the liver, while PPAR γ protects the myocardium from excess FA and lipotoxicity by redistributing the FA fluids into adipocytes. PPAR β / δ is the main regulator of lipid metabolism in muscles, constituting up to 50% of body weight. The PPAR / PGC 1 α system (mainly PPAR α / PGC 1 α) controls mitochondrial biogenesis and, thus, makes it possible for myocardium to adapt to a sudden (stress) load. Regulatory system dysfunction PPAR / PGC 1 α may be one of the pathogenetic mechanisms of cardiomyopathy development, and the signaling pathways of this system may be subject to therapeutic effects.

2.4 PPAR γ

Numerous studies have shown that in peritoneal processes, PPARs play a role (peroxisome proliferator-activated receptor, receptors that activate proliferation by peroxisome- γ), stimulation of which reduces the level of triglycerides, has an antiproliferative effect and improves endothelial function, including in patients with diabetes and kidney damage. A low level of adiponectin is considered as the most important risk factor for the development of insulin resistance, obesity, MS, cardiovascular risk. Adiponectin levels the negative effects of leptin, IL 6 and TNF α , PAI 1 and angiotensin II concerning insulin resistance, endothelial function, vascular elasticity, atherogenesis, platelet aggregation, and non-infectious inflammation. PPAR γ agonists enhance adiponectin production, but at the same time, their activity itself depends on the level of adiponectin secretion.

2.5 PPAR α

The main physiological role of PPAR α is to respond by activation to the supply of fatty acids and their derivatives to the liver and xenobiotics, called peroxisome proliferators (hence the name of the receptors). Activation of PPAR α triggers transcriptional programs for capturing, activating and oxidizing fatty acids in peroxisomes, microsomes, and mitochondria in hepatocytes, which provides the necessary energy and several substrates for all other functions of the liver. The genes for the synthesis of very-low-density lipoproteins (VLDL) and

triglycerides (TG) are also expressed. The former is exported to the blood; the latter is deposited in the form of intracellular chylomicrons. The liver detoxification function is also under the control of PPAR α . The PPAR α receptor is present in significant amounts in organs and tissues that are characterized by a high level of fatty acid catabolism: in the liver, skeletal muscle, brown adipose tissue, heart, kidney, and cells in the area of atherosclerotic lesions (endothelial cells, smooth muscle cells, macrophages). Thus, PPAR α activity in the liver and other organs is manifested by a decrease in intracellular fatty acid concentrations, which leads to a decrease in very-low-density lipoproteins (VLDL) and a decrease in plasma triglyceride levels in patients receiving PPAR α receptor agonists.

2.6 Activation of peroxisome proliferator activated receptors

Nuclear receptors combine the functions of a receptor and a transcription factor: they recognize various hydrophobic components of food or their derivatives (fatty acids, vitamin D, retinoic acid, bile salts, etc.), and then change the activity of the genes regulated by them. It will be about how fatty acids and their derivatives affect the activity of certain receptors. These are peroxisome proliferator-activated receptors (PPARs), a group of nuclear receptors that function as a transcription factor.

2.7 PPARS Drugs Modulators (Pharmacological role of PPARs agonists in human disease)

Receptors that activate the proliferation of peroxisome (PPAR), activated by ligands of the nuclear transcription factors from the family of hormone receptors. All isoforms (PPAR α , PPAR β/δ , PPAR γ) expressed in the liver, regulate the metabolism of fats and carbohydrates, cholesterol and bile acids, the processes of inflammation, regeneration and differentiation/proliferation of liver cells. The role PPAR β/δ is still to be explored, while the role of PPAR α and PPAR γ in the development of metabolic illnesses resulting liver (insulin resistance, dyslipidemia, hepatic steatosis, viral and neoplastic diseases levant) is well known. Agonists of these receptors may be a means of prevention and treatment of these diseases. The use of PPAR α agonists that induce cancer of the liver and bladder, in the treatment of liver cancer remains a subject of debate. Prolonged use of full agonists PPAR γ causing the maximum activation of these receptors in humans might not be known side effects of these drugs. Currently developed approaches with the use of "partial" activators, for example,

telmisartan. It is also necessary to explore the possibility of change "double" and "triple" agonists.

2.8 Structure of PPAR

Molecular structure of PPARs generally are consist of following function domains: (A/B) N terminal region, (C) DBD (DNA binding domain), (D) flexible hinge region, (E) LBD (ligand-binding domain) and (F) C terminal section (Diradourian, Girard, & Pégrier, 2005; Renaud & Moras, 2000). The DBD contains two zinc finger motifs, which bind to specific sequences of DNA known as hormone response elements when the receptor is activated. The LBD has an extensive secondary structure consisting of 13 alpha-helices and a beta-sheet. Natural and synthetic ligands bind to the LBD, either activating or repressing the receptor. The transcriptional activating function (AF 1) motif is present in the N terminus and it is not activated by ligands. On the other hand, E/F domain or LBD also contains a transcriptional activating function (AF 2) motif at the C terminus helix 12, which is activated by ligands (Diradourian et al., 2005). A large number of synthetic and natural ligands like eicosanoids, fatty acids, linoleic acid derivatives, oxidized and nitrated fatty acids, bind to the large binding pocket present on the E/F (LBD) domain. The dimerization of PPARs with the 9 cis retinoic acid receptor (RXR) requires both the D and E/F domains. Then this dimerized PPARs and RXR bound to their respective peroxisome proliferator-activated receptor response elements (PPREs) present on the DNA molecule (Blitek & Szymanska, 2019).

2.9 Diabetes-Associated Complications

With good control, discipline and a healthy lifestyle, complications of diabetes can easily be minimized or even completely prevented. Taking care of your body is your main responsibility, and it begins with awareness of your illness. Understanding what diabetes is, how it is treated and what changes it requires in lifestyle can be difficult at the first stage. To assimilate all the information presented is not an easy task, but it is important to obtain as much accurate information as possible. This first step enables many people with diabetes to successfully live a long and healthy life, subject to continuous monitoring of the disease. Improper management of blood sugar levels over a long period can lead to problems with organs, and in this case, serious complications can occur. Since diabetes directly affects the blood vessels and nerves, no part of the body is protected from deterioration and even complete failure. Short-term and

late complications of diabetes mellitus depend on improper treatment affecting your body, and how poorly you regulate blood sugar levels over a long period.

2.10 Computer aid drug design

Computational methodologies are valuable instruments to translate and direct tests to speed up the anti-toxin tranquilize configuration process. Structure-based medication plan (SBDD) and ligand-based medication structure (LBDD) are the two general kinds of PC supported medication structure (CADD) approaches in presence. SBDD strategies investigate macromolecular objective 3-dimensional auxiliary data, normally of proteins or RNA, to distinguish key locales and communications that are significant for their individual natural capacities. Such data would then be able to be used to plan anti-microbial medications that can contend with fundamental associations including the objective and, in this way, intrude on the organic pathways basic for the endurance of the microorganism(s).

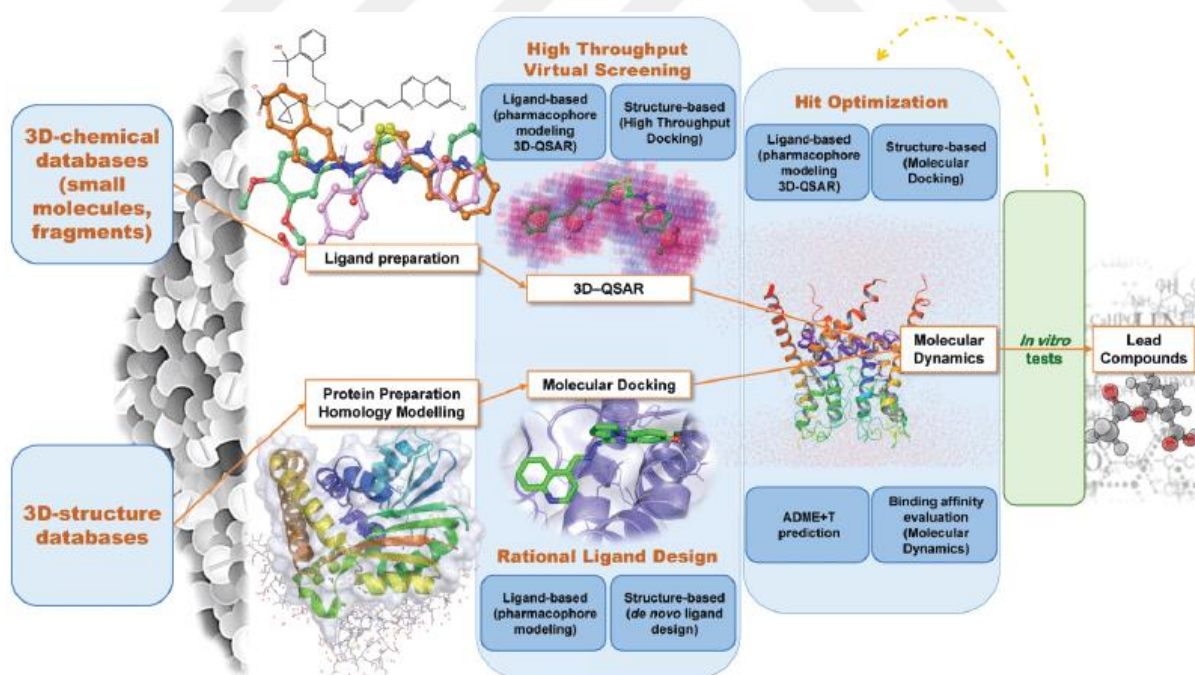


Figure 2. 3 Computer aid drug design. Different computational methods with different potential applications during the drug discovery process. Adapted from (G & S, 2017).

2.10.1 Docking Studies

A molecular docking study can predict the binding conformations and free energies of the ligands, which are candidate drug molecules at the corresponding target binding site (Ferreira, Dos Santos, Oliva, & Andricopulo, 2015). Many counting functions are designed to predict the interaction between a ligand and its protein through docking. Some of these include CHEM Score, AUTODOCK4, FRESNO, GOLD SCORE, Cdocker, LigandFit (Beaver & Venkatachalam, 2003), LeDock (Zhao & Caflisch, 2013), AutoDock Vina (Ambrus et al., 2010), rDock (Ruiz Carmona et al., 2014), UCSF Dock (Allen & Luo, 2015), and many other dockings can occur in the following forms: flexible docking protein-ligand, flexible protein-protein flexible ligand hard protein or hydrophobic docking (Shore, 2012).

2.10.2 Pharmacophore

The IUPAC describes the pharmacophore term as “an ensemble of steric and electronic features that is necessary to ensure the optimal supramolecular interactions with a specific biological target and to trigger (or block) its biological response”. Pharmacophoric signs are usually understood pharmacophoric centers and the distances between them, necessary for the manifestation of this type of biological activity. Typical pharmacophore centers here are hydrophobic regions, aromatic rings, hydrogen bond donors and acceptors, anionic and cationic centers. For a more detailed description of a pharmacophore, hydrophobic and excluded volumes are often used, as well as the allowable intervals of the angular orientation of the hydrogen bond vectors and planes of aromatic rings. In pharmacophore search, a match is conducted between the description of the pharmacophore and the characteristics of molecules from the database that are in acceptable conformations.

2.10.3 Virtual screening

The strategy of using computer analysis for the selection of compounds that can bind to a specific (specified) receptor uses the available information in the field of studying the nature of receptor binding sites, as well as ligands, productively binding to these receptors. Used in all areas of the study of living, and especially in structural biology, molecular biophysics, and genetics. Most often, virtual screening is used in the development of new drugs to search for chemical compounds with the desired type of biological activity. In the latter case, the virtual screening procedure can be based either on knowledge of the spatial structure of the biological

target or on knowledge of the structure of the ligands to the molecule of the given biological target. Several monographs and review articles are devoted to virtual screening.

2.10.4 Toxicity and ADME Properties

ADMET (absorption, distribution, metabolism, excretion, toxicity) furthermore, toxicological investigations are basic pieces of any medication improvement program and basic for consistency with administrative rules. Generally, they were led distinctly on medicating applicants that had to endure the rigors of substance streamlining, process improvement, and pharmacological profiling. The purpose behind this isolation was basically that such examinations perpetually included entire creature models and accordingly were tedious and costly. It was not monetarily solid to consume such assets on competitors that were not immovably dedicated to advancement by other determination criteria. Shockingly, when an ADMET issue was at long last recognized, it was at late investigational new medication arrangement or even in the facility. Such occasions made genuine interruption of the improvement procedure and frequently brought about the conclusion of the task and a lost chance. The parallel advancement of a few up and comers from a similar compound class has been a standard methodology to maintain a strategic distance from venture end in case of the rise of an untoward impact. The extensive expense conferred by this methodology was supported as being important for venture endurance. Today, the circumstance is changing quickly and drastically. ADMET and toxicology advancements have developed to allow the utilization of fast and more affordable techniques that have made the early appraisal of medication applicants appealing to the pharmaceutical business. Substantial, organizations are moving ADMET evaluation to turn into a basic piece of the application determination process. Expenses are as yet significant yet supported.

2.10.5 Molecular dynamics simulations

Molecular dynamics simulations have developed into a full-grown procedure that can be utilized viably to comprehend macromolecular structure to work connections. Present recreation times are near organically important ones. Data assembled about the dynamic properties of macromolecules is sufficiently rich to move the standard worldview of auxiliary bioinformatics from examining single structures to dissect conformational troupes. Here, we depict the establishments of atomic elements and the enhancements made toward getting such

gathering. Explicit utilization of the procedure to three primary issues (allosteric guideline, docking, and structure refinement) is examined.



3. MATERIALS AND METHODS

Generally. This research study was done by using computer-aided drug design tools, (in-silico) approach. It also has shown two main methods that were performed to reach and obtain the results: Ligand-based pharmacophore model and second, Structure-based pharmacophore model. Figure 3.1 Illustration of Material and methods of this research study for obtaining the potential of dual PPAR α (1I7G) / γ (2PRG).

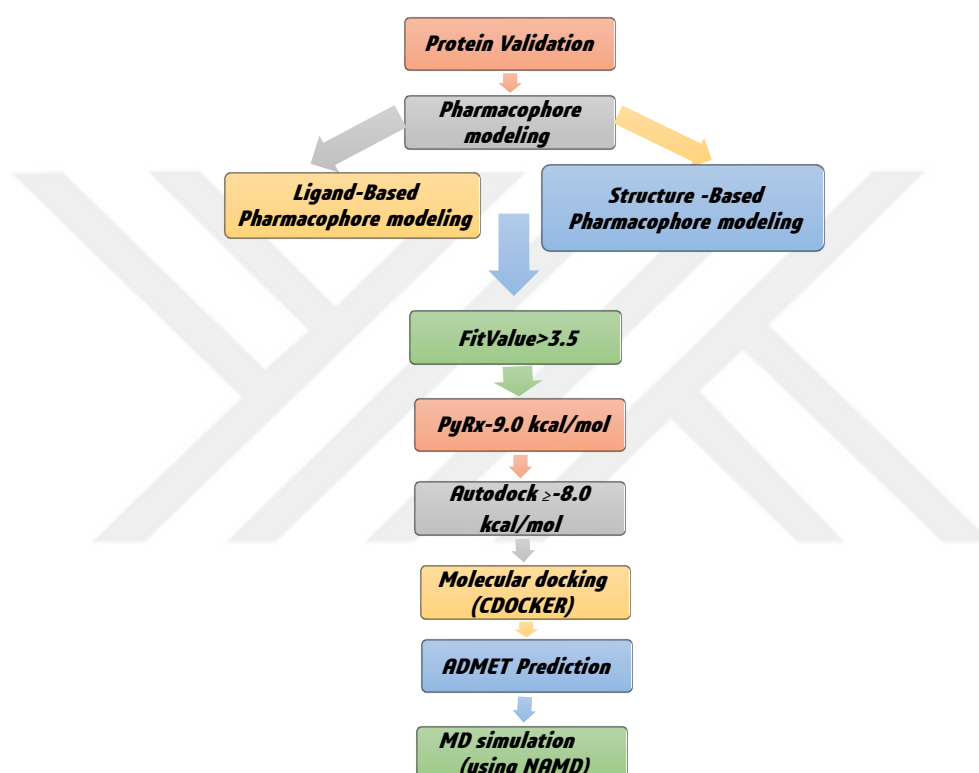


Figure 3. 1 The diagram of procedure steps and the criteria that were followed while choosing the best inhibitor.

Firstly, use approach (protein validate) by a macromolecule that has known inhibition value, by two way:

1. by constructing a common feature that is found in these inhibitors (chemical group which is the pharmacophore features are assume that too fundamental).
2. the receptor-ligand interaction a protocol which is consider the maker for building the pharmacophore feature.

The purpose of this research is to be achieved throughout (in silico approach) by using a computer simulation which by:

1. The crystal structure of targeted PPAR α/γ receptors obtained from The RSCB protein databank (PDB).
2. Using the "prepared protein" protocol in Accelrys Discovery Studio, for the two targeted receptors (1I7g, 2PRG) to dock.
3. During the aforementioned research, two approaches were utilized to -earned promising inhibitors PPAR α/γ receptors (proteins):
 - Firstly, prepared ligands by using protocol prepared ligands in discovery studio visualizer.
 - Secondly, the ZINC25' and the ZINC15 Chemical Library use for getting ligands that could serve as a drug promising inhibitor of PPAR α/γ receptors (proteins). Thousands of ligands were obtained from these library and convert to PDB files by using discovery studio for the main purpose of docking via PyRx and Autodocktools4.
4. PyRx initially use for docking the converted ligands, those have a binding the affinity of upper than - 8.00 Kcal/mol or lower were selected for furthermore dock using Autodocktools. Ligands do not still within the threshold -8.00 Kcal/mol were not further, do processed. Inhibitors with a lower inhibition constant (K_i) taken to discovery studio for the generating (2D -3D) structures for observed the interactions.

3.1 Screening and preparation the ZINC15 Chemical Library

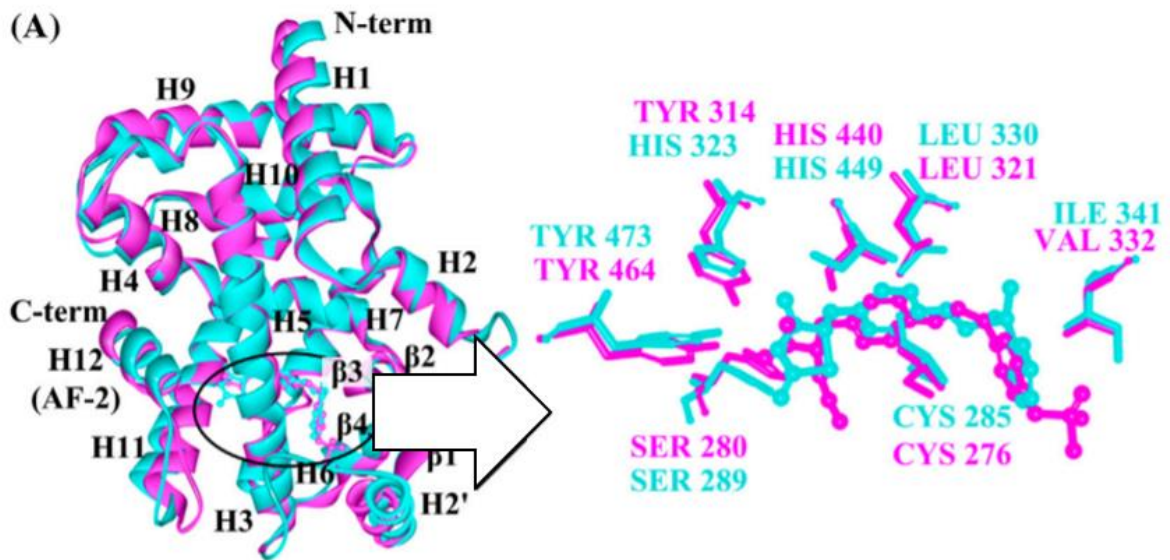
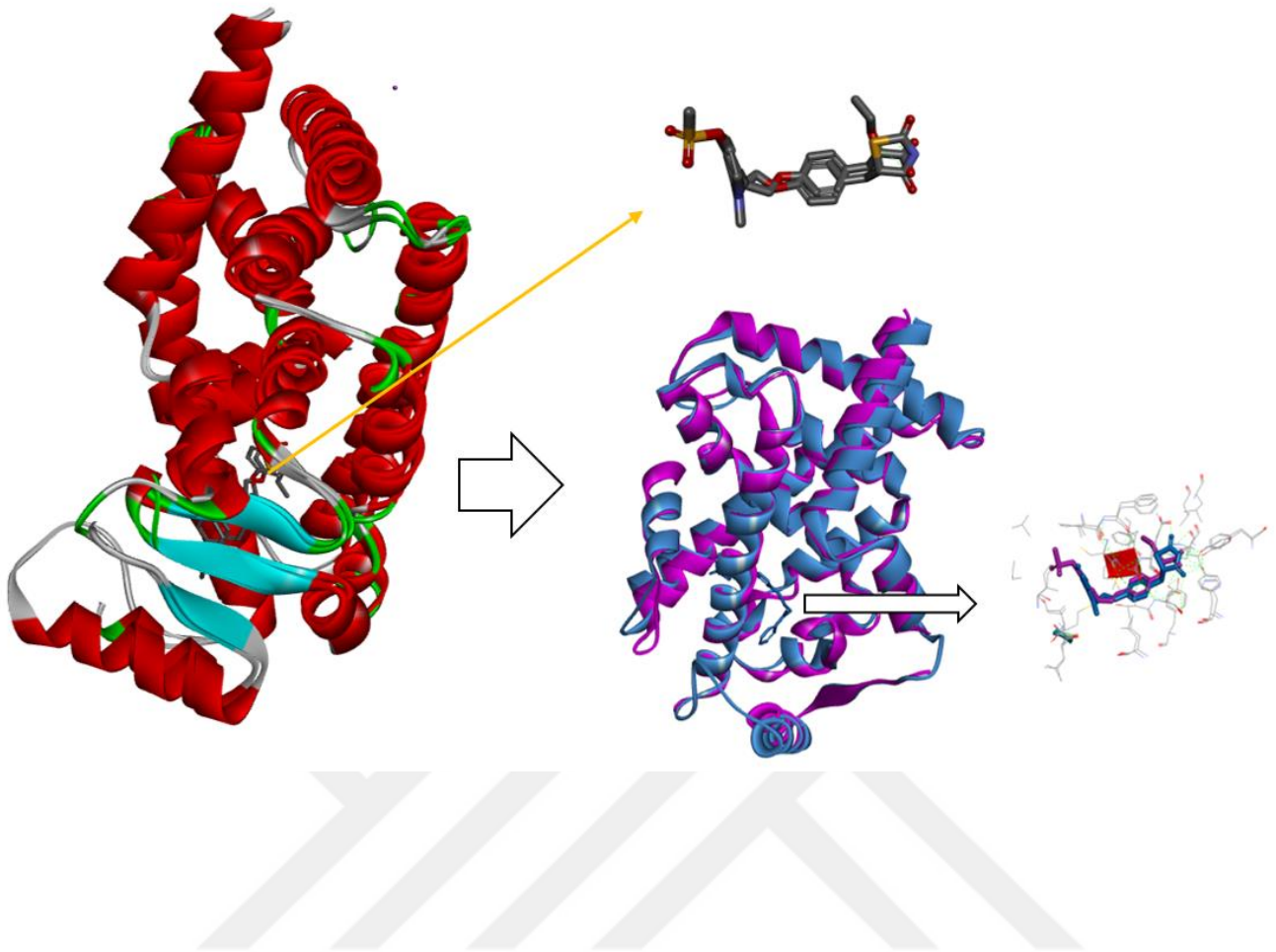
The protocol "Build 3D Database" in Bio via Discovery Studio was utilized to construct a 3D database used in this study. The Zinc15 database was first chosen with moreover than two hundred and fifty million compounds commercially accessible to download (Sterling & Irwin, 2015). All compounds were pre-synthesized and prepared due for virtual screening. The compounds are classified according to diverse filters; moving horizontally from left to right across the Zinc15 platform shows an increase in the molecular weight of the compound and moving vertically from upward to downward across the Zinc15 platform, the logo factor increases figure 3.2. The new advanced platform of Zinc15, Tranches, provided a beneficial feature of choosing according to Lipinski's rule of five.

		Molecular Weight (up to, Daltons)											
		200	250	300	325	350	375	400	425	450	500	>500	Totals, by LogP
LogP (up to)	-1	25,006	97,108	1,270,570	1,858,918	2,255,140	476,680	376,427	76,464	46,111	22,810	2,305	6,480,228
	0	163,292	937,316	6,802,472	10,182,378	13,498,255	2,512,145	650,898	347,288	344,239	183,226	3,304	35,458,217
	1	515,770	3,761,092	20,908,294	13,317,993	24,671,609	6,772,203	1,024,908	361,186	280,692	339,523	3,369	71,437,500
	2	722,952	8,791,595	24,606,591	47,614,252	17,820,237	29,837,694	3,804,167	402,484	71,997	371,520	31,411	133,320,537
	2.5	277,224	3,287,917	18,800,852	19,488,948	20,086,887	13,293,595	2,776,191	455,583	87,853	77,134	24,412	78,354,960
	3	151,465	3,252,289	16,961,147	11,532,516	25,239,184	34,199,798	3,464,288	503,218	131,328	384,632	42,991	95,668,400
	3.5	82,574	1,390,317	15,995,827	15,175,621	13,719,740	15,361,472	2,820,827	218,778	175,114	539,446	66,725	65,397,142
	4	45,000	442,962	7,082,941	8,245,012	10,710,019	3,694,434	22,205,834	6,154,354	204,622	562,226	192,600	59,302,404
	4.5	14,413	55,029	598,582	6,781,458	5,710,395	5,273,771	1,624,506	4,977,902	201,521	589,486	110,285	25,812,650
	5	93	3,813	103,226	333,436	72,655	148,332	124,120	155,614	167,508	587,125	172,672	1,695,829
	>5	27	788	14,312	53,706	44,733	113,702	120,582	193,354	227,358	488,172	850,305	0
Totals, by Weight		0	22,019,438	113,130,502	134,530,532	133,784,121	111,570,124	38,872,166	13,652,871	1,710,985	3,657,128	0	573M Protomers 9.8K Tranches

Figure 3. 2 Table shows LogP versus molecular weights obtained from Zinc15 databases in order to get the best compounds which fulfils the Lipinski rule.

3.2 Structure and superimposition of PPAR α and PPAR γ

To distinguish the closeness and contrast among PPAR α and PPAR γ , we adjusted the previous structure of 1I7G with 2PRG. The superimposed outcome was shown in figure 3.2, we could find that the gem structures of PPAR α and PPAR γ were fundamentally the equivalent, and the comparability of the two successions is 80.8%. They all made out of 12 α helices masterminded in an antiparallel helix sandwich and a four-stranded antiparallel β sheet. The ligand restricting pocket of PPAR α/γ is Y molded and shaped by commitments from helices 3, 5, 6, 7, 11, 12, and the β sheet (van Marrewijk, Ybema, Smits, Clegg, & Pitsis, 2016). The helix 12 (AF 2 helix) shows generally conformational varieties in various previous stones and assumes basic jobs in enactment of PPAR receptors. The coupling site of CYS 276, SER 280, TYR 314, LEU 321, VAL 332, HIS 440, and TYR 464 of PPAR α was fascinating to superpose well with deposits CYS 285, SER 289, HIS 323, LEU 330, ILE 341, HIS 449, and TYR 473 of PPAR γ , separately. Similar buildups for SER 280 and SER 289, CYS 276 and CYS 285, LEU 321 and LEU 330, TYR 464 and TYR 473 from PPAR α to PPAR γ , individually, showed nearly a similar dynamic restricting depression. In the accompanying, the entire examinations were directed with the two receptors.



(B)

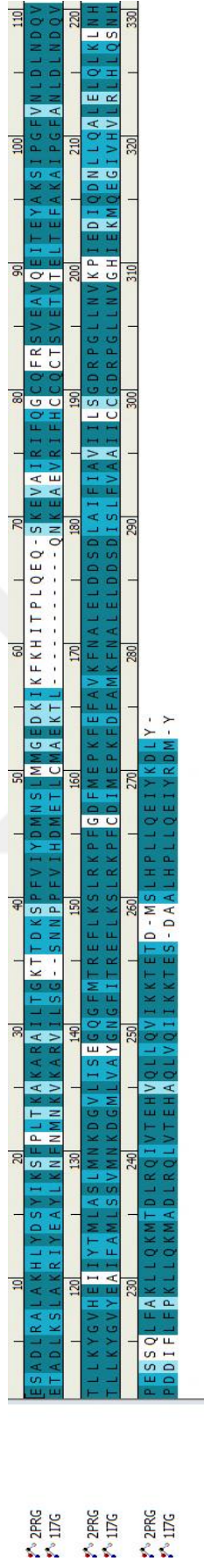


Figure 3. 3 Structure of PPAR α/γ after structure alignment as shown above with molecules AZ242 and BRL using Biovia, then colored for distinguished as observed on A. (A) Superimposition plots of PPAR α/γ with the key residues. PPAR α : magenta, PPAR γ : cyan. (B) Sequence alignment of PPAR α/γ , dark blue color showed that the amino acid residues of both receptors were identical, the shallower, the more difference in structure.

3.3 Principles of Structure-Based Drug Design

3.3.1. Rationale and Target Selection

Structure-Based Drug added Design SBDD is most of a powerful tool that utilized information of the three-dimensional (3D) structure of that that a biological target to expeditiously search the chemical groups for ligands with high binding affinity. Indeed, 83.8% of the entire macromolecule structures within (PDB) as of December 2018 were determinative X-ray physics for these cases within which not through an experimentally determined structure is on the market. Medicine targeting protein-protein interactions (PPIs) are more and more being pursued by drug discovery teams (Center for Substance Abuse Treatment, 2012; Jones, Willett, Glen, Leach, & Taylor, 1997; Simmons, Chopra, & Fishwick, 2010; Tuma, J. M., & Pratt, J. M. (1982). Clinical child psychology practice and training: A survey. \ldots of Clinical Child & Adolescent Psychology, 137(August 2012) et al., 1989). Also, these programs solely account for side-chain flexibility, which may be low once modeling a lot of complicated macromolecule backbone motions as within the case of receptors (Pagadala, Syed, & Tuszynski, 2017).

3.3.2 Methods of SBDD

(SBDD) structure-based drug design is the most useful method when the biological target is determined, and the 3D structure is available. Based on information on the targeted 3D structure, SBDD methods can serve the process of selecting ligand with good-affinity with the protein binding-site (Lionta, Spyrou, Vassilatis, & Cournia, 2014). Accordingly, SBDD approaches being a promising tool for serving to design new drugs against DM. Overall, SBDD is divided into three main methods: (1) Docking protein-ligand; (2) structure-based pharmaceuticals; and (3) molecular dynamics (Mottin et al., 2018). Once ,design a new ligands as a lead-compound with a structural information, it had been required to screen the library of 332447 compounds against PPAR (α/γ) by the following ,the grid-box dimension: 60, 60, 60 A; and grid-box center: α (X = 37.354) ,(Y = 34.871),(Z = 39.222), γ (Y = 49.720800), (Y = 36.982840), (Z = 19.294840) A. (Oleg Trott & Olson, 2009). In the first method, the compounds were filtered due to their energy values ($\Delta G > \text{or} = -8\text{kcal/mol}$), from this criterion a wholly of 110 been achieved. Second, the highest 42 protein-ligand complexes were analyzed for the orientation of ligands during a binding-site. This approach depends on the interaction between the receptor-ligand within the 3D structure as previously mentioned. Secondly, been

using the protocol for generating the hypothesis is an analysis of the chemical group in the pockets and their locative-relations. The receptor-ligand-complex method used in this study was performed to identify the interacting groups between the ligands and the receptors.

3.3.3 Protein Preparation

Obtained from RCSB PDB, the ID of the crystal structures of human PPARalpha is 1I7G; besides, PPARgamma is 2PRG (Feng et al., 2019). The compounds of these targets, named as the native fragments (co-crystallization ligand) of 1I7G, its known ligand is presentative PPAR α agonist dihydro cinnamate and its molecular form is identical to Rosiglitazone. Though Rosiglitazone (BRL) is 2PRG (PPAR γ), an anti-drug for treat diabetic. As regulation pieces, PPARalpha and PPARgamma AZ242 and BRL (Rosiglitazone) were investigated as independent disciplines. The ligands were from the ZINC15 table, and the known inhibitors (the experimental) were from ChEMBL. The protocol that performed the process was preceded by cleaning the protein from the native ligand, water molecule, and non-interacting ions. During the process, the hydrogen atom added to the protein and the "Clean Geometry tool" used to optimize geometry using the forcefield. The final step includes "Preparing Macromolecule" protocol that cleans common issues that present in the protein structure and include the addition of the missing hydrogen based on the protonation state of the residue sat PH of 7.4 using Biovia Discovery Studio (DS) 4.5 program (Accelrys Inc., 2017; Kemmish, Fasnacht, & Yan, 2017).

3.3.4 Pharmacophore Generation

The pharmacophore models were produced by using a Biovia Discovery Studio, the protocol of pharmacophore receptor-ligand complexes was performed (Gaurav & Gautam, 2014). During the process find the best pharmacophore-model, through choosing the robust matching and conformational approach, the 'BEST' method was developed using only the matching pharmacophore system. The process of production of pharmacophores is ranked as 'FAST' and 'BEST' Use of 'FAST' and 'RIGID', the pharmacophore model was better created by using 'BEST'. The major six features will be comprised:

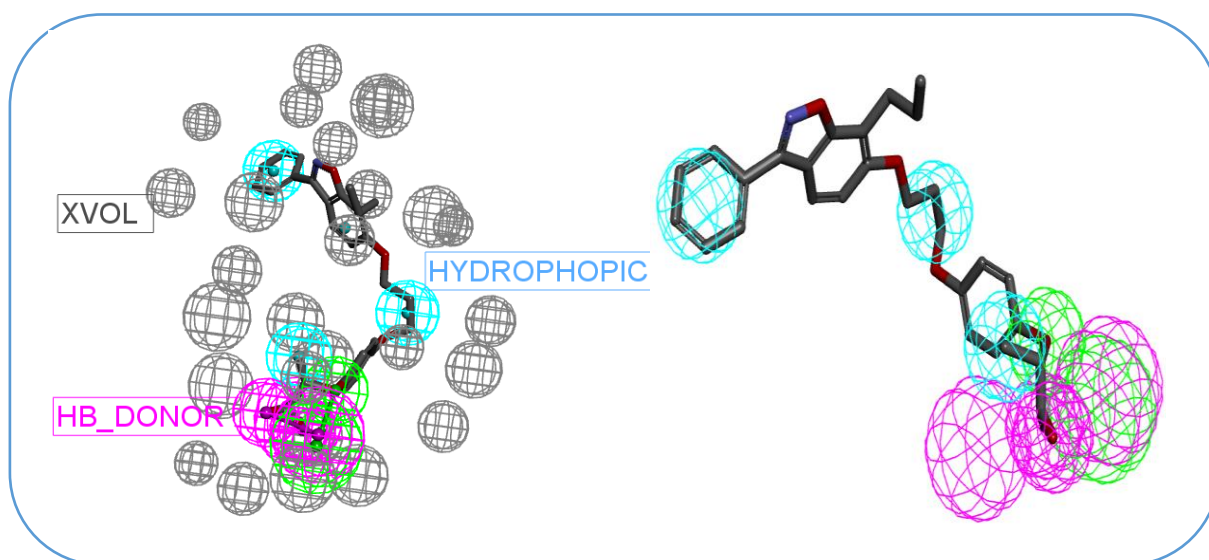
1. Hydrogen bond acceptors (HBA) colored as green.
2. Hydrogen bond donors (HBD) colored as magenta.
3. Hydrophobicity (HY) colored as cyan.
4. Negative ionization (NI) colored as red.

5. Positive charge (PI) colored as blue.

6. Cyclic aromatic (RA) colored as orange, brown.

To construct the CBP (complex based pharmacophore) pattern, the parameters were set by the default value. The generated-hypothesis mimics a binding-site between the receptor and the ligand; however, it will be used later for virtual screening to find similar but better ligands than the existing ones. The 1I7G and 2PRG PDB complexes were showed pharmacophore models with either ≥ 6 features numbers that were found between the receptor-ligand interacting point, AAHRR or different-sets of features as illustrating it in Table 3.1. In each of these models, and the selectivity scores to the receptors were found more than (6,6413) which was shown in the protocol report. The validation of the pharmacophore was taken into consideration while choosing the best model between these three generated models, as shown in Table 3.1 are presented the pharmacophores, of the PPAR (α/γ) CHEMBL24458, CHEMBL427299, CHEMBL326015 complexes. The best pharmacophore-model was selected according to control ligands (AZ242, BRL) as shown in Figure 3.2,3,4,5, which can observe the interaction between the ligand and the receptor. According to a recent study, that assesses the pharmacophore feature flexibility while using the molecular dynamics simulation, the hydrophobic feature is the most stabilized interaction out of the other features (Wieder, Perricone, Boresch, Seidel, & Langer, 2016).

(A)



(B)

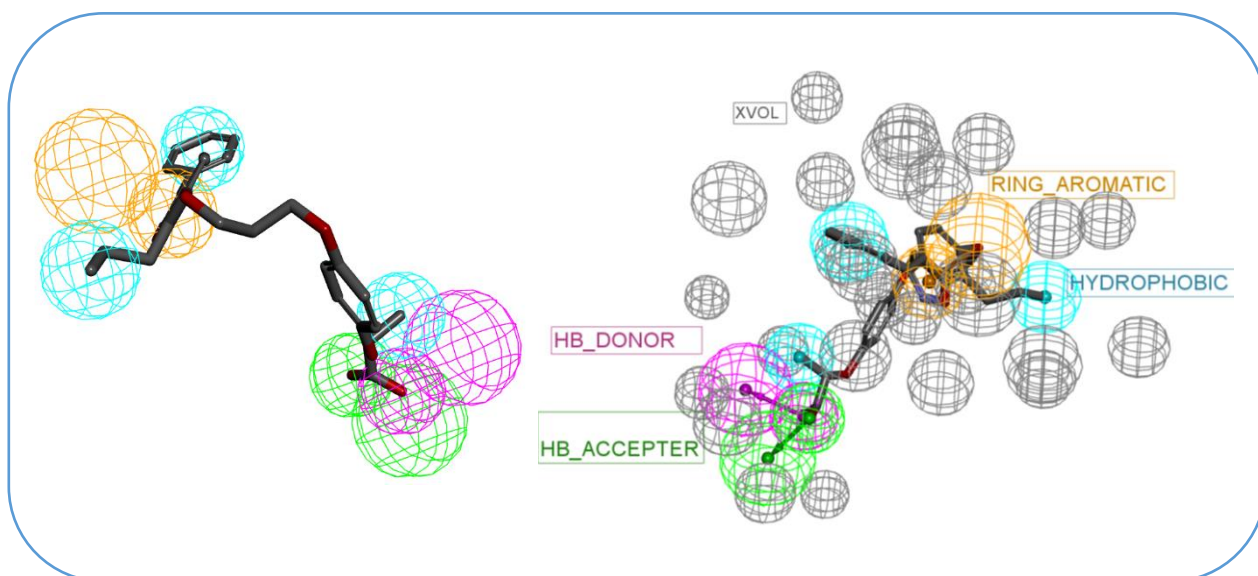
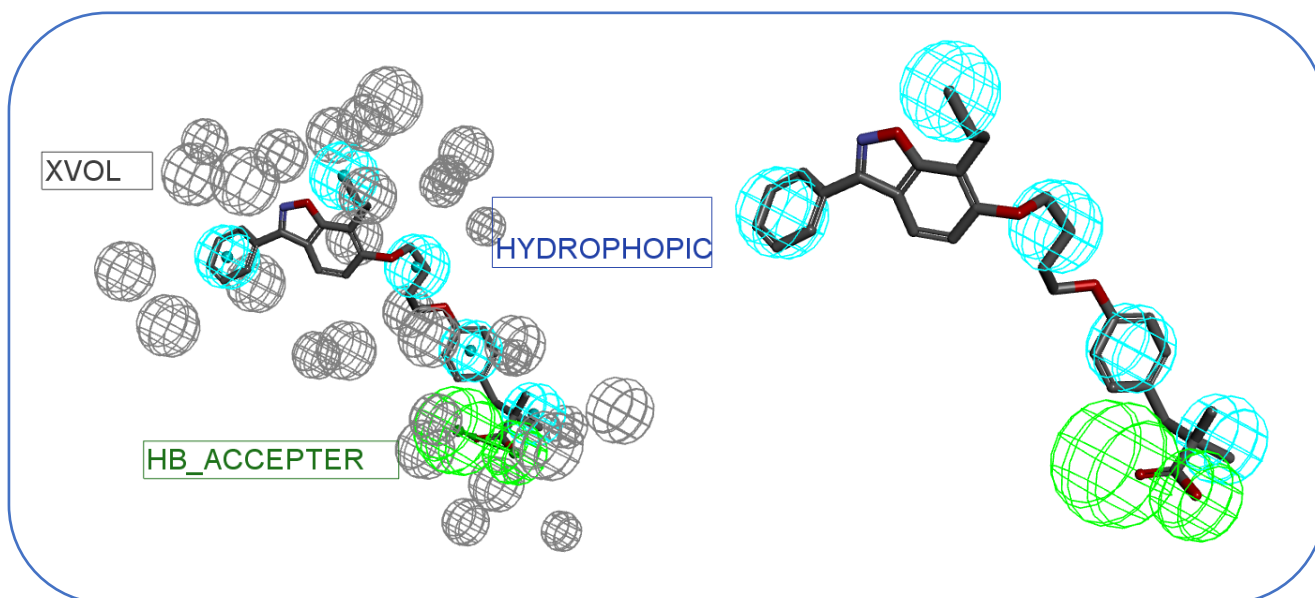


Figure 3. 4 Overlay of training set compounds upon the pharmacophores. A) 3D (CHEMBL427299). Best pharmacophore model of PPAR α complex. B) 3D (CHEMBL427299). Best pharmacophore model due the selectivity score of PPAR γ complex.

(A)



(B)

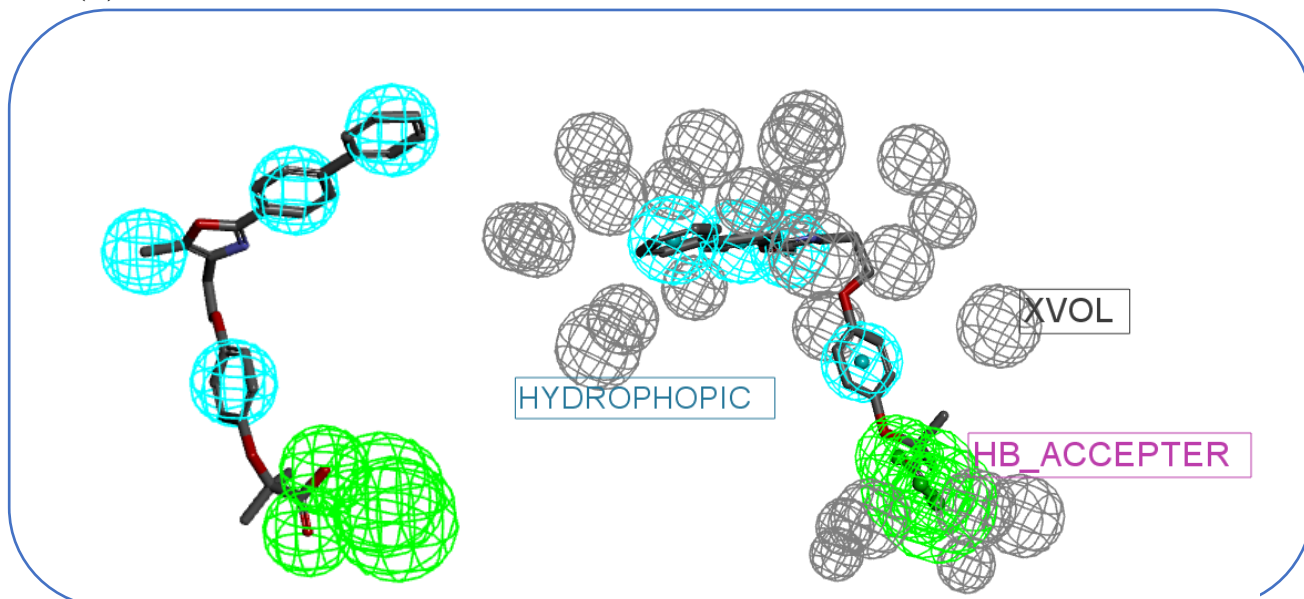
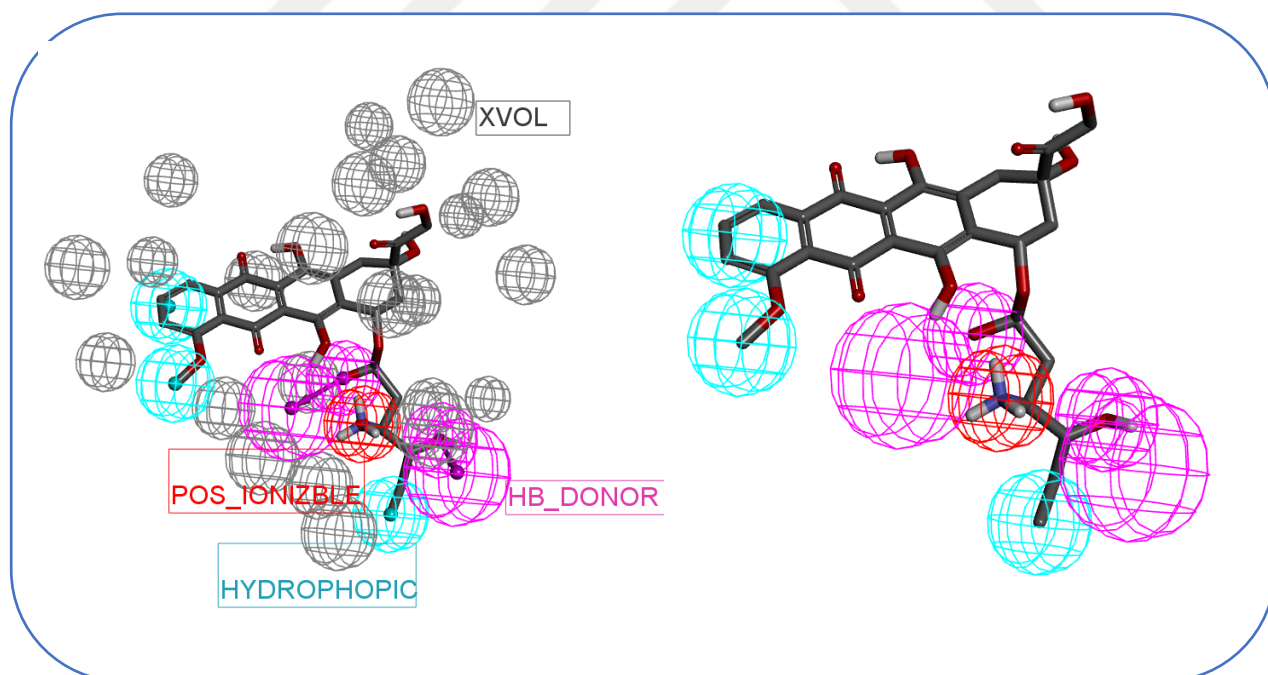


Figure 3. 5 Overlay of training set compounds upon the pharmacophores. A) 3D (CHEMBL24458). Best pharmacophore model of PPAR α complex. B) 3D CHEMBL24458 Best pharmacophore model due the selectivity score of PPAR γ complex

(A)



(B)

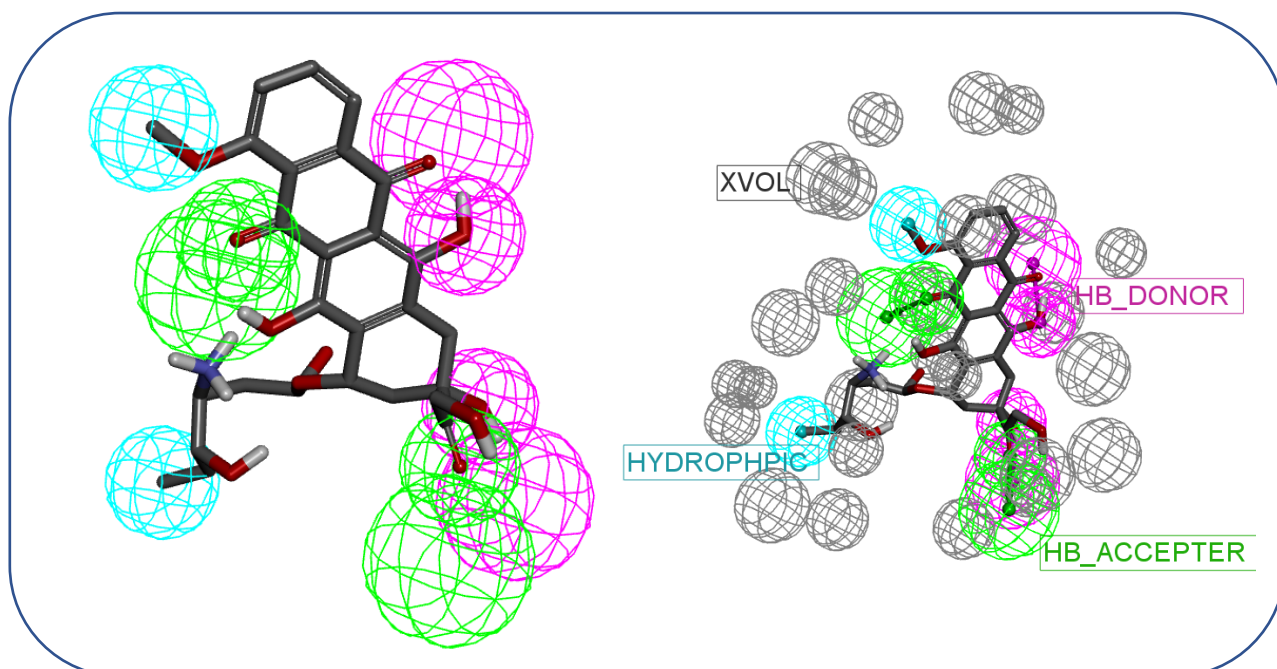
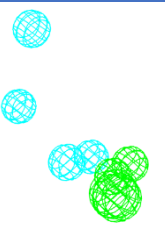
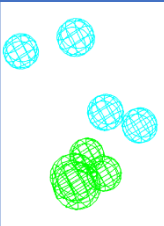
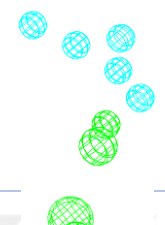

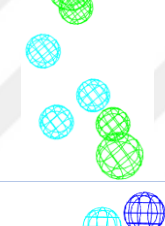
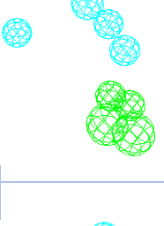
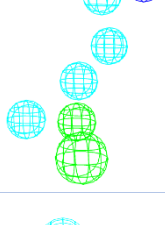
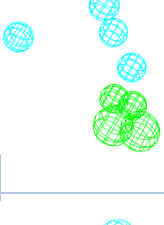
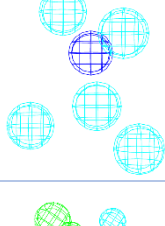
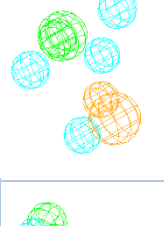
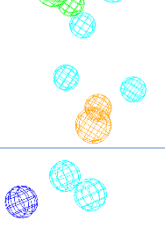
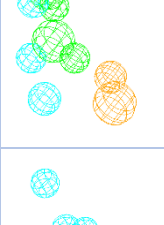

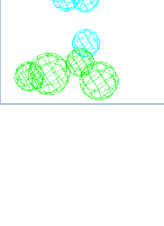


Figure 3. 6 Overlay of training set compounds upon the pharmacophores. A) 3D (CHEMBL326015). Best pharmacophore model of PPAR α complex. B) 3D CHEMBL326015 Best pharmacophore model due the selectivity score of PPAR γ complex.

No.	Hypothesis	No# Of_ PH	No #of _F	Set of_ F	Ss	Figure	No# Of_ PH	No #of _F	Set of_ F	Ss	Finger
		1i7g	1i7g	1i7g	1i7g	1i7g	2prg	2prg	2prg	2prg	2prg
1.	CHEMBL5 65198	01	6	AAH HHH	9.8 767		01	6	AA HH HH	9.94 53	
2.	CHEMBL4 35523	01	6	AHH HHH	9.8 081		01	6	AA HH HH	9.94 53	
3.	CHEMBL1 72490	01	5	AAH HH	7.9 504		01	6	AA HH HH	9.73 95	
4.	CHEMBL3 67311	01	6	AHH HHN	11. 405		01	6	AA HH HH	9.73 95	
5.	CHEMBL5 3463	01	6	HHH HHN	10. 925		01	6	AH HH HR	9.53 37	
6.	CHEMBL2 53417	01	6	AHH HHR	9.8 767		01	6	AA HH HR	9.67 09	
7.	CHEMBL1 73409	01	6	AHH HHN	11. 611		01	6	AA HH HH	9.60 23	

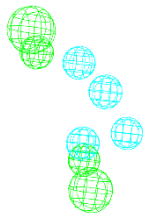
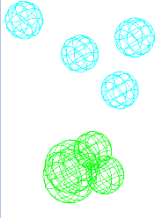
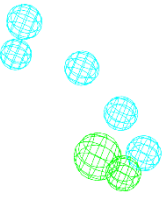
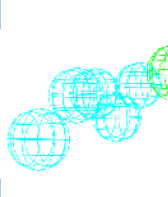

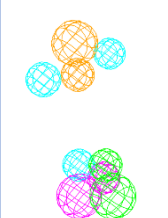
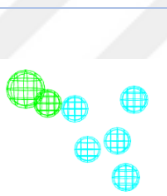
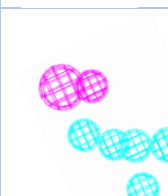
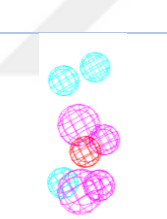
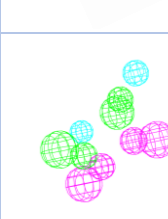
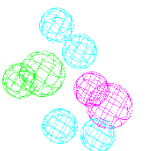
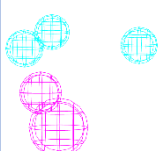
8.	CHEMBL1 73285	01	6	AAH HHH	9.6 023		01	6	AA HH HH	9.60 23	
9.	CHEMBL2 4458	01	6	AHH HHH	10. 082		01	6	AH HH HH	9.87 67	
10.	CHEMBL4 27299	01	6	ADD HHH	12. 115		01	6	AD HH HR	11.0 65	
11.	CHEMBL9 4306	01	6	AHH HHH	9.3 966		01	6	DH HH HH	10.5 16	
12.	CHEMBL3 26015	01	6	DDH HHP	12. 823		01	6	AA DD HH	11.7 72	
13.	CHEMBL1 73159	01	6	ADH HHH	10. 173		01	4	DH HH	6.93 75	

Table 3. 1 PPAR (α/γ) The validation outcomes of the 13 pharmacophore models on the activity of active compounds by using "Receptor-Ligand Pharmacophore" protocol. From the highlighted three of these ligands' hypothesis represent the pharmacophores that which highlighted red color has the best Selectivity score will selected for the screening. From Figures, observing, functional features are represented by distinct color codes: hydrogen bond acceptor (green), hydrogen bond donor (magenta), hydrophobic group (cyan), aromatic ring (orange), and positive charge group (red) , the(blue) is the negative charge group . The Hypothesis that was generated using the data set obtained from the literature.

Note: No # of pharmacophore (No#Of_PH), No #of Feature (No #of_F), Set-of Feature (Set of_F), Selectivity score (Ss).

3.4 Ligand-Based Approach

3.4.1 Protein Preparation

The crystal structure of the two proteins of human PPAR α (PDB ID 1I7G) was obtained from RCSB Protein Information Bank (Protein Data Bank, 2019; Rose et al., 2013), as well as PPAR γ (PDB ID 2PRG), (Cronet et al., 2001). We have chosen from the literature PPAR α (PDB ID 1I7G) with a resolution of 2.2 °A, PPAR γ (PDB ID 2PRG) with a resolution of 2.3 °A. Though PPAR γ and PPAR α residues as mentioned early in figure 3.3. These residues interact with thiazolidinedione and fibrates which includes rosiglitazone, it drastically maintains the AF 2 helix inside the energetic conformation, consequently selling the binding of coactivator proteins. But there is a lot of the reverse outcomes along with Weight gain and pulmonary edema related to an increased risk of congestive failure. The proteins mentioned earlier downloaded from the Protein data bank in PDB format. They prepared for the next step by removing all water molecules from Each structure using the Biovia Discovery Studio 2016.

3.4.2 Known Inhibitor, Molecular Docking Validation

The determination of the quality of the PDB structure was chosen conducted by selecting a known inhibitor of this enzyme. These inhibitors were obtained from the literature resembling the well-known inhibitor of this enzyme. The Auto dock automated docking tools (ADT) is a visualized tool and a generator of the docking files according to the ligand-receptor binding. It was employed to obtain the docking files that includes a grid parameter file (GPF) containing a map that stores all the potential energy of each atom in a ligand and a receptor that is used in the calculation in further steps. The second docking file is the docking parameter file (DPF) which has the receptor and the ligand names in PDBQT format, docking and search parameters (Esiyok, Çakar, & Kurtulmuşoğlu, 2017; Karpuz, Kockar, & Esiyok, 2014). In Table 3.2 the ligands were docked into the binding site of the receptor to assure its accuracy. As have mentioned before, the parameter was used for the (GPF) for each and every ligand 60, 60, 60 and the coordinates were PPAR (α/γ) using the following grid box dimension: 60, 60, 60 Å; and grid box center: α (X = 37.354), (Y = 34.871), (Z = 39.222), γ (Y = 49.720800), (Y = 36.982840), (Z = 19.294840) Å, respectively. Lastly, the Lamarckian Genetic algorithm was

chosen and all the parameters were kept as default except the number of energy evaluation, that was needed for the docking, it was set for twenty five million, and the number of the GA runs was set to twenty to observe different conformations.

<i>Is</i>	<i>EXP</i> <i>Ki/IC₅₀</i>	<i>PPAR alpha</i> <i>(1I7G)</i>		<i>PPARgamma</i> <i>(2PRG)</i>		<i>S ID</i>	<i>R</i>
		<i>Ki</i> <i>nM</i>	<i>ΔG</i> <i>kcal/mol</i>	<i>Ki</i> <i>nM</i>	<i>ΔG</i> <i>kcal/mol</i>		
1) <i>CHEMBL3</i> <i>827820</i>	<i>IC₅₀</i> <i>>15000</i>	<i>132.65</i>	<i>-9.38</i>	<i>527.26</i>	<i>-8.56</i>	<i>BDBM50</i> <i>189566</i>	<i>ACS Med</i> <i>Chem</i> <i>Lett 7: 590-</i> <i>4 (2016)</i>
2) <i>CHEMBL1</i> <i>785028</i>	<i>12</i>	<i>30.58</i>	<i>-10.25</i>	<i>43.02</i>	<i>-10.05</i>	<i>BDBM50</i> <i>418557</i>	<i>J Med</i> <i>Chem 41: 5</i> <i>020-</i> <i>36 (1999)</i>
3) <i>CHEMBL4</i> <i>91751</i>	<i>IC₅₀</i> <i>85</i>	<i>497.79</i> <i>pM</i> <i>(picomolar)</i>	<i>-12.69</i>	<i>2.17</i>	<i>-11.82</i>	<i>BDBM50</i> <i>248410</i>	<i>Bioorg</i> <i>Med Chem</i> <i>Lett19:145</i> <i>1-6 (2009)</i>
4) <i>CHEMBL4</i> <i>35704</i>	<i>7.3</i>	<i>4.28</i>	<i>-11.42</i>	<i>34.46</i>	<i>-10.18</i>	<i>BDBM50</i> <i>124377</i>	<i>Bioorg</i> <i>Med Chem</i> <i>Lett 13: 93</i> <i>1-5 (2003)</i>
5) <i>CHEMBL4</i> <i>35523</i>	<i>7.2</i>	<i>4.88</i>	<i>-11.34</i>	<i>128.16</i>	<i>-9.40</i>	<i>BDBM33</i> <i>283</i>	<i>Bioorg</i> <i>Med Chem</i> <i>Lett 13: 93</i> <i>1-5 (2003)</i>
6) <i>CHEMBL4</i> <i>27299</i>	<i>11</i>	<i>67.54</i> <i>nM</i>	<i>-9.78</i>	<i>91.10</i>	<i>-9.60</i>	<i>BDBM50</i> <i>124383</i>	<i>Bioorg</i> <i>Med Chem</i> <i>Lett 13: 93</i> <i>1-5 (2003)</i>
7) <i>CHEMBL4</i> <i>26878</i>	<i>15</i>	<i>211.94</i>	<i>-9.10</i>	<i>565.76</i>	<i>-8.52</i>	<i>BDBM50</i> <i>194968</i>	<i>Bioorg</i> <i>Med Chem</i> <i>Lett 16: 61</i> <i>20-3 (2006)</i>
8) <i>CHEMBL4</i> <i>26550</i>	<i>7</i>	<i>118.18</i>	<i>-9.45</i>	<i>446.11</i>	<i>-8.66</i>	<i>BDBM50</i> <i>194957</i>	<i>Bioorg</i> <i>Med Chem</i> <i>Lett 16: 61</i> <i>20-3 (2006)</i>

9) CHEMBL4 25639	11	152.33	-9.30	304.56	-8.89	BDBM50 194955	Bioorg Med Chem Lett 16: 61 20-3 (2006)
10) CHEMBL3 75370	300	122.72	-9.43	559.27	-8.53	BDBM50 195080	Bioorg Med Chem Lett 16: 61 16-9 (2006)
11) CHEMBL3 74448	16	129.69	-9.40	985.85	-8.19	BDBM50 194961	Bioorg Med Chem Lett 16: 61 20-3 (2006)
12) CHEMBL3 69053	100	15.81	-10.64	117.55	-9.45	BDBM50 124385	Bioorg Med Chem Lett 13: 93 1-5 (2003)
13) CHEMBL3 68371	23	5.73	-11.24	20.18	-10.50	BDBM50 124375	Bioorg Med Chem Lett 13: 93 1-5 (2003)
14) CHEMBL3 67311	93	18.11	-10.56	81.55	-9.67	BDBM50 124386	Bioorg Med Chem Lett 13: 93 1-5 (2003)
15) CHEMBL3 67019	14	1.87	-11.91	33.79	-10.19	BDBM50 124369	Bioorg Med Chem Lett 13: 93 1-5 (2003)
16) CHEMBL3 46219	1.22E+ 8	19.53	-10.52	106.51	-9.51	BDBM50 418571	Eur J Med Chem 43: 7 3-80 (2008)
17) CHEMBL3 26015	618	146.67	-9.32	510.74	-8.60	BDBM50 132570	Bioorg Med Chem Lett 13: 31 85- 90 (2003)
18) CHEMBL2 21525	15	135.49	-9.37	1.20 uM (micro molar)	-8.08	BDBM50 194971	Bioorg Med Chem Lett 16: 61 20-3 (2006)

19) CHEMBL2 21123	15	225.64	-9.07	241.18	-9.03	BDBM50 194971	Bioorg Med Chem Lett 16: 61 20-3 (2006)
20) CHEMBL1 98529	IC ₅₀ 120	6.02	-11.21	18.39	-10.55	BDBM50 194971	Bioorg Med Chem Lett 16: 61 20-3 (2006)
21) CHEMBL1 73494	213	51.11	-9.95	118.74	-9.45	BDBM50 124384	Bioorg Med Chem Lett 13: 93 1-5 (2003)
22) CHEMBL1 73409	133	6.11	-11.21	92.34	-9.60	BDBM50 124370	Bioorg Med Chem Lett 13: 93 1-5 (2003)
23) CHEMBL1 73285	54	61.85	-9.83	107.11	-9.51	BDBM50 124379	J. Med. Chem. (2008) 51:2689- 2700
24) CHEMBL1 72931	121	17.95	-10.57	95.88	-9.57	BDBM50 124374	Bioorg Med Chem Lett 13: 93 1-5 (2003)
25) CHEMBL1 72490	255	59.70	-9.86	53.36	-9.92	BDBM50 124378	J. Med. Chem. (2008) 51:2689- 2700
26) CHEMBL1 04850	560	99.71	-9.55	350.25	-8.81	BDBM34 017	Bioorg Med Chem Lett 11: 31 11-3 (2001)
27) CHEMBL9 4306	60	23.28	-10.41	53.44	-9.92	BDBM50 131503	J Med Chem 47: 4 118- 27 (2004)

28) CHEMBL8 2602	4	77.98	-9.70	188.99	-9.17	BDBM50 145710	<i>J Med Chem</i> 47: 4 118- 27 (2004)
29) CHEMBL6 5805	0.400	149.88	-9.31	498.37	-8.60	BDBM50 287729	<i>Bioorg Med Chem Lett</i> 6: 212 1- 2126 (1996)
30) CHEMBL2 5259	170	22.14	-10.44	24.98	-10.37	BDBM50 100442	<i>J Med Chem</i> 47: 4 118- 27 (2004)
31) CHEMBL2 4458	330	99.97	-9.55	1.07 uM (micro molar)	-8.14	BDBM50 075315	<i>Bioorg Med Chem Lett</i> 22: 70 75-9 (2012)
32) CHEMBL3 978392	IC ₅₀ 4000	8.63	-11.00	33.56	-10.20	BDBM50 211660	<i>Bioorg Med Chem</i> (2017) 25:4723- 4744
33) CHEMBL9 4306	60	23.28	-10.41	53.44	-9.92	BDBM50 131503	<i>J Med Chem</i> 47: 41 18- 27 (2004)
34) CHEMBL5 3463	3.45E+ 3	251.50	-9.00	3.24 uM (micro molar)	-7.49	BDBM22 984	<i>Bioorg Med Chem Lett</i> 26: 535 0- 5353 (2016)
35) CHEMBL1 73159	20	6.29	-11.19	31.13	-10.24	BDBM50 124389	<i>J Med Chem</i> 47: 4 118- 27 (2004)
36) CHEMBL2 53417	89	12.01	-10.81	23.55	-10.41	BDBM50 234372	<i>Bioorg Med Chem Lett</i> 18: 16 17- 22 (2008)
37) CHEMBL5 65198	18	15.84	-10.64	41.92	-10.06	BDBM50 294690	<i>Bioorg Med Chem Lett</i> 19: 26 83-7 (2009)

38) <i>CHEMBL3</i> 781727	<i>IC₅₀</i> 4500	356.64 <i>pM</i> (picomolar)	-12.89	2.99	-11.63	<i>BDBM50</i> 155328	<i>Eur J Med Chem</i> 114: 191-200 (2016)
39) <i>CHEMBL3</i> 695843	<i>IC₅₀</i> 20	524.10 <i>pM</i> (picomolar)	-12.66 <i>kcal/mol</i>	11.40	-10.84	<i>BDBM25</i> 3949	<i>US Patent</i> US9 464092 (2016)
40) <i>CHEMBL5</i> 56643	18.4	8.76	-10.99	6.07	-11.21	<i>BDBM50</i> 294688	<i>Bioorg Med Chem Lett</i> 19: 26 83-7 (2009)
41) <i>CHEMBL5</i> 54562	33	33.26	-10.20	89.34	-9.62	<i>BDBM50</i> 294692	<i>Bioorg Med Chem Lett</i> 19: 26 83-7 (2009)
42) <i>CHEMBL2</i> 63029	2.4	10.03	-10.91	53.59	-9.92	<i>BDBM50</i> 124394	<i>Bioorg Med Chem Lett</i> 13: 93 1-5 (2003)

Table 3. 2 The known ligand used for validation of both PPAR(α/γ) receptors. ΔG (Estimated Free Energy of Binding), K_i (Estimated Inhibition Constant), IC_{50} (is the concentration of an inhibitor where the response (or binding) is half due there, reduced, Experimental (EXP), Structure ID (S ID), Reference (R), Inhibitors (Is).

3.4.3 Data sets

The data set was obtained from literature containing the known inhibitor for individual PPAR α crystal structures (PDB ID 1I7G) as well as PPAR γ (PDB ID 2PRG) 2PRG's main ligand (co-crystallization ligand) is the antidiabetic medication Rosiglitazone (BRL). The main focus was to obtain a different compound that has a diversity structure, an active compound which able to inhibit the PPARs (α/γ) and functioned as an anti-diabetic agent. Also, the binding interaction of these well-known inhibitors with receptors was taken into the account. All the inhibitors have IC_{50} and K_i and were synthesized and tested experimentally; some of them are in verity stages of the FDA clinical trial.

3.4.4 Pharmacophore Generation

The pharmacophore was generated using both the "Common Features Pharmacophores Toolkit" and "Receptor Ligand Pharmacophore Generation Toolkit" in Bio via Discovery Studio 2016, where the conformation generation was set to best. The Maximum number of conformation generated was 255 along with the energy threshold of 20 kcal/mol at the global minimum. "Best" and "Flexible" method was used for the confirmation generation and fitting. The docked pose (DockRMSD) of the compound 0.5A obtained from the literature was used as a reference. The principal was set to 2 and Max Omit Feat value was chosen as 0, and as for the remaining ligands, the first one was set to 1 and the second to 2 respectively (Wieder et al., 2016). Figure 3.6 shows the alignment of the compound used. After aligning the known inhibitors figure 3.7 that were obtained from the literature Table 3.3, 13 pharmacophore hypotheses Table 3.1 were generated using the protocol mentioned earlier. These hypotheses were assessed, along with the hypothesis from the Structure-Based approach, one by one using the Günner Henry method which will be mentioned later in this chapter. Figure 3.7 The compound that forms the ligand-based approach.

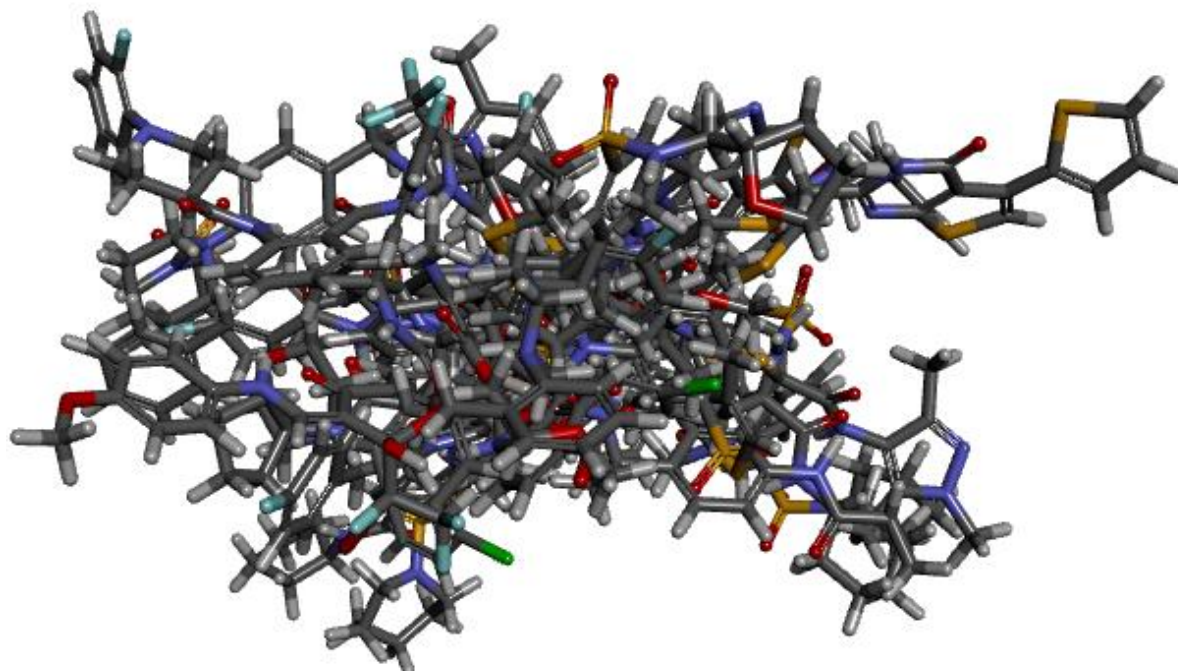
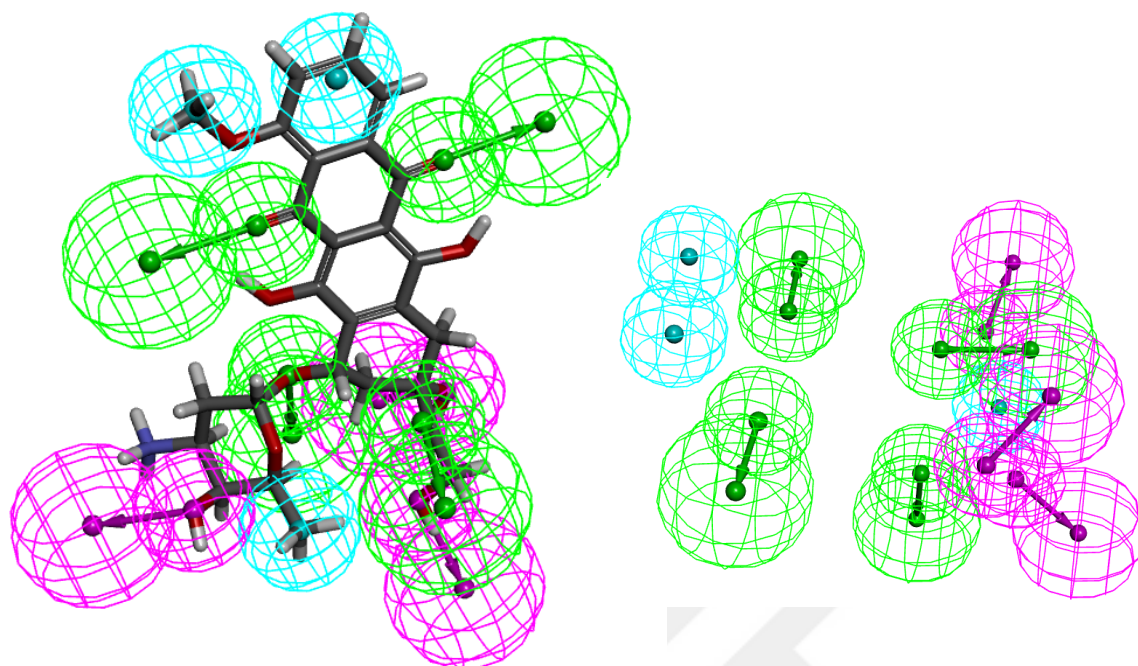
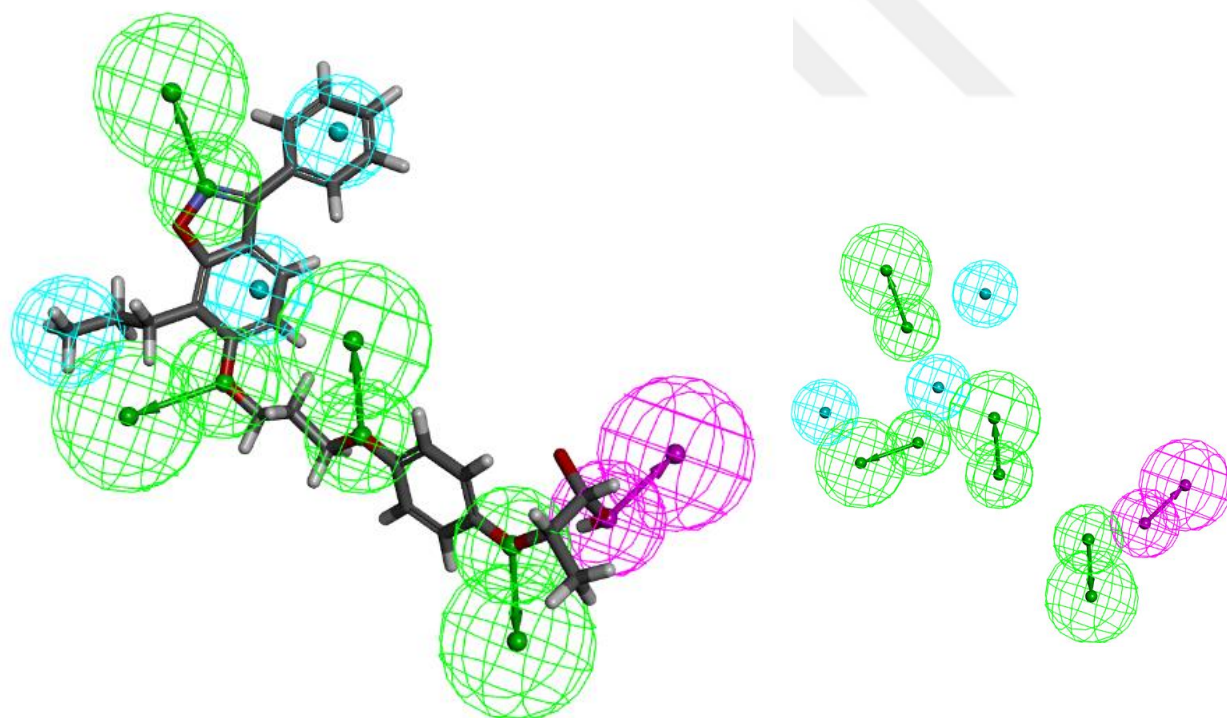


Figure 3. 7 The compound that form the ligand-based approach

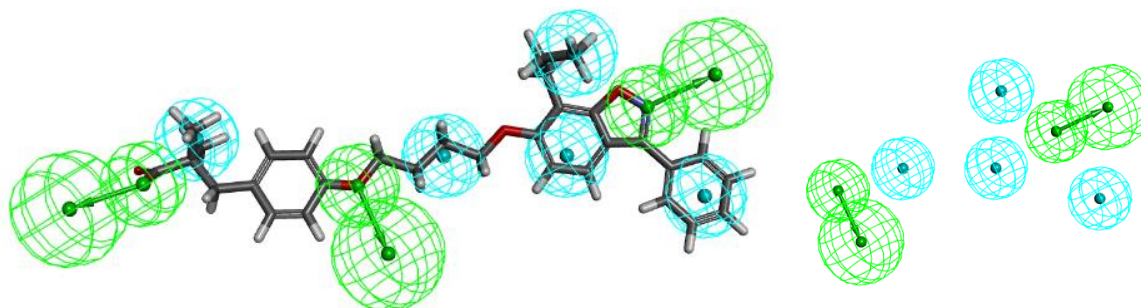
(A)



(B)



(C)



(D)

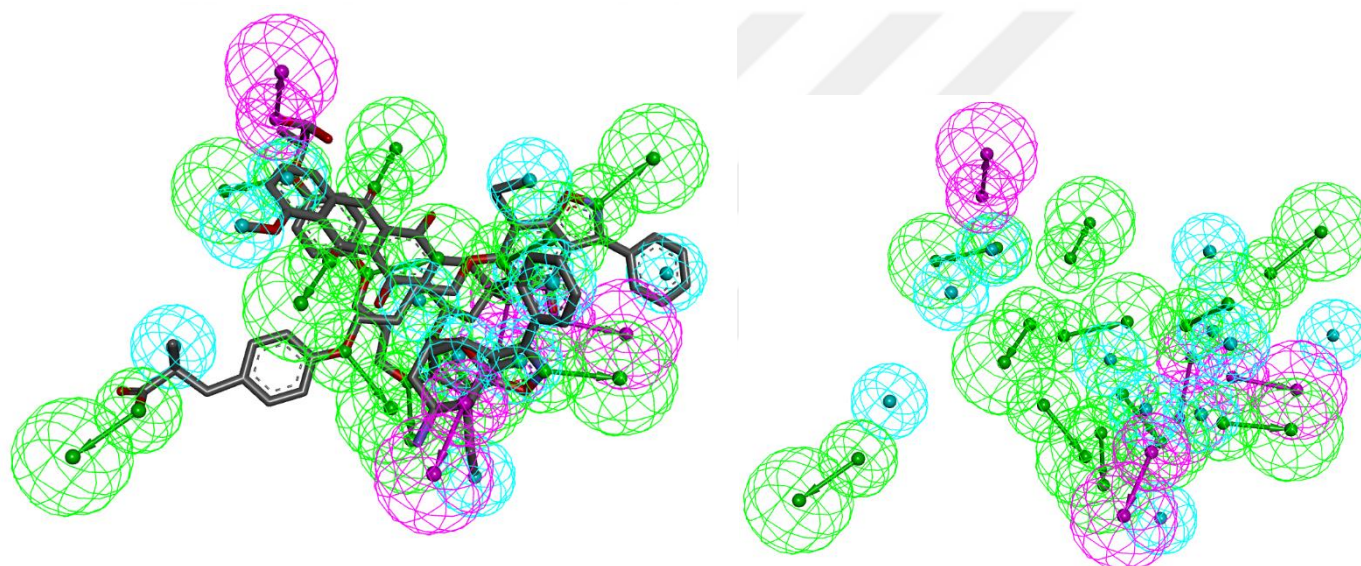


Figure 3. 8 The Hypothesis that was generated using the data set obtained from the literature. (A) The Inhibitor CHEMBL326015, from the data-set hypothesis where the green represents hydrogen bond acceptor, the blue is the Hydrophobic feature and the purple hydrogen bond donor. (B) The Inhibitor CHEMBL427299, from the data-set hypothesis where the green represents hydrogen bond acceptor, the blue is the Hydrophobic feature and the purple hydrogen bond donor. (C) The Inhibitor CHEMBL24458, from the data-set hypothesis where the green represents hydrogen bond acceptor, the blue is the Hydrophobic feature. (D) The three compounds CHEMBL326015 CHEMBL24458, CHEMBL427299 from the data set aligning together and Mapping the pharmacophore hypothesis where the green represents hydrogen bond acceptor and the blue is the hydrophobic feature and the purple hydrogen bond donor.

3.5 Pharmacophore validation

For the validation of the pharmacophore hypotheses that were generated using Biovia Discovery Studio 4.5, an active set was prepared to contain 13 active molecules got from BindingDP (BindingDB2015), and the native PDB ligand, which has K_i and IC_{50} (Table 3.2 and 3.1). The inactive set was prepared using DUD.E (MysingerMM2012), and a program called Decoy-Finder 2.0; the set was taken from the Zinc database which generates molecules inactive to the receptor that is used for pharmacophore generation (Table 3.4 5 6) illustration the mean of CBP approaches (Adrià, Garcia Vallvé, & Pujadas, 2012). The generated pharmacophore was tested using the equation provided by Günner Henry method:

% A: The number of all the active compound in the database (accuracy).

H_a : The reiterative active hit (true positives).

A: The active molecule in the database.

% Y: The percentage of the active molecule extracted from the decoy set.

H_t : The number of hits in the database.

D: The number of the compound in the database.

E: The Enrichment Factor.

GH: The Goodness of the Hit.

$$Y\% = \frac{H_a}{H_t} \times 100\%$$

$$\% A = \frac{H_a}{A} \times 100\%$$

$$E = \frac{H_a \times D}{H_t \times A}$$

$$GH = \frac{H_a(3A + H_t)}{4H_t A} \left(1 - \frac{H_t - H_a}{D - A} \right)$$

Hypothesis	D	A	H _t	H _a	%A	Y%	E	GH
1. CHEMBL565198	41	13	--	---	-----	-----	-----	-----
2. CHEMBL435523	41	13	7	7	53.8461538462	100	3.15384615385	0.88461538461
3. CHEMBL427299	41	13	8	8	61.5384615385	100	3.15384615385	0.90384615384
4. CHEMBL367311	41	13	---	---	-----	---	-----	-----
5. CHEMBL326015	41	13	10	9	69.2307692308	90	2.83846153846	0.81778846153
6. CHEMBL253417	41	13	---	---	---	---	---	-----
7. CHEMBL173409	41	13	7	7	53.8461538462	100	3.15384615385	0.88461538461
8. CHEMBL173285	41	13	8	8	61.5384615385	100	3.15384615385	0.90384615384
9. CHEMBL173159	41	13	2	2	15.3846153846	100	3.15384615385	0.78846153846
10. CHEMBL172490	41	13	1	1	7.69230769231	100	3.15384615385	0.76923076923
11. CHEMBL94306	41	13	---	---	-----	---	-----	-----
12. CHEMBL53463	41	13	1	1	7.69230769231	100	3.15384615385	0.76923076923
13. CHEMBL24458	41	13	8	7	53.8461538462	87.5	2.75961538462	0.7626201923

Table 3. 3 This is when decoy 41 of best 13 and obtained hypothesis. The pharmacophore validation result for both Ligand-Based approaches, and Structure-Based approaches.

Hypothesis	Features	Rank	Direct Hit	Partial Hit	Max Fit
01	HHAAA	178.305	1111111111111111	00000000000000	5
02	HAAA	152.317	1111111111111111	00000000000000	4
03	HAAA	151.730	1111111111111111	00000000000000	4
04	HHAA	149.563	1111111111111111	00000000000000	4
05	HHAA	148.883	1111111111111111	00000000000000	4
06	HAAA	148.486	1111111111111111	00000000000000	4
07	HAAA	148.306	1111111111111111	00000000000000	4
08	HHAA	147.835	1111111111111111	00000000000000	4
09	HHAA	147.660	1111111111111111	00000000000000	4
10	HHAA	147.209	1111111111111111	00000000000000	4

Table 3. 4 HIP-HOP table decoy42 with best13 and obtain 55(active and inactive) The pharmacophore validation result Ligand-Based Approaches. In this Table, respectively. Direct hit means whether “1” or not “0” a molecule in the training set map every pharmacophore feature in the hypothesis means no missing features. Partial hit indicates whether “1” or not “0” this molecule a particular one in the training set been-mapped all but one pharmacophore feature in the hypothesis, which indicates no missing features. The max fit of these ten pharmacophore hypotheses models is 4, Rank scores the range of the ten models from 147.209 kcal·mol⁻¹ to 178.305 kcal·mol⁻¹.

Hypothesis	D	A	H _t	H _a	Y%	A%	E	GH	SE	SP
01	55	13	15	13	86.6666666667	100	619.66	0.85714285714	0	2
02	55	13	18	13	72.2222222222	100	990	0.69742063492	0	5
03	55	13	17	13	76.4705882353	100	935	0.74509803921	0	4
04	--	--	--	--	--	-----	-----	--	-----	-----
05	55	13	16	13	81.25	100	880	0.64836774553	0	3
06	55	13	17	13	76.4705882353	100	935	0.74509803921	0	4
07	55	13	20	13	65	100	1100	0.61458333333	0	17
08	55	13	18	13	72.2222222222	100	990	0.69742063492	0	5
09	55	13	16	13	81.25	100	880	0.64836774553	0	3
10	55	13	17	13	76.4705882353	100	935	0.74509803921	0	4

Table 3. 5 Statistical parameters for generating pharmacophore models are listed as top ten pharmacophore hypotheses generated by implementation protocol for the pharmacophore validation result Ligand-Based Approaches.

The sensitivity and specificity reveal the ability of those patterns to if wherever active and inactive molecules. These ten generate hypotheses are assesses by rank scores and fit values and also to indicate the properties of each pharmacophore which is the result of decoy42 with best13 and obtain 55(active and inactive). SE(sensitivity) = False negatives (A – H_a), SP (specificity) = False positives (H_t – H_a). Competence of the model between (active and inactive) compounds was more powerful consistent with the higher results 0-1-2 ,Moderated score 3-4-5,Lower score higher than 5. (SP and SE).

However, rank scores and fit values alone cannot easily determine any of the best or best hypotheses, you can get the scores and keep the appropriate values. Therefore, the Güner-Henry (GH) scoring method was used to determine the best pharmacological model. A data collection database used to identify and validate the pharmacophore model (Li, Wang, Wang, Wang, & Cheng, 2015).

		PPAR gamma Receptors (2PRG)								PPAR alpha Receptors (1i7g)							
Hypothesis		D	A	H _t	H _a	%A	%Y	E	GH	D	A	H _t	H _a	%A	%Y	E	GH
1.	CHEM BL5651 98	39	13	12	9	69.2 3076 9230 8	75	2.2 5	0.650702 66272	39	13	2	2	15.38 4615 3846	100	3	0.78846153 846
2.	CHEM BL4355 23	39	13	4	4	30.7 6923 0769 2	100	3	0.826923 07692	39	13	10	7	53.84 6153 8462	70	2.1	0.58350591 716
3.	CHEM BL4272 99	39	13	10	9	69.2 3076 9230 8	90	2.7	0.815458 57988	39	13	17	11	84.61 5384 6154	64.7 058 823 529	1.94 117 647 059	0.53602506 091
4.	CHEM BL3673 11	39	13	11	9	69.2 3076 9230 8	64.7 058 823 529	2.4 54 54 54 55	0.726196 88004	39	13	7	7	53.84 6153 8462	100	3	0.88461538 461
5.	CHEM BL3260 15	39	13	11	8	61.5 3846 1538 5	72.7 272 727 273	2.1 81 81 81 82	0.618612 15707	39	13	7	5	38.46 1538 4615	71.4 285 714 286	2.14 285 714 286	0.58326289 095
6.	CHEM BL2534 17	39	13	6	6	46.1 5384 6153 8	100	3	0.865384 61538	39	13	2	2	15.38 4615 3846	100	3	0.78846153 846
7.	CHEM BL1734 09	39	13	10	8	61.5 3846 1538 5	80	2.4	0.695857 98816	39	13	7	6	46.15 3846 1538	85.7 142 857 143	2.57 142 857 143	0.72907861 369
8.	CHEM BL1732 85	39	13	12	10	76.9 2307 6923 1	83.3 333 333 333	2.5	0.754437 86982	39	13	11	8	61.53 8461 5385	72.7 272 727 273	2.18 181 818 182	0.61861215 707

9. CHEM BL1731 59	39	13	8	8	61.5 3846 1538 5	100	3	0.903846 15384	39	13	2	2	15.38 4615 3846	100	3	0.78846153 846
10. CHEM BL1724 90	39	13	--	-	--	-	-	-----	39	13	--	-	--	-	-	-----
11. CHEM BL5346 3	39	13	--	-	--	-	-	-----	39	13	--	-	--	-	-	-----
12. CHEM BL2445 8	39	13	5	2	15.3 8461 5384 6	40	1.2	0.299408 28402	39	13	5	1	7.692 3076 9231	20	0.6	0.71597633 136
13. CHEM BL9430 6	39	13	--	-	--	-	-	-----	39	13	--	-	--	-	-	-----

Table 3. 6 Positive Goodness of the Hit Results of both PPAR (α/γ) Could know the differences between each table that depend on D. The pharmacophore validation result for Structure-Based approaches.

Hypothesis	D	A	Ht	Ha	%A	%Y	E	GH
Pharm01	1033	13	794	13	100	1.637279597	1.301007557	0.061455709
Pharm 02	1033	13	819	13	100	1.587301587	1.261294261	0.054948646
Pharm 03	1033	13	826	13	100	1.573849879	1.250605327	0.053130786
Pharm 04	1033	13	856	13	100	1.518691589	1.206775701	0.045358885
Pharm 05	1033	13	849	13	100	1.531213192	1.216725559	0.04716968
Pharm 06	1033	13	857	13	100	1.516919487	1.205367561	0.045100327
Pharm 07	1033	13	878	13	100	1.176537585	1.176537585	0.039677687
Pharm 08	1033	13	878	13	100	1.480637813	1.176537585	0.039677687
Pharm 09	1033	13	867	13	100	1.499423299	1.191464821	0.042516452
Pharm 010	1033	13	789	13	100	1.64765526	1.309252218	0.062760008

Table 3. 7 Negative Goodness of the Hit Results Common Feature Pharmacophore Generation of 42 as active training set 13 as selective training set and test set decoys number are 1991.

3.6 Virtual Screening

According to the previously validated results for both approaches, the selected models were searched via a 3D query toolkit by Biovia Discovery Studio. Zinc15 with over 6 million compounds with over 400 thousand compounds were screened. The Filtration was set to best and only the compounds with Fit Value higher than 3.5 were processed to the next step. Furthermore, utilized to SPOT-ligand: Virtual Ligand-Screening based on Binding-Homology from Protein 3D Structure is also used (Yang, Zhan, & Zhou, 2016).

3.7 PyRx

PyRX is a free virtual scanning tool that uses the Autodock vina for screening several drug potentials targets. They were, then, extracted from the databases in the form of the PDB format file. For both approaches, the resulted compounds were docked in the macromolecules that were selected. In the ligand-based approach, the compounds with a fit value of more than 3.5 were all docked into the macromolecules 1I7g and 2PRG that was selected for the method. As for the structure-based approach, the compounds were docked to macromolecules. In a process called cross-docking, all compounds were screened against the two macromolecules to ensure the output compounds are highly selective. During this process, the docking tool PyRx was used to obtain high-affinity compounds. The criteria of the binding energy were set to 9.0 kcal/molar higher by which the compounds were selected. The first one thousand compounds or each one of the hypotheses proceeded through PyRx docking.

3.8 AutoDock

The filtered compounds are tested for accurate docking of PPARalpha and PPARgamma. Firstly, the clean Protein module at Discovery Studio 4.0 technologies designed the crystal complex. Second, Prepare Ligands prepared all the obtained compounds and applied CHARMM forcefield (Puratchikody, Umamaheswari, Irfan, & Sriram, 2018). Successively, the active sites are identified based on the initial PPARalpha and PPARgamma ligands. Docking process, the Autodock tools were used to obtain the binding energy and the Ki. The files were first generated using the grid parameter file (GPF) for each ligand and were set to 60, 60 and 60 in each dimension. The X, Y and Z Coordinates were set according to each macromolecule where the points in which the binding occur between macromolecule and ligand were extracted and used. The Lamarckian genetic algorithm was chosen while

generating the docking parameter file (DPF). The GA run was set to 20 and the docking simulation run was set to 10,000,000 energy evaluations (Maruthanila et al., 2018). Then Small In the binding site, molecules are docked to display Higher energy concentrations than the original PPAR ligands and docking ratings (Hasan, Mazumder, Chowdhury, Datta, & Khan, 2015). Eventually, for further study, cdocker energy, hydrogen bond, and VDW interactions are visualized and used.

3.9 Molecular-docking approach (CDOCKER)

Four compounds with higher docking scores and greater affinity than the initial ligands (AZ242 and BRL) were collected. By high-throughput fundamental scanning and detailed docking review. The first three compounds names, structures, and docking energies have been identified according to the docking scores and interaction patterns (Das et al., 2015; Wu, Robertson, Brooks, & Vieth, 2003).

3.10 ADMET-prediction

In this project, the blends are tested for ADMET prediction and toxicity expectation (TOPKAT), (Kalathiya, Padariya, & Baginski, 2016). ADMET target descriptors are chosen to include liquid solvency, blood brain barrier (BBB), cytochrome enzyme restriction rate P450 2D6, hepatotoxicity stage, human intestine-absorption (HIA), authoritative plasma protein barrier (PPB). The parameters are set in the TOPKAT is projected to include Ames Mutagenicity, Rabbit Oral LD50, Biodegradability Aerobic, and Natural Call (Male Rat) cancer-causing NTPC. We used AZ242 and BRL(Rosiglitazone) for the first ligand Positive checks. The atoms with strengthened pharmacokinetic properties and reduced toxicity were selected by applying these methods over. It was necessary to predict pharmacological and pharmacokinetic effects. Harmfulness tests include disease which induces mixtures, biodegradable oxygen, AMES mutagenicity and eye and skin disruption (Wang et al., 2014). They re-analyzed these criteria to investigate a few low lethality's and strong assimilation atoms.

3.11 Molecular dynamics simulations

Both the free PPARs and their complexes with the respective best ligand identified via virtual screening were submitted to MD simulations using NAMD software (Phillips et al., 2005).

Input files for NAMD were generated using CHARMM GUI (CHARMM36), (Lee et al., 2016). Ligand parameterization was carried out using the CHARMM General Force Field (CGenFF) server. CGenFF server was used to perform ligand atom typing and assignment of parameters and charges by analogy in a fully automated design. The systems' energy was minimized for 10000 steps by the steepest descent method (Bibi et al., 2013; Kausar et al., 2013). Following a 2 ns equilibration run at a constant number of particles, volume and temperature (NVT) ensemble, three parallel unrestrained 10 ns production MD simulations with different initial velocities were performed for each system at constant temperature and pressure (NPT) ensemble. During the production run, the time step and collection interval were set to 3 fs and 2ps respectively, however, the simulated for 30 nanoseconds and then the last frame was selected to continue the study. Structural stability of the systems was compared by analyzing the average values of radius of gyration (Rg), root means squared deviation (RMSD) and root mean squared displacement (RMSF) profiles throughout the trajectories. The findings are evaluated by analyzing the time path of the root mean square deviation (RMSD), the root mean square fluctuation (RMSF) residues, and the length of H bonds. Gyration radius (Rg) calculates the protein structure's compactness. To evaluate hydrogen bonding interactions, the effects of the MDs are evaluated and checked whether they are compatible with the docking tests. In operating the centos 7.1 Linux Operating System, the screened compounds (ZINC000002805504, ZINC000058367624) analyzed the whole molecular dynamics simulations and their stability was contrasted to the PPAR α (free without ligand in the system) and PPAR α AZ2 (free without ligand in the system) complexes PPAR α BRL. The functional The root mean square deviation (RMSD) quantitative metric was used to assess the stability of protein and protein-ligand complexes (Thangapandian, John, Lee, Kim, & Lee, 2011).

4. RESULTS AND DISCUSSION

In this chapter, the consequences of the previous chapters will be discussed. The ligand-based pharmacophore hypotheses and the structure base pharmacophore hypotheses were screened after validation. The data bases had been screened the use of the Biovia Discovery Studio. After filtration using molecular modeling software, PyRx, and Autodock4, the outcomes had been obtained. The final docking of the structure based and the ligand Based pharmacophore screening has yielded from 110 then 42 then 13 compounds, when doing basic pharmacophore validation (training set 13 and selective training set 3 which obtained after implementation common feature pharmacophore, test set (the Decoys in active compound) not always worked, due to considered 13 are training set and CHEMBL24458, CHEMBL427299, CHEMBL326015 considered as selective training set. Give a good GH as shown at chapter 3, Table 3.3,4,5 used different number of decoys all with low number due to obtained a good result which is when using high numbers of decoy not return back a good result as shown on Table 3.6 where used high number and considering the active training set 13 and selective training set 3. Ten hypotheses with GH, obtained only high GH as shown on Table 3.5. Particularly when select CHEMBL326015 with the thirteen, the result of these hypotheses their fit value 5, also, when docked the result has good binding energy with the ZINC database. As for when select either CHEMBL24458 or CHEMBL427299 with the thirteen, the result of these hypotheses their fit value 4 also, when docked the result has good binding energy with the ZINC database, but better than CHEMBL326015. The Ligand Based approaches provided 1 compound that obtained from hypothesis of GH (0.85714285714) the result of search 3D database on DS program are fit value 5 and 4 had obtained only 10 compound as output from this step which is expected as Penultimate step and discard compound with fit value 4 that have been docked to each one of the two macromolecules and the Structure Based approaches have 10 output compounds. That was twice cross docked to every one of the two macromolecules 1I7G and 2PRG to confirm the succeeded. Moreover, to make certain the efficiency of these compounds criteria of ≥ 9.0 kcal/mol, the threshold was to be used for implied, and the research continues for more validate. Furthermore, also aligned these compounds with the known inhibitor considered us promised drug (ZINC000002805504) to both PPAR(α/γ) receptors. From 4 zinc compound that aligned with

the BRL (inhibitor) inside the crystal structure (2PRG) (ZINC000010853984, ZINC000002805504, ZINC000033275541, ZINC000058367624). While all ZINC compound that aligned with the AZ242 (inhibitor) inside the crystal structure(1I7G) but the well aligned are 5 (ZINC000010853984, ZINC000002805504, ZINC000033275541, ZINC0000252503037, ZINC000058367624). According to similarity on aligned Zinc compound result of both PPAR(α/γ) receptors, are (ZINC000010853984, ZINC000002805504, ZINC000033275541, ZINC000058367624). Finally, for a review of the stability of the complexes PPAR α , PPAR α AZ242, PPAR α ZINC000002805504, PPAR α ZINC000058367624 of PPAR γ , PPAR γ BRL, PPAR γ ZINC000002805504, PPAR γ ZINC000058367624 follow in the 30 ns production MD simulation done with (RMSD), (RMSF), (Rg).

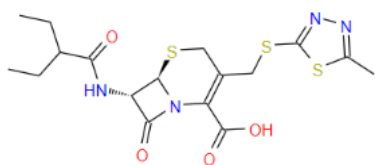


NO.	CODE	M _{WT}	LOGP
1.	ZINC000067287165	445.516	2.141
2.	ZINC000010853984	448.483	2.433
3.	ZINC000002805504	442.588	2.113
4.	ZINC000008706134	438.532	2.355
5.	ZINC000022139684	429.473	1.97
6.	ZINC000033275541	435.528	2.242
7.	ZINC000252503037	435.525	2.468
8.	ZINC000008790155	447.557	2.155
9.	ZINC000019699752	440.544	1.852
10.	ZINC000058367624	428.489	0.965

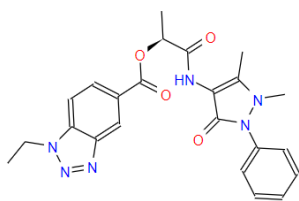
Table 4. 1 The compounds and properties obtained from structure-based approaches.

NO.	Code	Mwt	LogP	ΔG	
				Value Kcal/mol	(Ki)nM
1	ZINC000067287165	431.514	2.87	-9.63	87.20
2	ZINC000010853984	440.543	0.861	-8.93	283.91
3	ZINC000002805504	425.47	2.174	-9.98	48.23
4	ZINC000008706134	435.502	1.334	-11.48	3.83
5	ZINC000022139684	438.44	0.396	-9.50	109.64
6	ZINC000033275541	447.509	2.735	-9.73	74.18
7	ZINC000252503037	447.509	2.735	-10.11	38.80
8	ZINC000008790155	440.543	0.861	-10.99	8.80
9	ZINC000019699752	438.436	1.988	-10.20	33.37
10	ZINC000058367624	432.436	2.659	-9.49	110.28

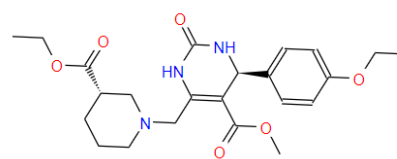
Table 4. 2 Ligand-Based approaches the resulting compounds and their properties.



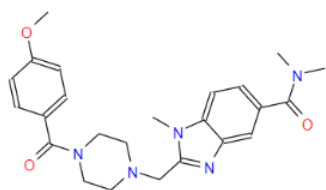
ZINC000002805504



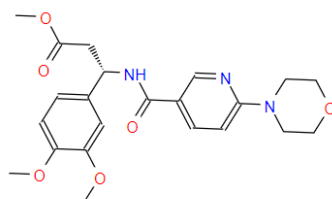
ZINC000010853984



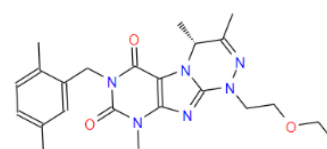
ZINC000067287165



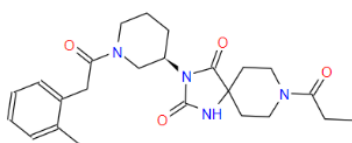
ZINC000033275541



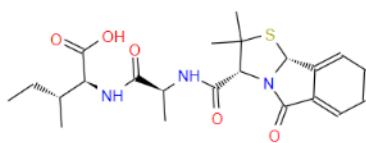
ZINC000022139684



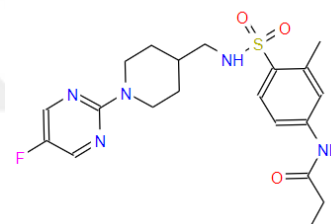
ZINC000008706134



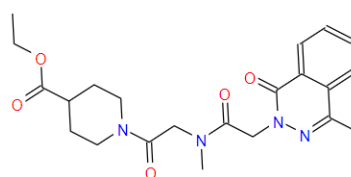
ZINC000019699752



ZINC000008790155



ZINC000252503037

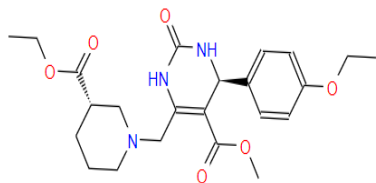


ZINC000058367624

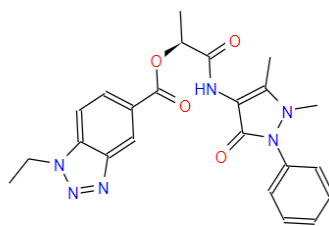
Figure 4. 1 2D scheme Structure of the Inhibitor from the Ligand-Based approaches.

Code	Mwt	LogP	PPAR-alpha (1I7G)		PPAR-gamma(2PRG)	
			ΔG	Inhibition	ΔG	Inhibition
			value Kcal/mol	constant (Ki) nM	value Kcal/mol	constant (Ki) nM
1. ZINC000067287165	445.516	2.141	-10.25	30.84	-9.51	106.91
2. ZINC000010853984	448.483	2.433	-10.23	31.64	-10.23	31.47
3. ZINC000002805504	442.588	2.113	-11.27	5.51	-11.10	7.28
4. ZINC000008706134	438.532	2.355	-10.22	32.49	-9.91	54.33
5. ZINC000022139684	429.473	1.97	-10.40	23.98	-9.29	155.72
6. ZINC000033275541	435.528	2.242	-10.29	28.89	-9.78	68.02
7. ZINC000252503037	435.525	2.468	-10.45	21.85	-10.05	42.63
8. ZINC000008790155	447.557	2.155	-9.54	101.50	-10.22	32.13
9. ZINC000019699752	440.544	1.852	-10.71	14.21	-11.14	6.79
10. ZINC000058367624	428.489	0.965	-10.94	9.58	-11.46	3.97

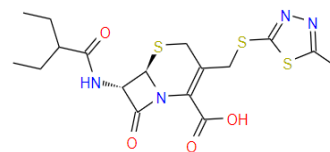
Table 4. 3 Structure-Based Cross-Docking between the different PDB Macromolecules.



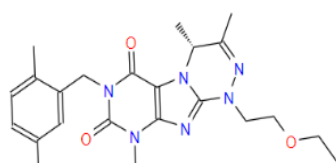
ZINC000067287165



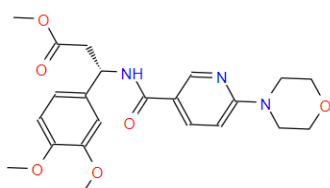
ZINC000010853984



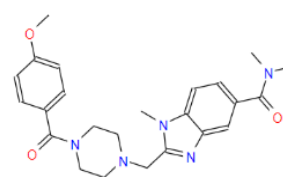
ZINC000002805504



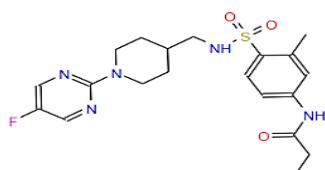
ZINC000008706134



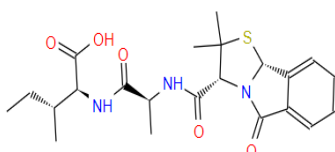
ZINC000022139684



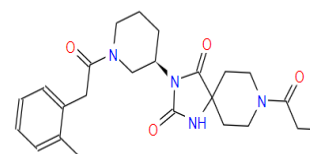
ZINC000033275541



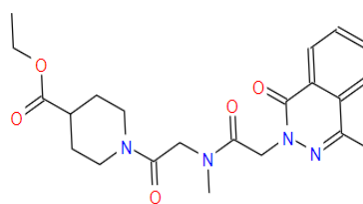
ZINC000252503037



ZINC000008790155



ZINC000019699752



ZINC000058367624

Figure 4. 2D Structure of the inhibitors from the structure-based approach

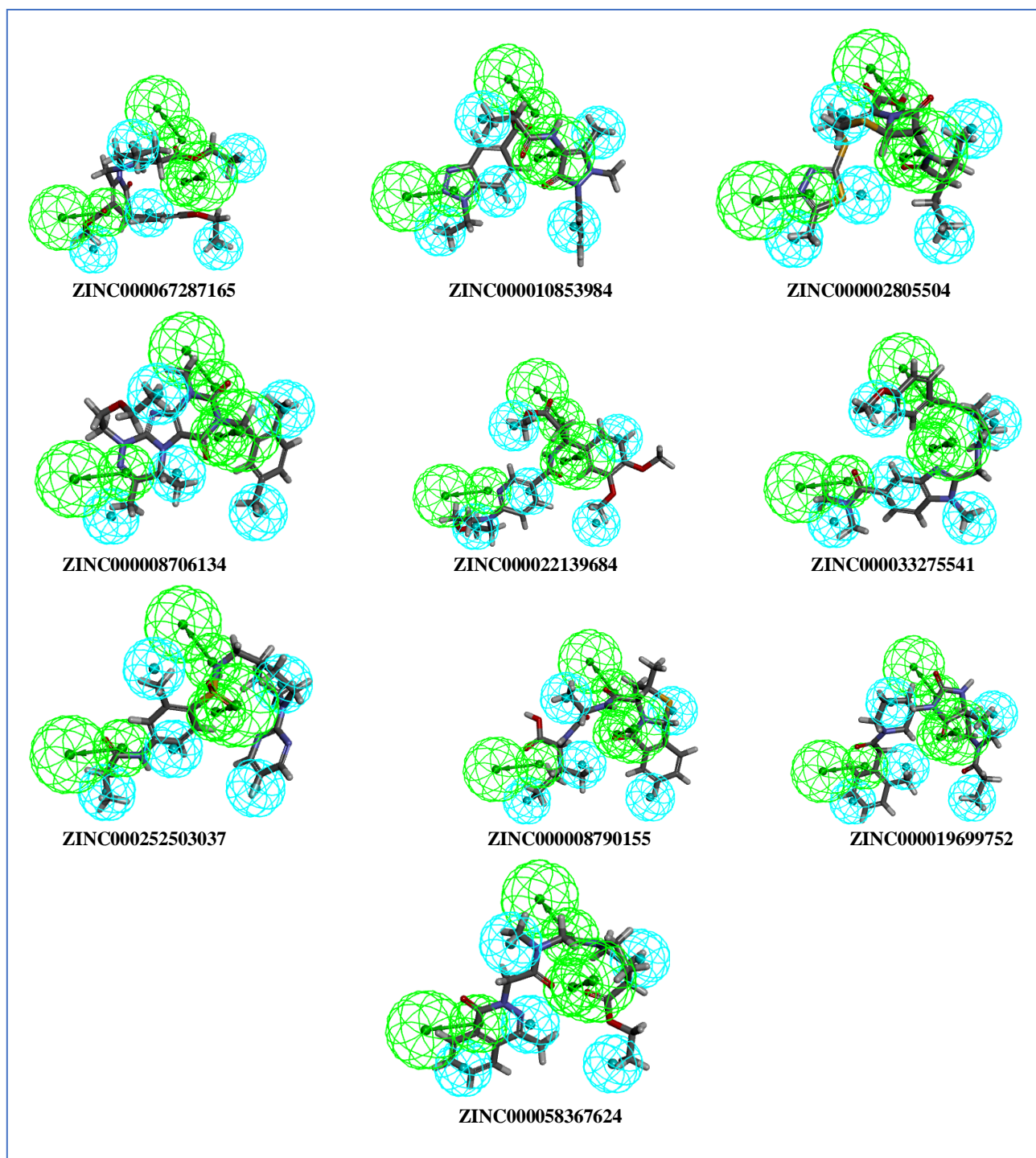
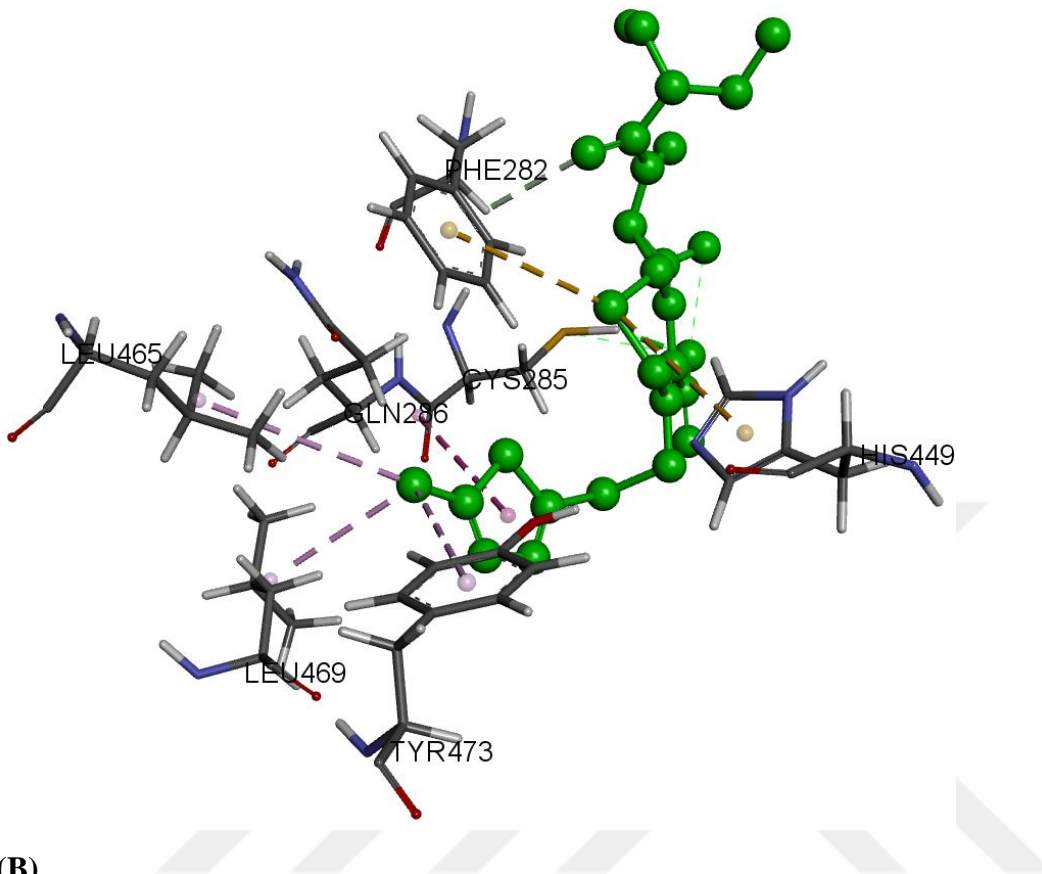


Figure 4. 3 10 best-fitting lead compounds that satisfied the geometric constraints of Hypo1 of the ligand CHMBL326015 identified by a 3D query against the “Zinc15” Database in Biovia DS 4.5. Represent two features HYDROPHOBIC=cyan and HB-ACCEPTER=green.

(A)



(B)

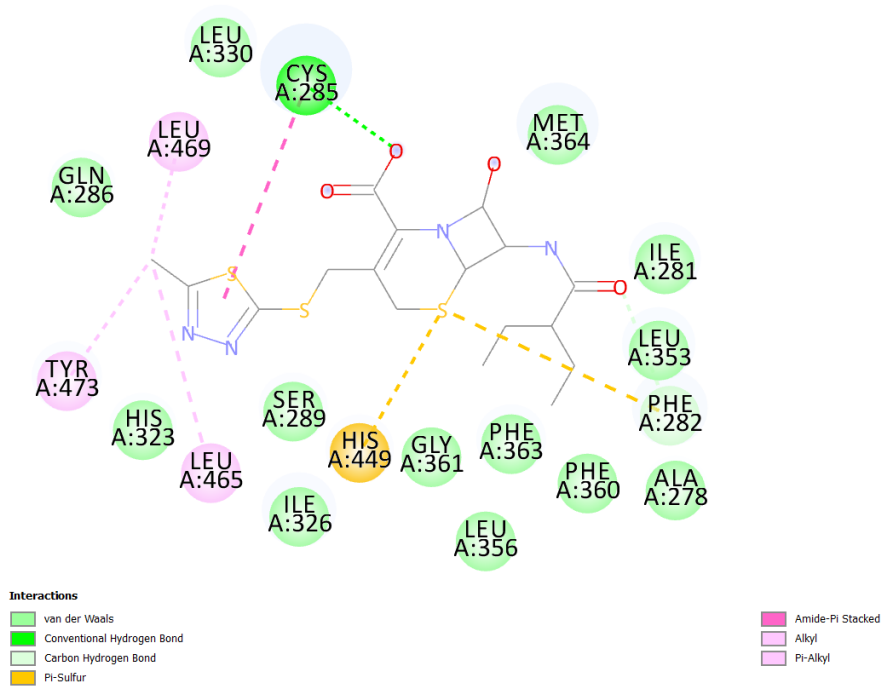
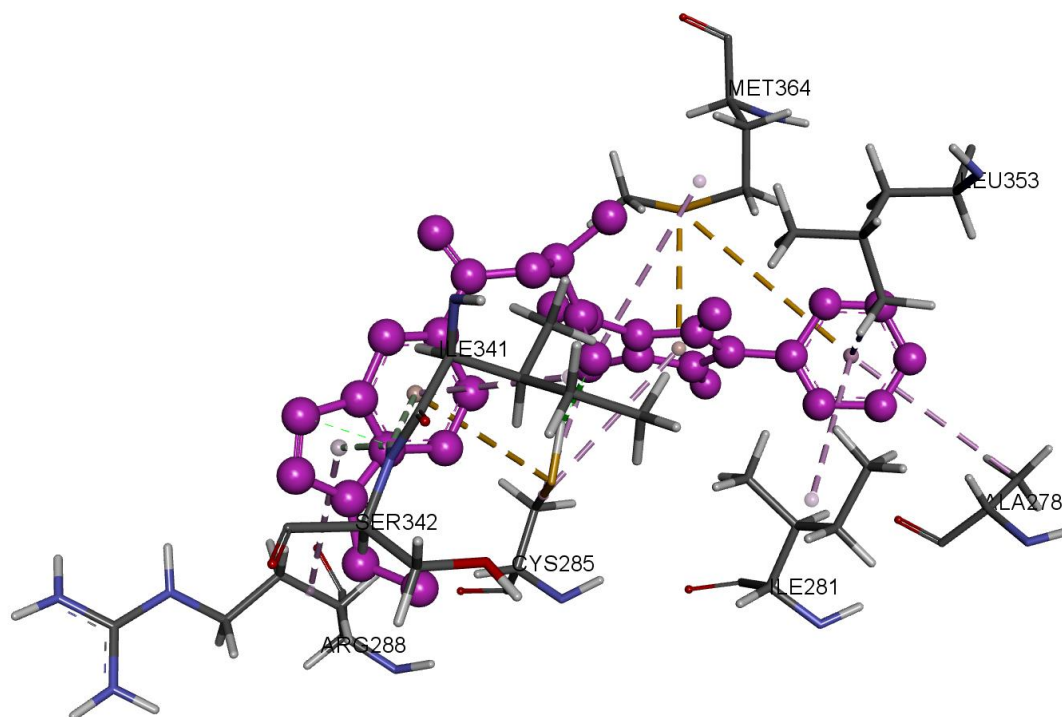


Figure 4. 4 A. 3D Interaction diagram between the amino acid residues and the binding pocket of 2PRG and ZINC000002805504. B) 2D interactions.

(A)



(B)

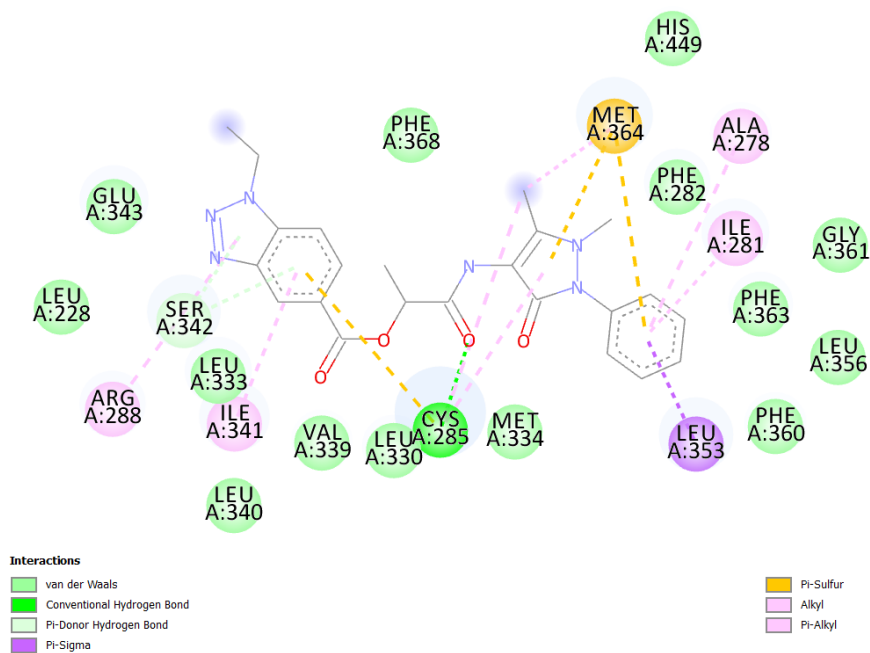
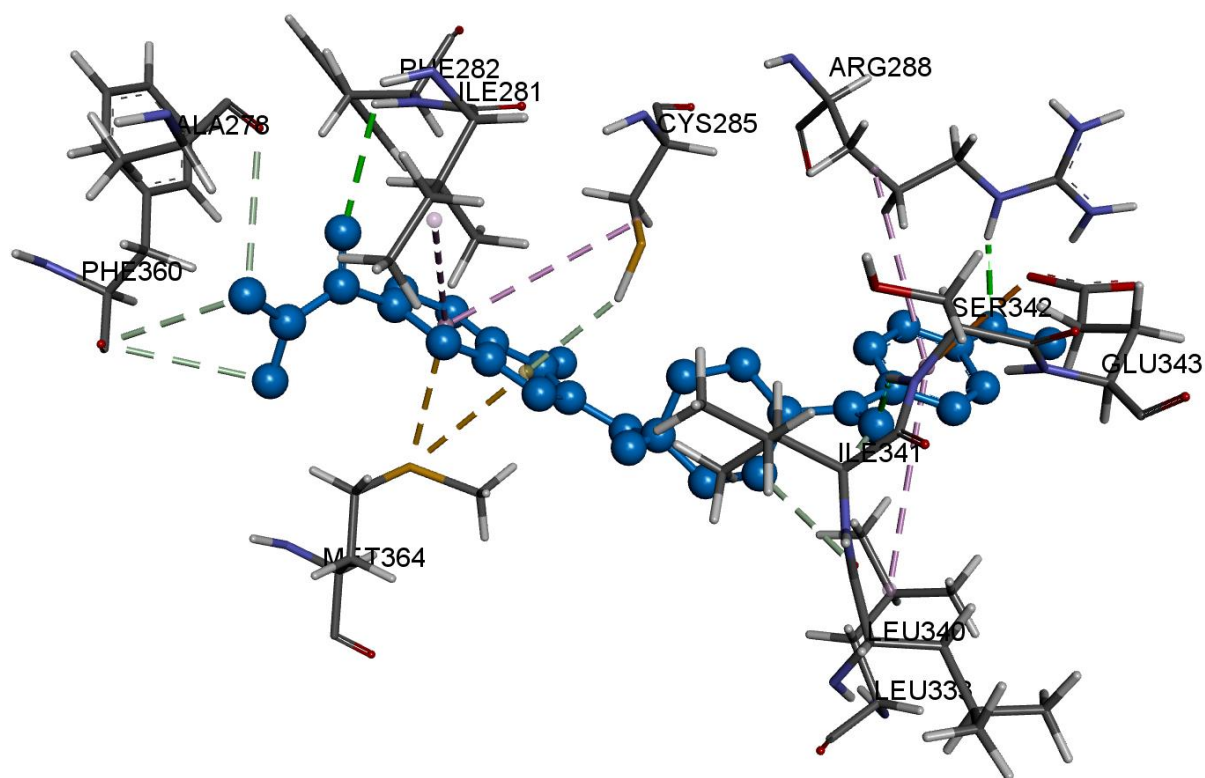


Figure 4. 5 A. 3DInteraction diagram between the amino acid residues and the binding pocket of 2PRG and ZINC000010853984. B)2D interactions.

(A)



(B)

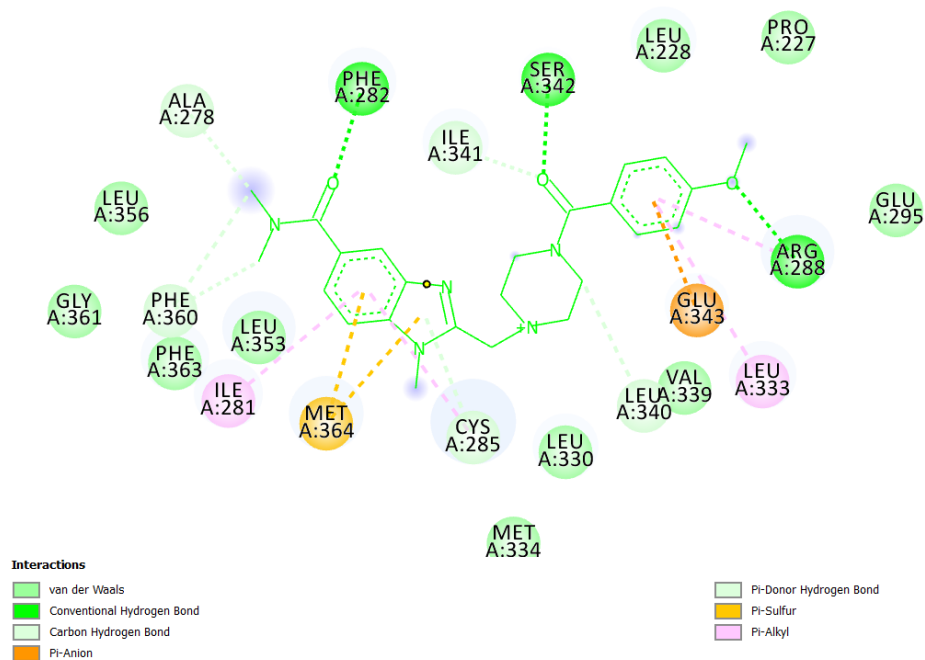
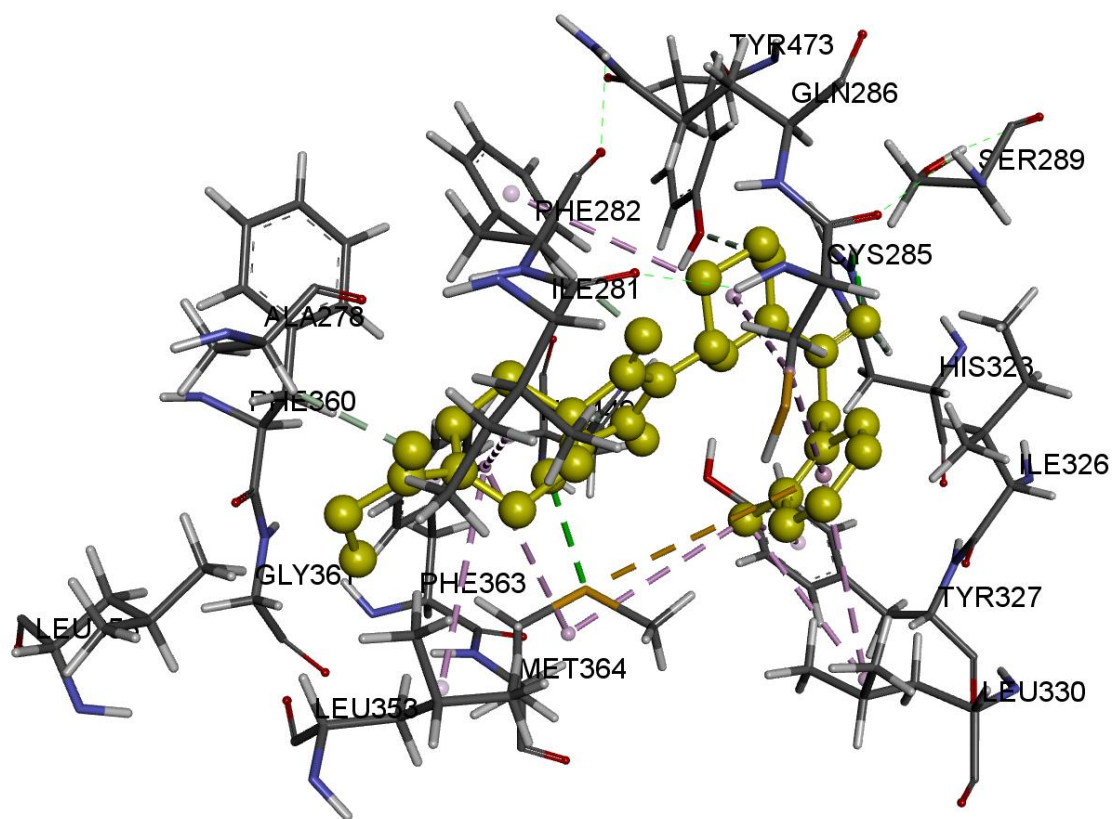


Figure 4. 6 A. 3DInteraction diagram between the amino acid residues and the binding pocket of 2PRG and ZINC000033275541. B)2D interactions.

(A)



(B)

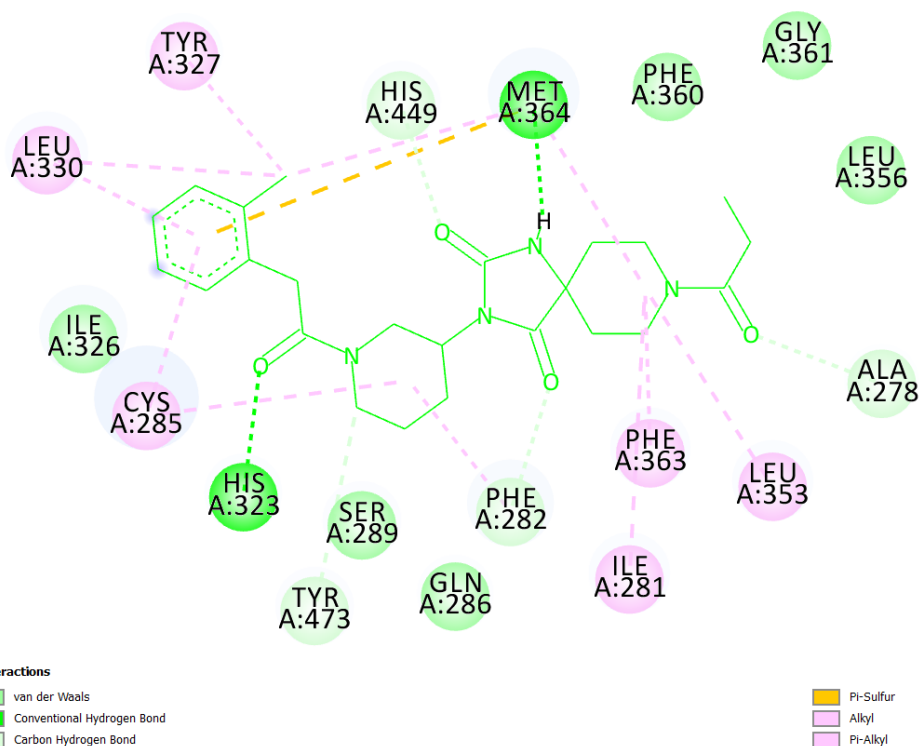
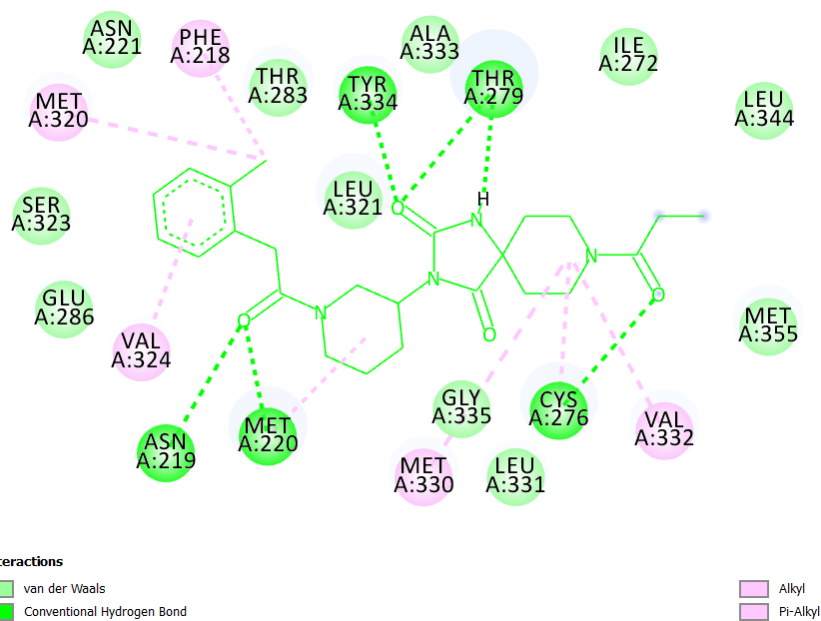


Figure 4. 7 A. 3DInteraction diagram between the amino acid residues and the binding pocket of 2PRG and ZINC000058367624. B)2D interactions.

(A)



(B)

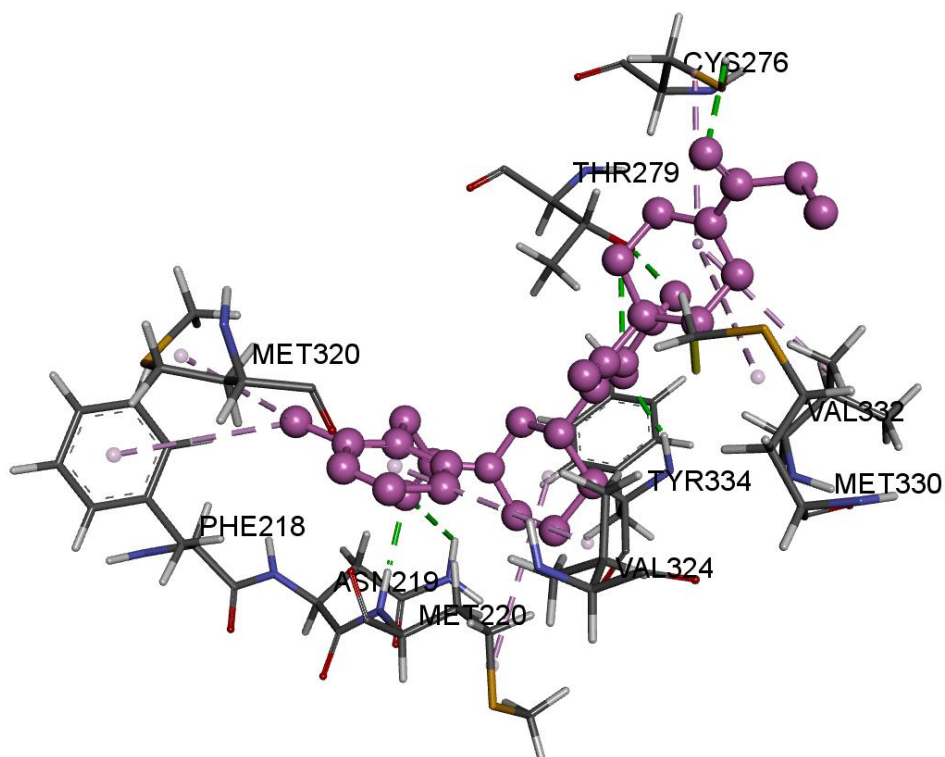
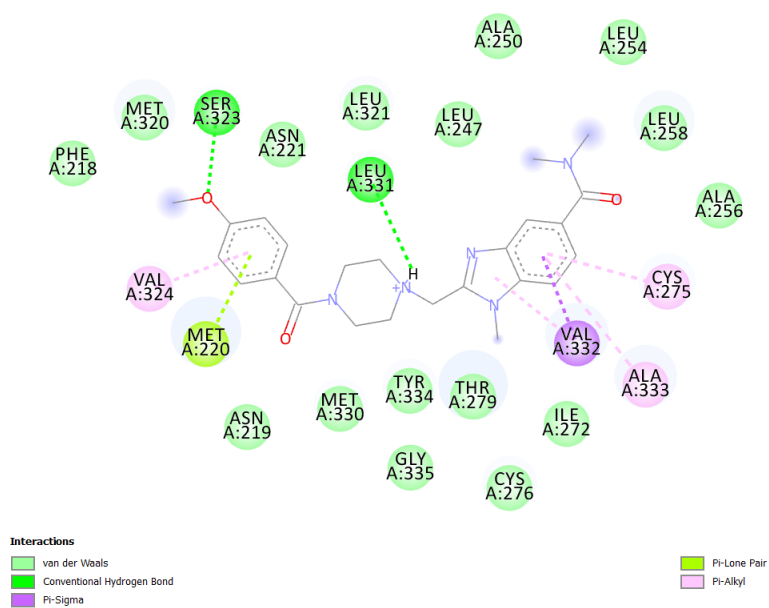


Figure 4. 8 A) 2D interactions. B) 3D Interaction diagram between the amino acid residues and the binding pocket of 1I7G and ZINC000058367624.

(A)



(B)

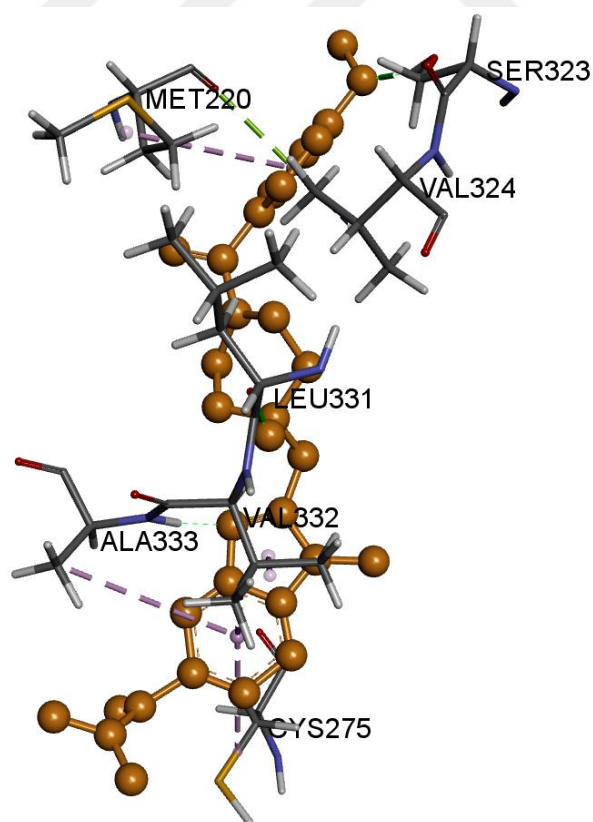
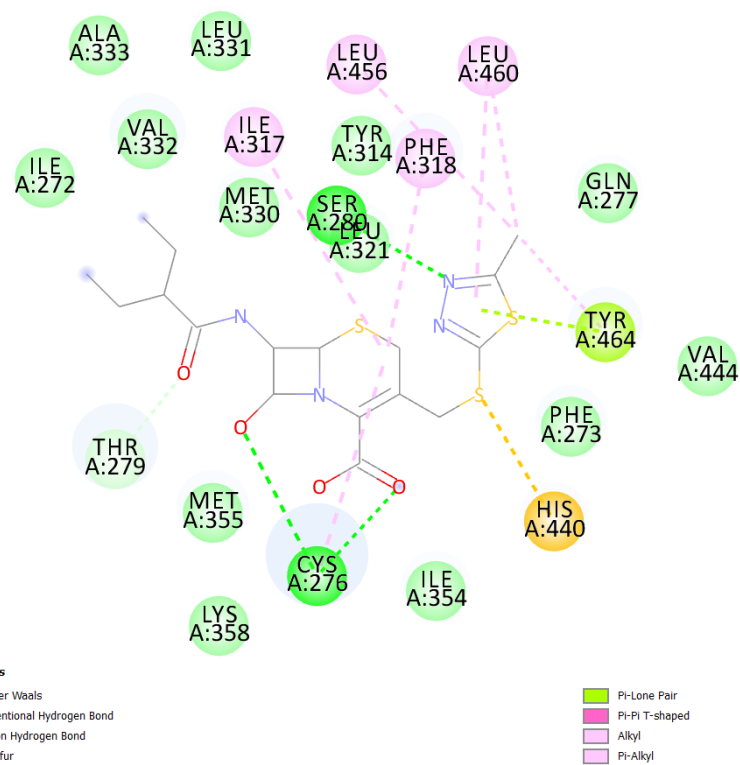


Figure 4. 10 A) 2D interactions. B) 3D Interaction diagram between the amino acid residues and the binding pocket of 1I7G and ZINC000033275541.

(A)



(B)

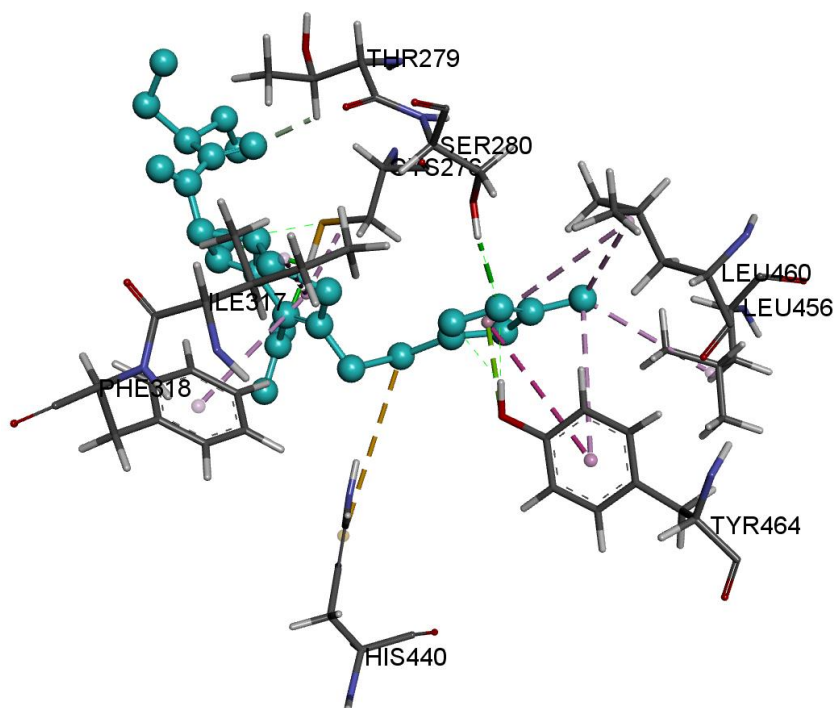


Figure 4. 11 A) 2D interactions. B) 3D Interaction diagram between the amino acid residues and the binding pocket of 1I7G and ZINC000002805504.

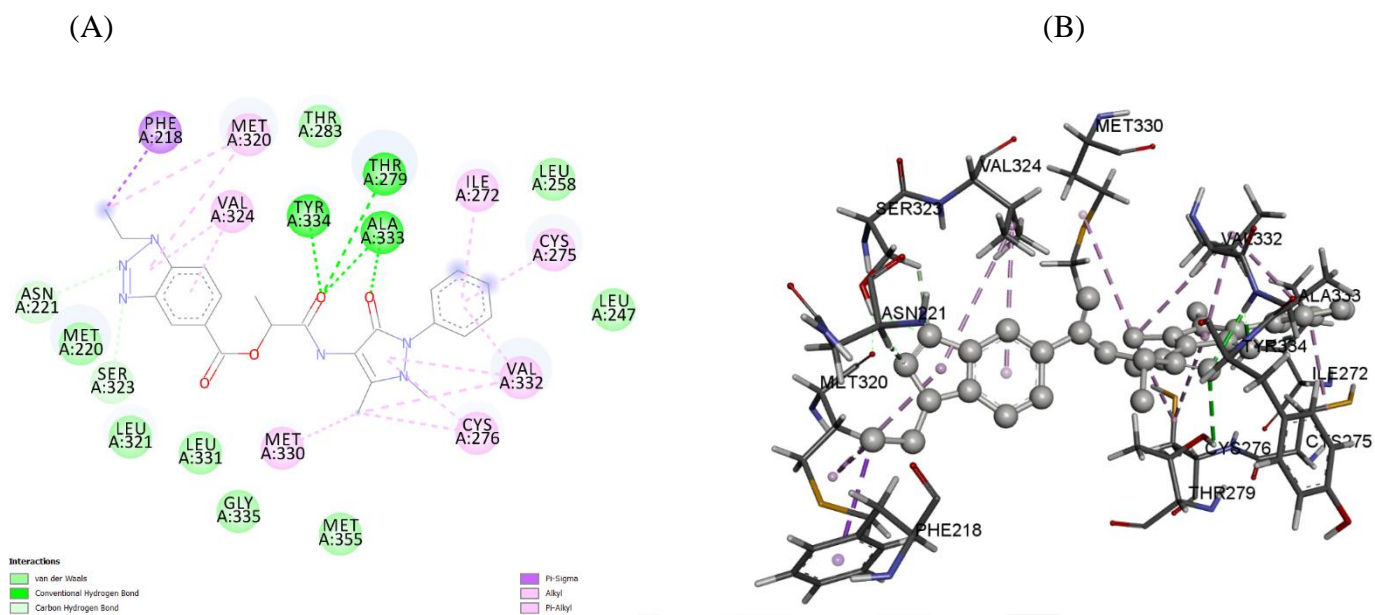


Figure 4. 12 A) 2D interactions. B) 3D Interaction diagram between the amino acid residues and the binding pocket of 117G and ZINC000010853984.

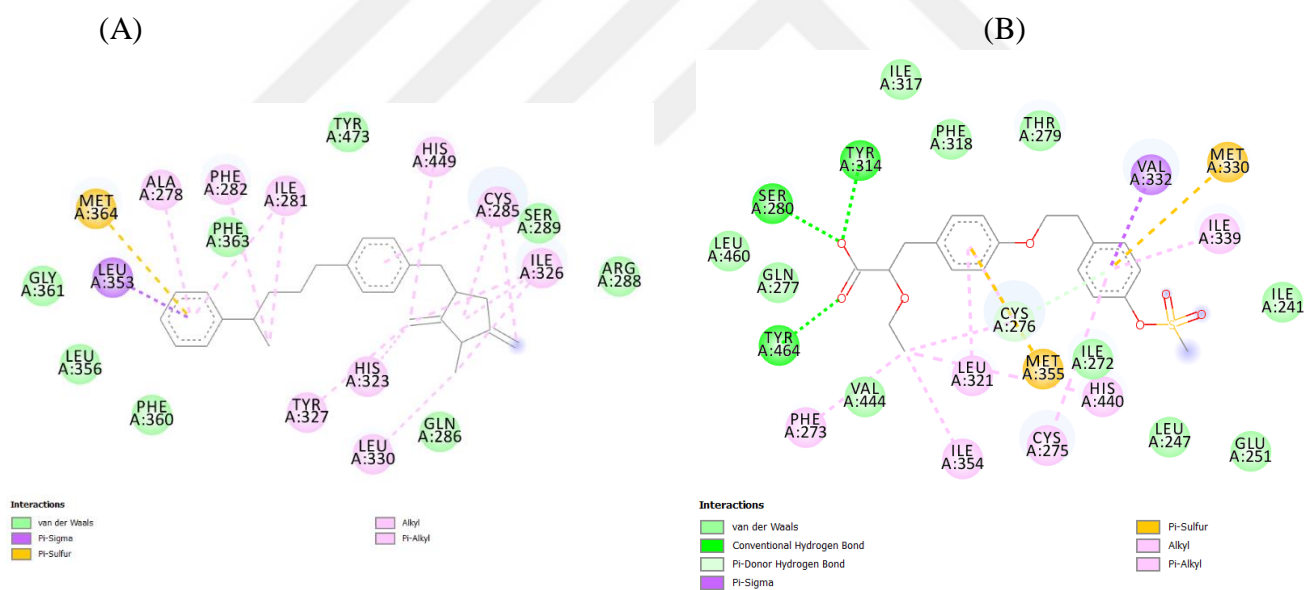


Figure 4. 13 The ligand-protein association with two-dimensional (2D) diagrams in the pocket of PPAR α and PPAR γ . (A) Ligand BRL docking diagram to PPAR γ . (B) AZ242 ligand docking reference to PPAR α .

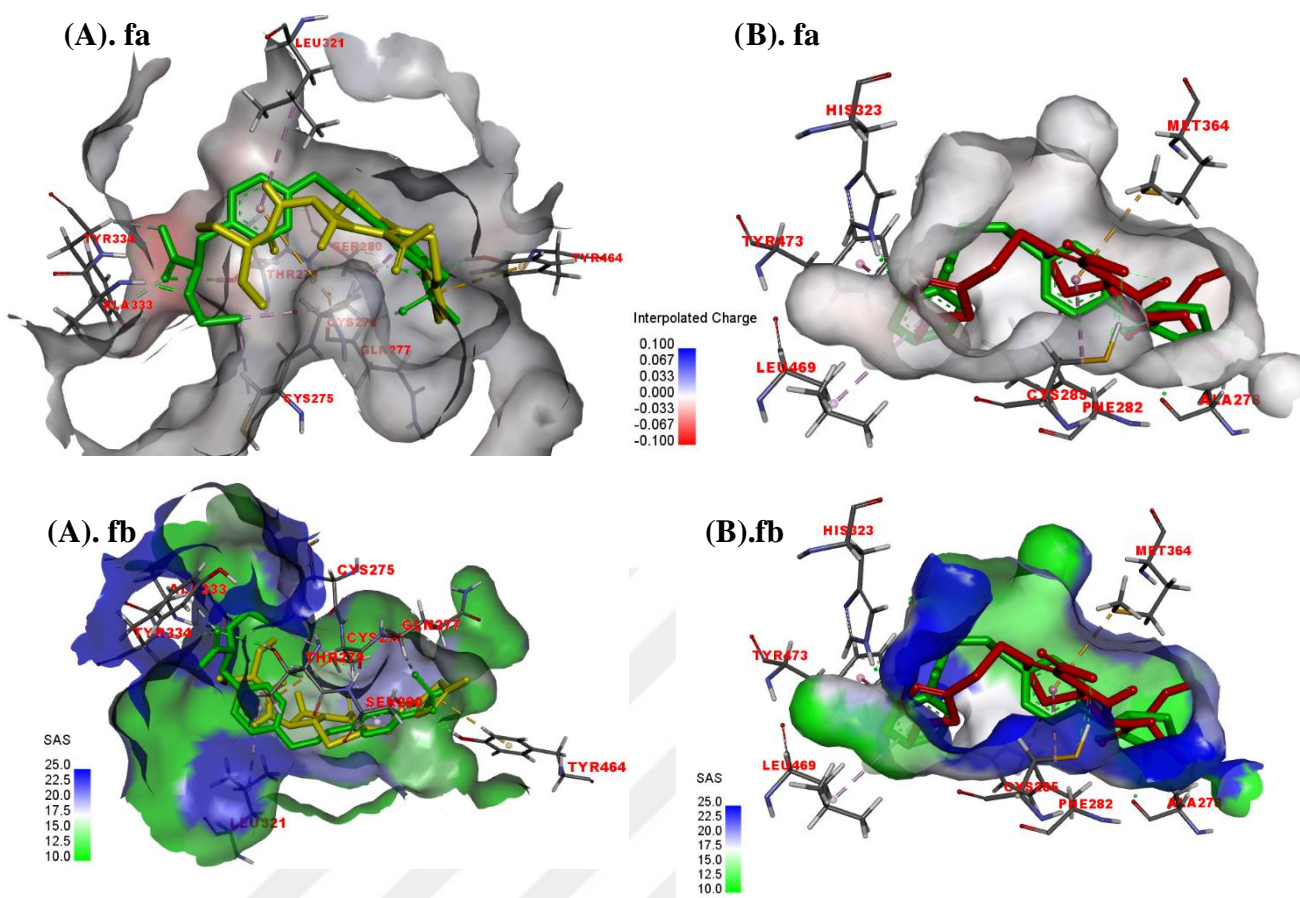


Figure 4. 14 (A)Interpolated charge surfaces and (B)Solvent accessibility surfaces (fa-b),the natural ligand binding layer AZ242 and BRL (green) and the PPAR α receptor pocket compound ZINC000002805504 (yellow)and PPAR γ (Red) ZINC000002805504 (green).

To review binding modes on filtered compounds and Receptor PPARs, the ZINC000002805504 compound was chosen as the representative for evaluating the docking mode and studying the ZINC000010853984 compounds, ZINC000033275541, ZINC000019699752. Figures above illustrate, attachment sequence of the PPAR alpha/gamma attachment pocket. We observed that the binding pocket held by ZINC000002805504 was virtually. Identical to AZ242 (PPAR α receptor) and BRL initial ligands (PPARgamma-receptor) in figure 4.14. Only, utilizing this compound ZINC000002805504 due it results as a lead compound, see the figure 4.4,11 for two dimensional graphs of protein-ligand interactions.

In this chart, the charged surface that creates an interpolated charge surface on the current receptor and also the open amino acid side was enclosed by a blue hollow amino acid ring and the circular diameter was proportional to the size of the solvent's accessible layer. As shown in figure 4.14 (A), figure 4.11 and FA FB. (A), figure 4.13. (B), The AZ242 and ZINC000002805504 carboxylate groups formed H bonds with several essential amino acids (SER280, TYR314, HIS440, and TYR464) active sites of PPAR α . The interactions of HBonds, mentioned above, played an important role in the AF 2 helix region. The interactions not only made the area of AF 2 helix secure but also played a vital role in the receptor combination and activation. In contrast to the carboxylic acid, the main association of the AZ242 ligand and ZINC000002805504 as showed on figures 2D diagram above with amino acid interaction. There were more hydrogen bonds generated by ZINC000002805504 Compared with the first AZ242 ligand. Thus, the docking scores were higher and a more secure linking mode. Figure 4.14 (B)fab. Displayed the ligand BRL and compound binding mode ZINC000002805504 docked with the active pocket of PPAR γ . From the figure 4.4 (B) and figure 4.13 (A), from it can observe that Ligand BRL thiazolidinedione part and ZINC000002805504 acid part both experienced in forming H Bonds interactions with HIS323 and TYR473. The ligand BRL which was almost like compound ZINC000002805504 that had been showed on figures 2D diagram above with amino acid interaction. Also, the compound ZINC000002805504 produced more hydrogen bonds and connections than the original ligand BRL. ZINC000002805504 This is more than the original BRL ligand. The green dabbed lines with the bolts showing the electron donor relates to the hydrogen keeping relations with the main amino acids. Total orange rows connote Pi-Pi conjugates. The green circles indicate the amino acids that are associated with the cooperation of van der Waals. H-bonds, polar connections or positive and negative interactions were illustrated by the pink circles.

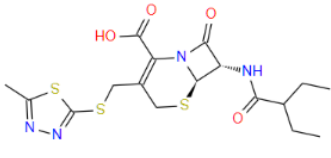
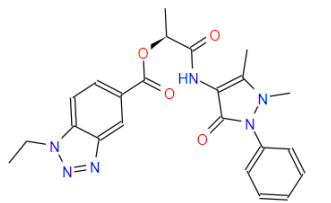
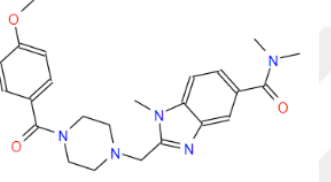
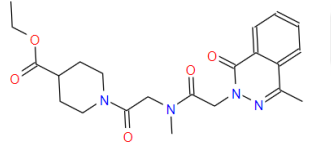
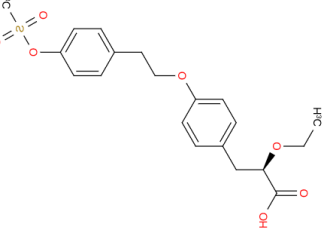
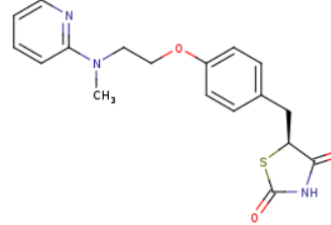
No.	Structure	Binding Energy		FV	-CDOCKER_ENERGY	
		Kcal/mol			PPAR α	PPAR γ
		PPAR α	PPAR γ			
ZINC000002805504		-11.27	-11.10	5.52 923	55.7684	53.4962
ZINC000010853984		-10.23	-10.23	5.30 434	52.656	46.2092
ZINC000033275541		-10.29	-9.78	5.26 093	50.5566	52.5815
ZINC000058367624		-10.94	-11.46	4.87 87	50.6474	52.2876
AZ242		-8.18	-----	3.86 799	46.5751	-----
BRL		-----	-8.58	4.54 764	-----	37.8628

Table 4. 4 The composition, energy(AutoDock and Cdocker),Fit values flow of small molecules. Note: FV (Fit Value)

In this part, utilizing the CDOCKER protocol to explore the binding mode of compounds (Feng et al., 2019). Which done by firstly select the active protein site was predicted and defined using the native ligand (AZ242 and BRL) module "Defining and Edit Binding Site" and the radius was set to 10A. The receiver collected was used as the parameter of the molecule "data receiver". All hit compounds undergoing initial sorting are identified as "Output Ligand" and docked into the active site of (PPAR Alpha 1I7G, PPAR Gamma 2PRG). To increase the diversity of the docked poses, the "Pose Cluster Radius" was described as 0.1A. The top hits were set to 10, meaning that the top 10 shapes were saved for each ligand based on scoring and ranking by the negative CDOCKER energy value. The parameters left are normal. Docking scores and correlation with ZINC000002805504's accessible complex crystal structure with the native ligand (AZ242 and BRL) were used to determine the best binding modes. We obtained 4 Better docking and better affinity molecules than the original ligands (AZ242 and BRL) for a quicker grid-based analysis (CDOCKER). The first four compounds' names, structures, and docking energies are identified (Table 4.4) According to ratings for docking and sequence of contact. In Table 4.4, the highest score of the ligand docking with PPARalpha was 55.7684, which was greater than the original ligand AZ242 (46.5751). The maximum score for receptor PPARgamma was 53.4962, which was also higher than the original ligand BRL (37.8628).

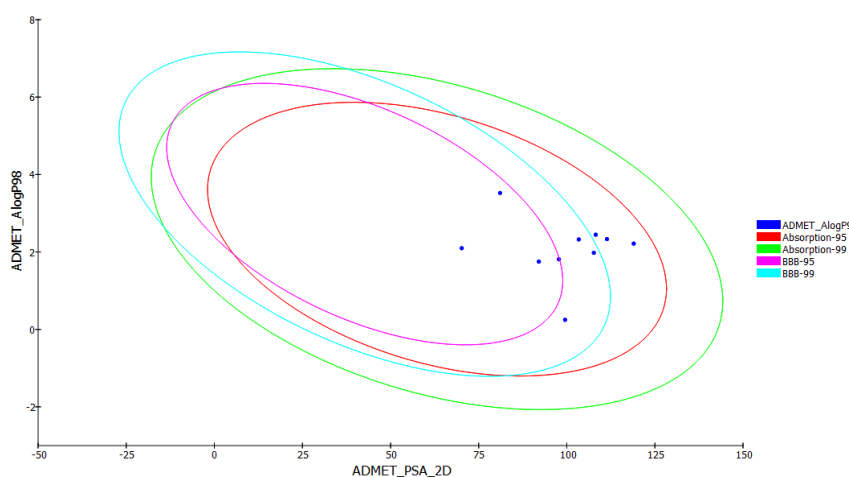


Figure 4. 15 The calculated ADMET properties for the Structure-Based inhibitors

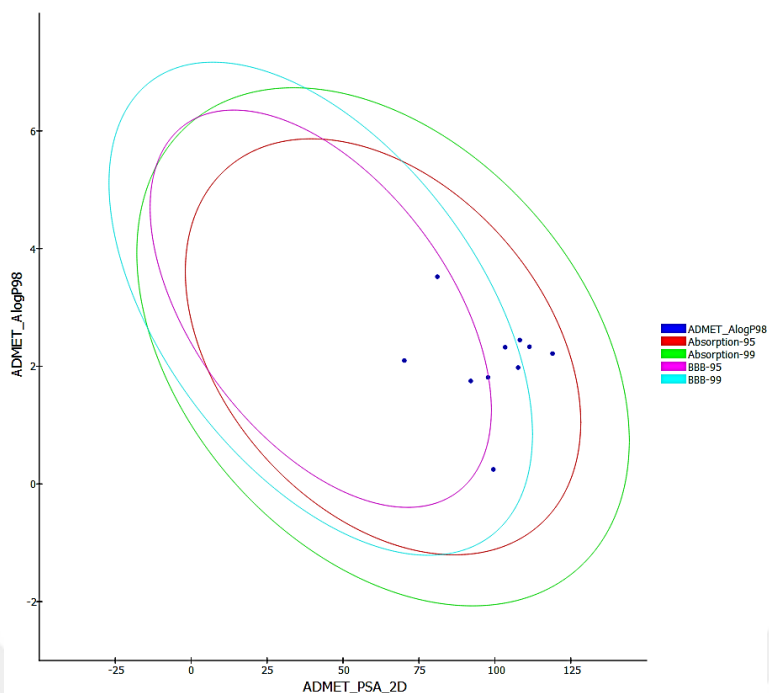


Figure 4. 16 The calculated ADMET properties for the Ligand-Based inhibitors.

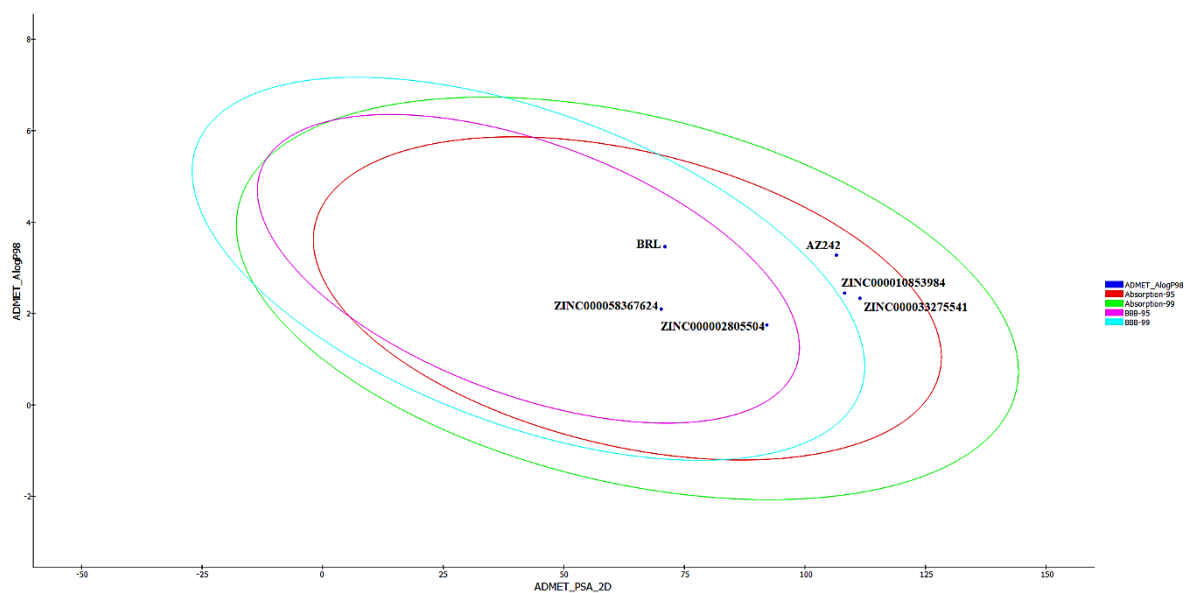


Figure 4. 17 The graph of ADMET PSA 2D vs AlogP98 (the trust mark between 95 and 99 percent ellipses According to the BBB and HIA ligands). The calculated ADMET properties for the Ligand-Based inhibitors (Selected compounds as previously mentioned).

In this chapter, we first dissected the result of the ADMET prediction on 10 Docking compounds, then analyzed the result of the ADMET prediction on 4 compounds. Such plots specifically identified the rate of ADMET PSA 2D vs ADMET Blood-brain barrier penetration (BBB) and human intestinal absorption (HIA) compounds with confidence ellipses of 95% and 99%, figure.4.14, 15, 16. All compounds fell at the level of human intestinal absorption within the ellipse of the confidence interval (95 percent). However, only one compound Penetration of the blood-brain barrier at the confidence interval was removed from the ellipse (99 percent). Studies have shown that the compound cannot cross the blood-brain barrier and therefore has a lower chance of neurotoxicity. It is not certain whether the compound was passing through the blood-brain barrier. Because it depended on where it was targeted and detected and its toxicity (Singh, Kumar, Mansuri, Sahoo, & Deep, 2016). The plasma protein binding, inhibition of Cytochrome P450-2D6 and hepatotoxicity. Some compounds (level 3 of solubility) are found to have lower aqueous solubility. The ranking for Bayesian is (2.8755) as a criterion for evaluating the binding of compounds with plasma proteins (Colmenarejo, Alvarez Pedraglio, & Lavandera, 2001). The higher score, the greater protein binding which provides the ability to know that all compounds have a strong binding outcome from the results. The CYP2D6 participates in the liver metabolism substrates. Despite this, all the substances could not know repressed the CYP2D6 because the Bayesian limit score is below (0.111). The Bayesian rating of approximately 0.4095 compounds shows that compounds do not have hepatotoxicity (Ahmad, Khan, Parvez, Akhtar, & Raisuddin, 2017), ZINC000002805504 had no toxicity. Likewise, TOPKAT prediction, revealed various Protein and protein-ligand cellular compatibility systems results suggested, there was no risk in most compounds as a potential drug tentatively. Researching ADMET prediction and TOPKAT prediction results, the ZINC000002805504 was the safe compound, and its molecular structure was almost like the original ligand structure. Hence, we deemed the PPAR α ZINC000002805504, ZINC000058367624 and PPAR γ ZINC000002805504, ZINC000058367624 as examples to conduct molecule dynamics simulations (MDs) by using the NAMD program for further exploring the binding pattern of protein-ligand complexes.

In this section, discussions of the results molecular dynamic by mean NAMD during the time of simulation 30ns as RMSD, RMSF, and Rg, by utilized VMD program.

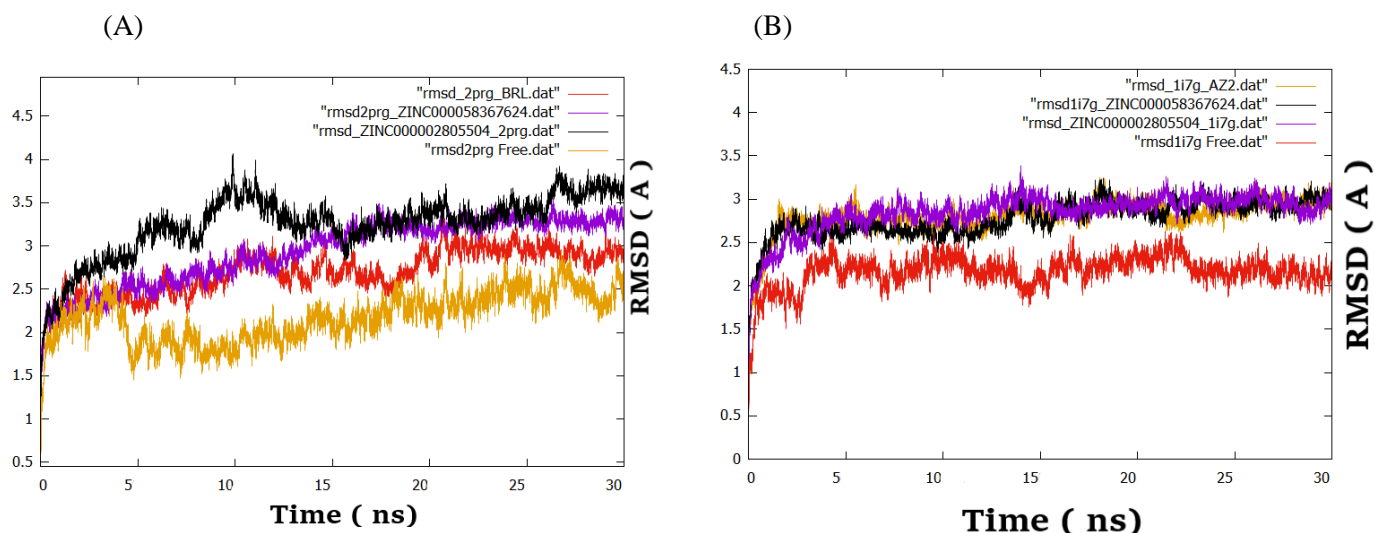


Figure 4. 18 During simulations of 30 ns, the RMSD trajectories of PPAR α / γ -ligand complexes. (A) PPAR γ BRL, PPAR γ free, PPAR γ ZINC000002805504, PPAR γ ZINC00000058367624, RMSD trajectories. (B) PPAR α RMSD trajectory, PPAR α AZ242, PPAR α ZINC000002805504, PPAR α ZINC000058367624.

This part is significant, where the quantitative root mean square deviation (RMSD) parameter is stable or not used to determine Protein and protein-ligand cellular compatibility systems. As shown in figure 4.17, on (A) Almost all compound tends to be in an equilibrium state especially PPAR γ , PPAR γ -BRL, PPAR γ -ZINC000058367624 after 5ns but PPAR γ -ZINC000002805504 after 16 ns of the 30 ns trajectories, on (B) Both compounds were in a state of equilibrium after simulation of 4ns. PPAR α 's maximum RMSD-value, PPAR α AZ242, PPAR α ZINC000002805504, PPAR α -ZINC000058367624. reached about (2.19559Å and 3.02400Å). While the RMSD values were PPAR γ 2.48989 Å, PPAR γ -BRL (2.88230Å), PPAR γ -ZINC000058367624 (3.25290 Å) and PPAR γ ZINC000002805504 (3.62350 Å), receptive during the time of harmony (acceptable range = 0 - 3,3.7 Å). The overall RMSD of the complexes seemed to have a minor reorganization of the conformation in the preceding step, but after that, the simulation or the final simulation cycle seemed to be stable due to the treatment of two proteins. Figure 4.17 (A) Showed that the RMSD range of complexes of PPAR γ , PPAR γ -BRL, PPAR γ - PPAR γ -ZINC000002805504, PPAR γ -ZINC000058367624

were around (2.68~3.55 Å) and PPAR α , PPAR α AZ242, PPAR α ZINC000002805504, PPAR α -ZINC000058367624 (2.11~3.26 Å) respectively. The capacity of every system reached attained to ± 0.6 Å when in equilibrium. Part of part from these, figure 4.18. (B) Of PPAR α , PPAR α AZ242, PPAR α ZINC000002805504, PPAR α -ZINC000058367624 their fluctuations kept in an α -relatively stable state. Compared with PPAR γ , PPAR γ -BRL, PPAR γ -ZINC000002805504, PPAR γ -ZINC000058367624 ligands value was higher. From the above discussion, the RMSD was remarkably more stable more for PPAR α and their complexes than PPAR γ their complexes.

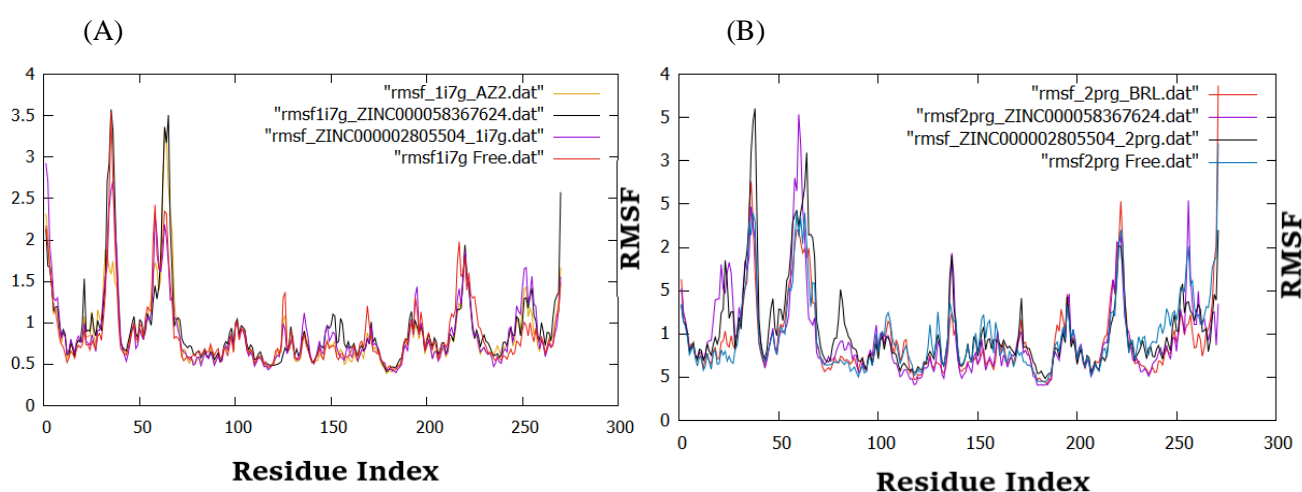


Figure 4. 19 Throughout the simulations, the RMSF maps of PPAR α and PPAR α/γ ligand complexes.(A) PPAR α , PPAR α -AZ242, PPAR α -ZINC000002805504, PPAR α -ZINC000058367624 MD simulations (NAMD) 30ns in their entirety. (B) Maps of the RMSF of PPAR γ , PPAR γ -BRL, PPAR γ -ZINC000002805504, PPAR γ -ZINC000058367624.

To know if the fluctuation of these amino acids as shown in figure 4.18 is constant, meaning RMSF. The root mean square fluctuations (RMSF) of the residues of amino acids used to calculate the average maximum atomic fluctuations of the given amino acids figure 4.17 (A) and (B)) (Shu et al., 2011; D. Zhang & Lazim, 2017; L. Zhang, 2017). For a few variations exceeding (3,3.5 Å), the RMSF for most amino acid residues were within Å. Where if the fluctuation of the active site and the main chain atoms were temperate, suggesting a slight change in conformity was appropriate (Priyadarshini et al., 2014). Figure 4.18 of (A) the fluctuation-region of PPAR α -ZINC000058367624 in black AF-2 area RMSF fluctuation are (Phe351, Cys352, Val437), PPAR α -ZINC000002805504 in magenta color AF-2 area RMSF fluctuation (Cys352, Phe365, Ala380), RMSF fluctuation of the AF-2 region PPAR α -AZ242

in yellow color AF-2 area RMSF fluctuation (Lys349, Cys352, Ile375, Ala380), PPAR α in red color RMSF fluctuation of the AF-2 region (Phe351, Ile375, Gln442) RMSF fluctuation are all stable in the Af-2 region near to the chain. (CYS 276, SER 280, TYR 314, LEU 321, VAL 332, HIS 440, and TYR 464 of PPAR α), the fluctuation-values of these residues of PPAR α -ZINC000002805504 and PPAR α -ZINC000058367624. These data showed that they were smaller than PPAR α -AZ242 and PPAR α . (PPAR α -ZINC000002805504 and PPAR α -ZINC000058367624) and key residue in between are both have strong hydrogen interactions.(B) The fluctuation region of PPAR γ -ZINC000002805504 in black color AF-2 area RMSF fluctuation are (Phe363-347, Asp383, Ala389, Ser382, Pro405, Lys457), PPAR γ -ZINC000058367624 in magenta color AF-2 area RMSF fluctuation are (Gln345, Arg350, Phe360, Leu384, Asp462), PPAR γ -BRL in red color AF-2 area RMSF fluctuation are (Phe360, Leu384, Ala389, Thr461), and PPAR γ in blue color RMSF fluctuation of AF-2 region are (Pro359, Asp362, Phe387, Ile391), totally they all showed stability on AF-2 region in spite of they have small fluctuation in that region as to PPAR γ , PPAR γ -BRL. The RMSF value of PPAR γ -ZINC000002805504, PPAR γ -ZINC000058367624 with previously mentioned about key-residues, they were lower than the PPAR γ -BRL complex system and PPAR γ free, meaning that key-residues generated stronger interactions between hydrogen bonds with both complexes PPAR γ -ZINC000002805504, PPAR γ -ZINC000058367624.

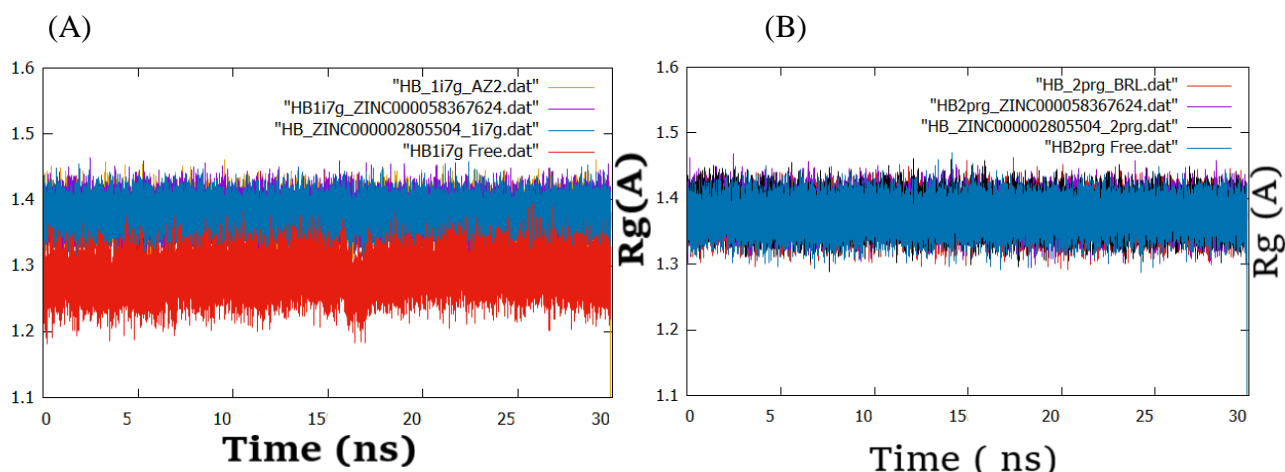


Figure 4. 20 Throughout the 30ns simulations, the Rg-maps of PPAR α/α and PPAR α/γ .

Lastly the analyzing for the radius of gyration (Rg) describe as the mass weighted root-mean square distance of a gathering of atoms from their common center of mass. Rg which means the measure of the compactness' of protein structure (M. I. Lobanov, Bogatyreva, &

Galzitskaia, 2008). The analyzing of radius of gyration provided an insight of the overall dimensions of the protein as shown in figure 4.19, illustrates the plot of, (A) PPAR α , PPAR α -AZ242, PPAR α -ZINC000002805504, PPAR α -ZINC000058367624 overall they are all stable due to their compactness very well accept the free PPAR α in red color found to be lower (1.18959,1.366228 A) throughout the simulation time 16 ns, and PPAR α -AZ242 in yellow color (1.29844,1.455007 A) simulation time 18 ns, PPAR α -ZINC000002805504 in blue color (1.27906,1.45634 A) simulation time 26 ns, PPAR α -ZINC000058367624 in magenta color (1.29502,1.46148 A) simulation time 7 ns found to be trend a little higher and mild throughout the whole simulation. (B) PPAR γ , PPAR γ -BRL, PPAR γ -ZINC000002805504, PPAR γ -ZINC000058367624 as observed these the free and complexes tend to be very stable and found to be higher compactness mean tend to be lower (1.29787,1.46433 A) simulation 18 ns until throughout the whole simulation 30 ns. However, as an indicator of protein structure compactness is the Radius of gyration. It is a concern by how regular secondary structures can are compactly packed into the 3D structure of the protein. α proteins having the highest radius of gyration in the range of protein sizes contemplated, indicating less leakage Compared to β - and ($\alpha + \beta$) proteins. The lowest radius of gyration and the tightest seal accordingly. Characteristics of α / β proteins. The radius of gyration normalized by the radius of gyration of a sphere. In the same volume, unlike compactness and number of contacts, independent of protein size per residue (M. Y. Lobanov, Bogatyreva, & Galzitskaya, 2008).

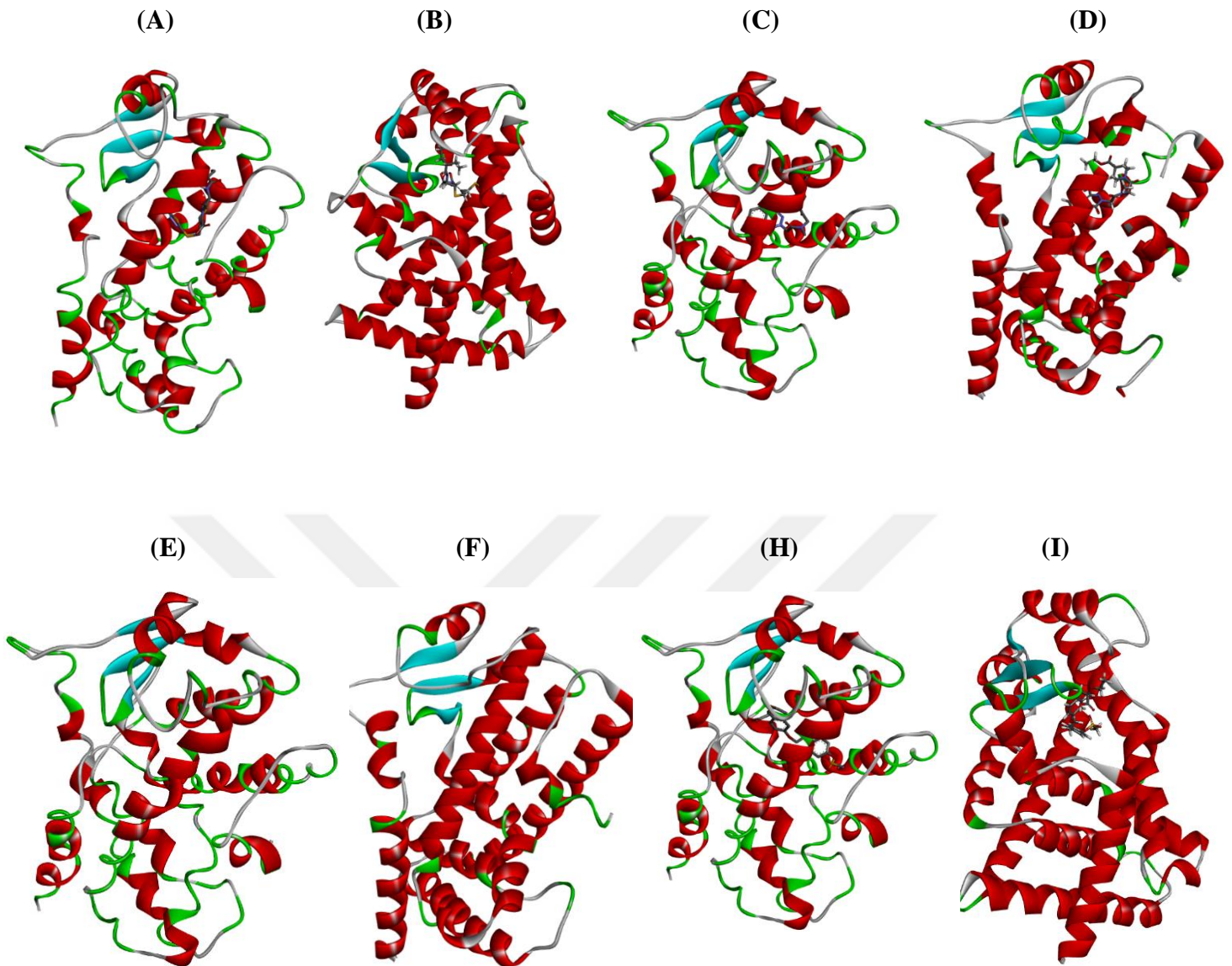
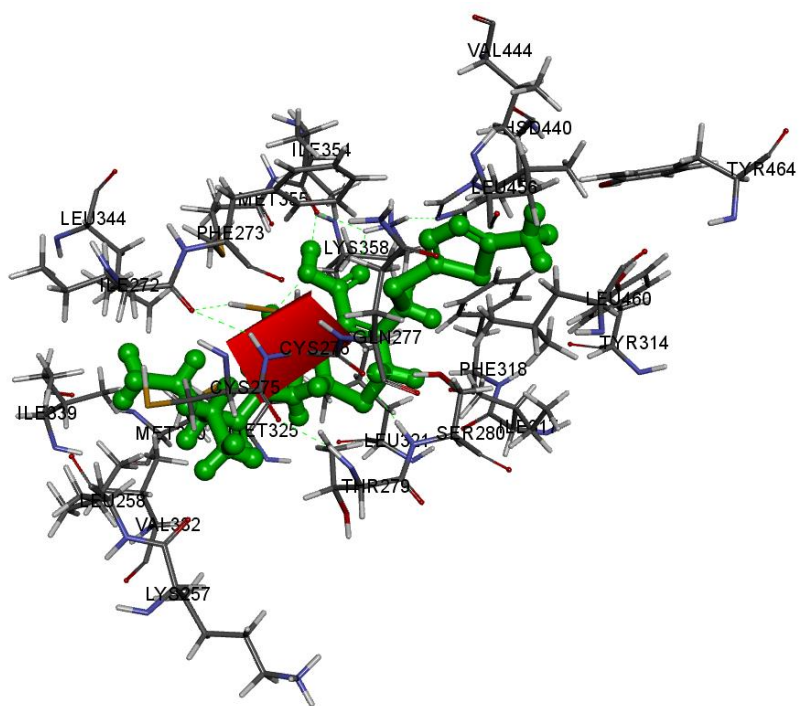


Figure 4. 21 From the final frame, The MD simulation results how it looks like before and after. The MD simulation result Complexes of PPAR α and PPAR α throughout the simulations 30ns. (A) PPAR α -ZINC000002805504 the MD simulation result before. (B) PPAR α -ZINC000002805504 PPAR α after The MD simulation result. (C) PPAR α -ZINC000058367624 before The MD simulation result. (D) PPAR α -ZINC000058367624 after The MD simulation result (E) PPAR α the free before The MD simulation result. (F) PPAR α the free after The MD simulation result (H) PPAR α -AZ242 before The MD simulation result, in the entire MD simulations (NAMD), 30ns. (I) PPAR α -AZ242 after The MD simulation result.

(A)



(B)

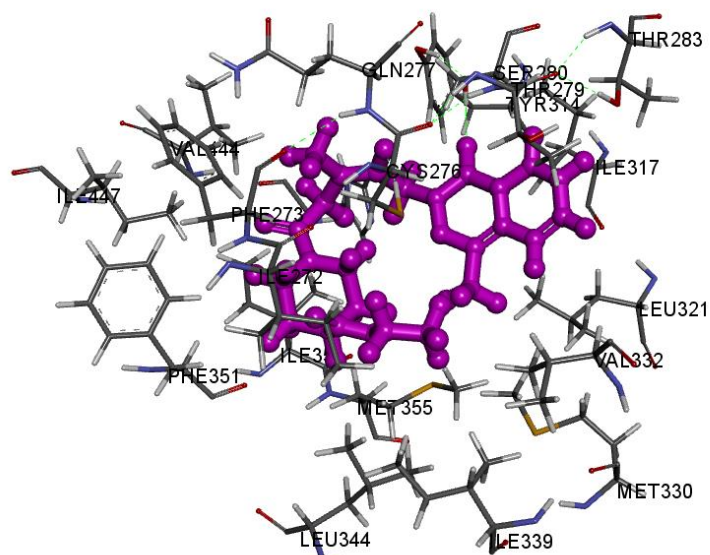
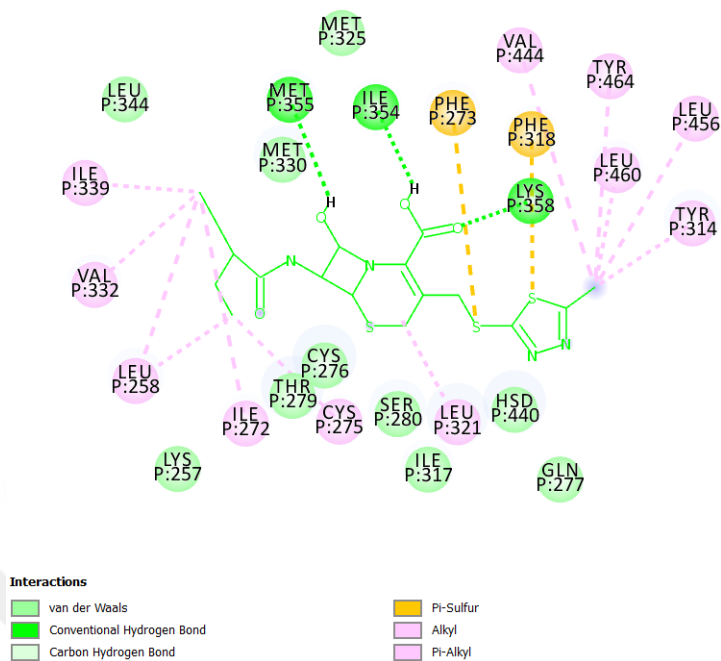


Figure 4. 22 The MD simulation result in the entire MD simulations (NAMD)30ns. 3D Ligand-protein interaction diagrams in a pocket of PPAR α . (A) 3DAmino acid residue interaction diagram with 1i7g (PPAR α) and ZINC000002805504 binding pocket. (B) 3DAmino acid residue association diagram with binding pocket (to PPAR α)1i7g and ZINC000058367624.

(A)



(B)

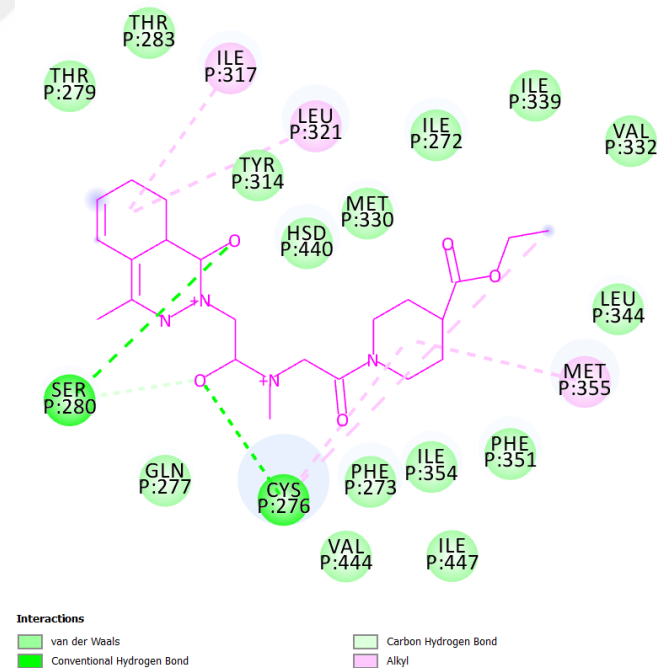


Figure 4. 23 2D-the MD simulation using (NAMD)30ns performance. The ligand-protein interaction two-dimensional (2D) diagrams in PPAR α a pocket. (A) MD ZINC000002805504 to PPAR α (117 G) simulation map. (B) MD ZINC000058367624 to PPAR α (117 G) simulation map

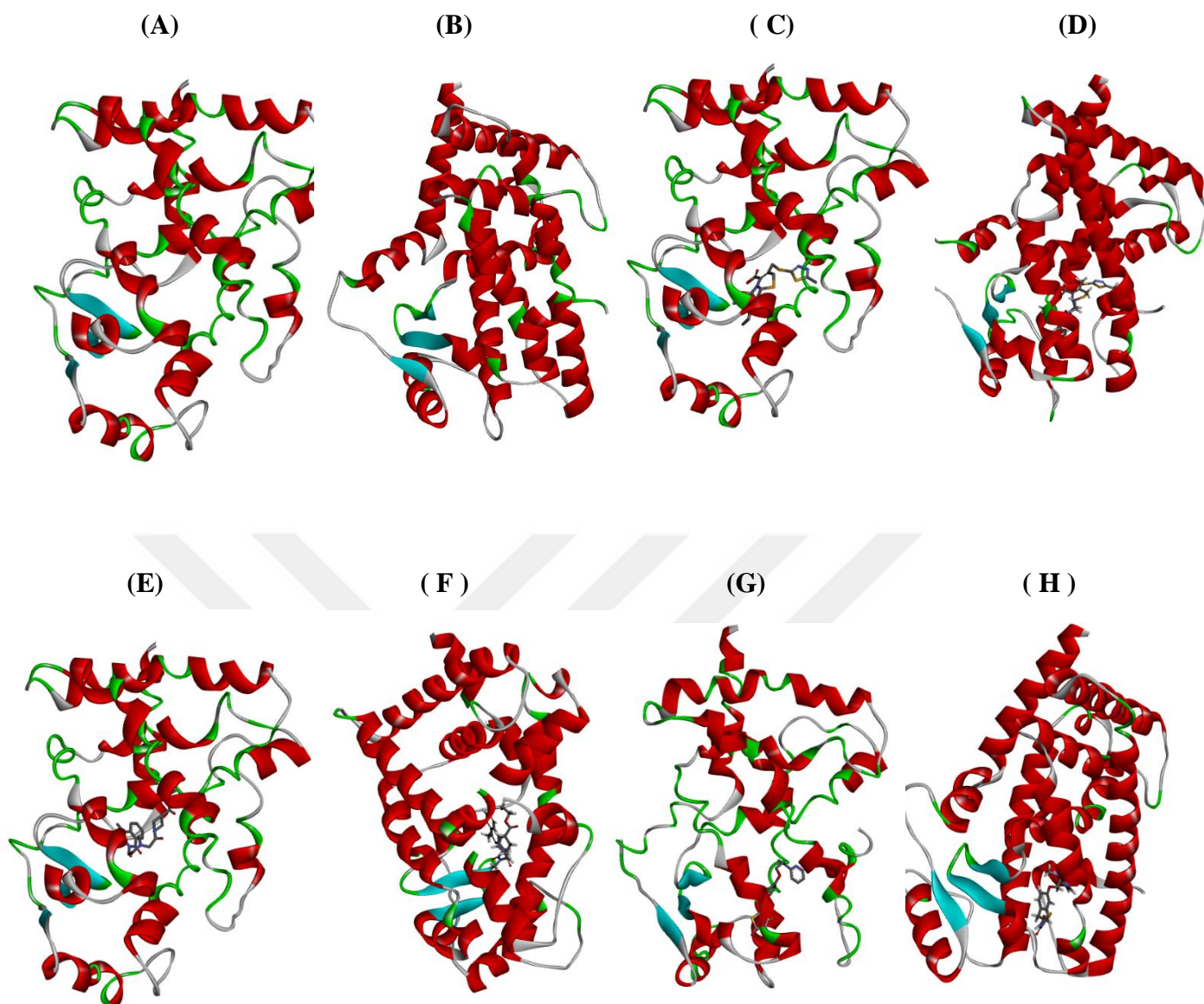


Figure 4. 24 From the final frame. The MD simulation results in how it looks like before and after. The MD simulation result of PPAR γ and PPAR γ Ligand complexes throughout the 30ns simulations. (A) PPAR γ free without ligand in the system, before the MD simulation result. (B) PPAR γ free without ligand in the system after. (C) PPAR γ -ZINC000002805504 before the MD simulation result. (D) PPAR γ -ZINC000002805504 after the MD simulation result. (E) PPAR γ -ZINC000058367624 before the MD simulation result. (F) PPAR γ -ZINC000058367624 after the MD simulation result. (G) PPAR γ -BRL before The MD simulation result. (H) PPAR γ -BRL after The MD simulation result, in the entire MD simulations (NAMD)30ns.

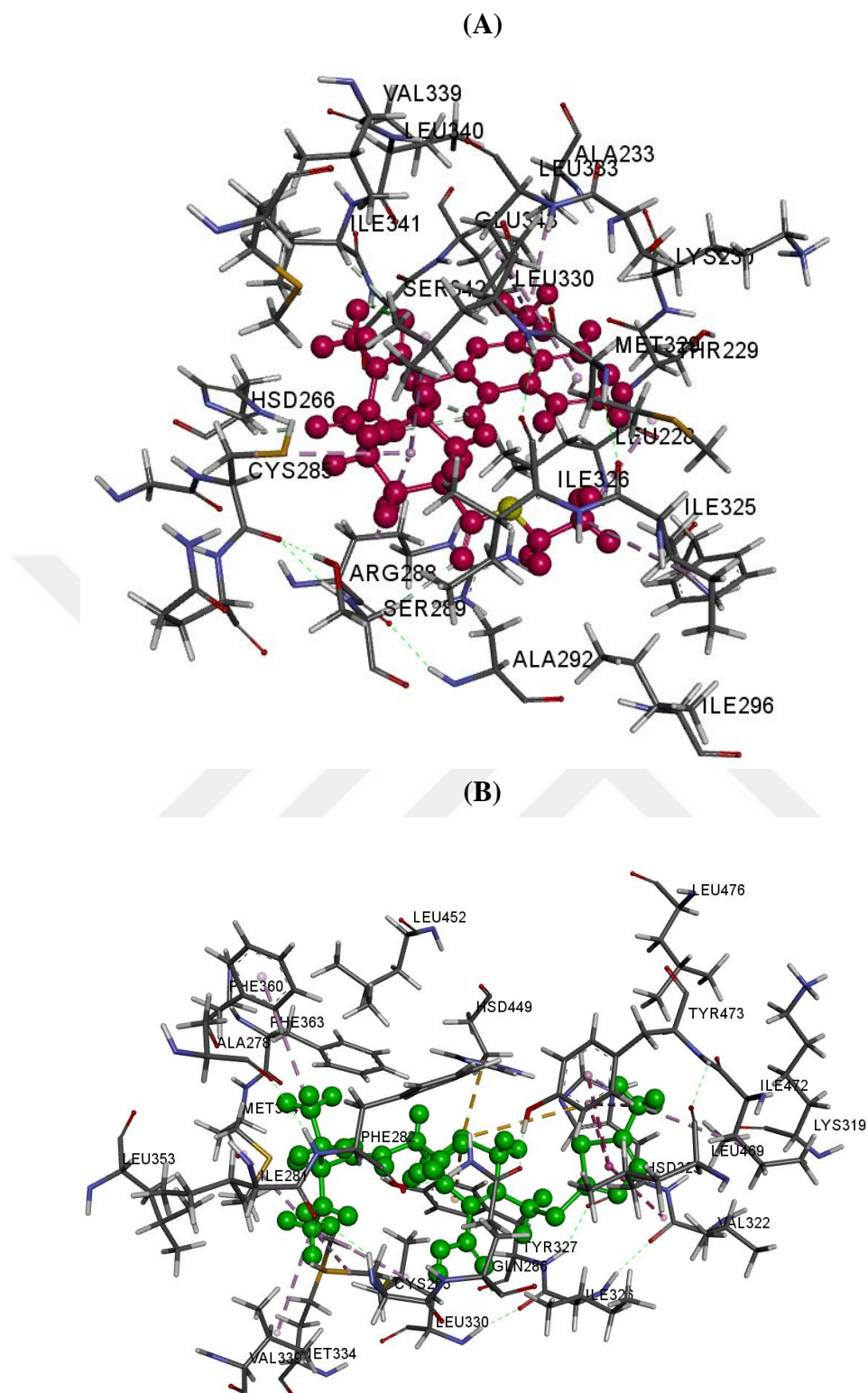


Figure 4. 25 3D-structure the MD simulation result in the entire MD simulations (NAMD)30ns. Ligand-protein interaction diagrams in the pocket of PPAR γ . (A) 3D diagram of the interaction between amino acid residues and 2PRG (PPAR γ) and ZINC000058367624 binding pockets. (B) 3DAmino acid residue interaction diagram with PPAR γ (2PRG) and ZINC000002805504 binding pocket.

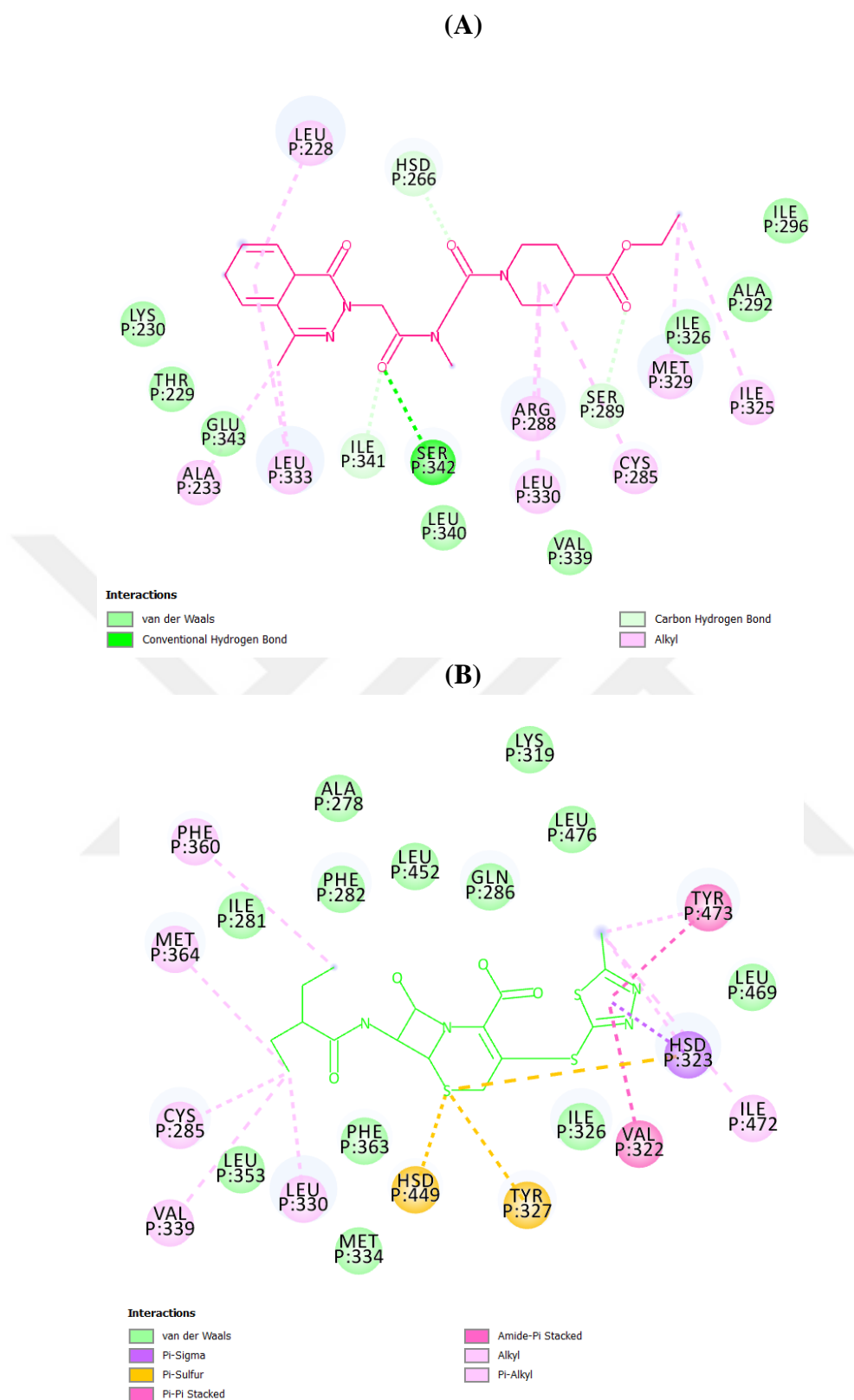


Figure 4. 26 2D structure the MD simulation all MD simulations (NAMD)30ns result. The ligand-protein interaction diagrams in PPAR γ (2PRG) pocket. (A) MD simulation-ZINC000002805504 ligand map to PPAR γ (2PRG). (B) MD ligand simulation map ZINC000058367624 to PPAR γ (2PRG).

5. Conclusion

DM is a chronic disease, a group of metabolic illnesses, there are two main-types of MD, T1DM (damage on beta-cell to produce insulin of the pancreas) and T2DM (pancreas it does not work correctly). PPARs family belongs to transcriptional nuclear receptors, that activated when it binds with specific ligands, for controlling some of the physiological process, which that reflected inside the body of a human. There are three kinds of PPARs are PPAR alpha (α), delta (δ), and gamma (γ), which they are located various positions and have different functions. The potential PPAR α / γ agonist plays a significant role in the part of DM treatment, however there is no real drug on the market, yet. PVS (pharmacophore virtual screening), Molecular Docking and analysis (C-DOCKER), ADMET estimate, molecule dynamics simulations (MD) tools were utilized to investigate the ZINC data bases in order to find some possible dual agonists for PPAR α / γ . From resulting 42 compounds only 13 best compounds were tested and through the virtual screening we obtain 10 compounds with fit value >3 . PyRx Virtual screening software was used to select possible candidates having binding energy less than (-9.0 kcal/mol) thresholds. Result of screening generated two compounds fulfilling this criterion such as ZINC000002805504(-10.56 kcal/mol) and ZINC000058367624(-10.31kcal/mol). Then, Autodock4, Autodocktools (ADT) and (CDOCKER) programs used putting the restriction of binding energy value not less than -8.0 kcal/mol of (CDOCKER_ENERGY). The obtained potential candidates were better than that of the native ligands for PPAR α / γ complexes (Table 4.4). Strategy is to generate good drug-candidates with high binding affinities and fit values are not enough without investigating its pharmacokinetics and pharmacodynamics properties. Further filtrations, accordingly, the following procedure was the ADMET prediction that was conducted using Biovia Discovery Studio2016. Molecular dynamics (MD) simulation confirmations indicated that the (ZINC000002805504, ZINC000058367624) are both stables inside the PPAR α / γ pockets. Finally, we gained compounds, (ZINC000002805504, ZINC000058367624), that they have higher fit value then the native one, better docking value, lower toxicity, and more desirable properties than the native-ligand conformation. All of the selected candidates passed these criteria. The results obtained in this research could be a reference to the further study to improve DM medicines.

References

- Accelrys Inc. (2017). BIOVIA Materials Studio.
- Adrià, C. M., Garcia-Vallvé, S., & Pujadas, G. (2012). DecoyFinder, a tool for finding decoy molecules. *Journal of Cheminformatics*. <https://doi.org/10.1186/1758-2946-4-S1-P2>
- Aekplakorn, W., Chariyalertsak, S., Kessomboon, P., Sangthong, R., Inthawong, R., Putwatana, P., ... Chaladthanyagid, K. (2011). Prevalence and management of diabetes and metabolic risk factors in Thai adults: The Thai national health examination survey IV, 2009. *Diabetes Care*. <https://doi.org/10.2337/dc11-0099>
- Ahmad, S., Khan, M. F., Parvez, S., Akhtar, M., & Raisuddin, S. (2017). Molecular docking reveals the potential of phthalate esters to inhibit the enzymes of the glucocorticoid biosynthesis pathway. *Journal of Applied Toxicology*. <https://doi.org/10.1002/jat.3355>
- Aleshin, S., Strokin, M., Sergeeva, M., & Reiser, G. (2013). Peroxisome proliferator-activated receptor (PPAR) β/δ , a possible nexus of PPAR α - and PPAR γ -dependent molecular pathways in neurodegenerative diseases: Review and novel hypotheses. *Neurochemistry International*. <https://doi.org/10.1016/j.neuint.2013.06.012>
- Allen, W. E., & Luo, L. (2015). Intersectional illumination of neural circuit function. *Neuron*. <https://doi.org/10.1016/j.neuron.2015.02.032>
- Ambrus, G., Whitby, L. R., Singer, E. L., Trott, O., Choi, E., Olson, A. J., ... Gerace, L. (2010). Small molecule peptidomimetic inhibitors of importin α/β mediated nuclear transport. *Bioorganic and Medicinal Chemistry*. <https://doi.org/10.1016/j.bmc.2010.08.038>
- Beaver, W., & Venkatachalam, M. (2003). Differential Pricing of Components of Bank Loan Fair Values. *Journal of Accounting, Auditing & Finance*. <https://doi.org/10.1177/0148558X0301800103>
- Berger, J., & Moller, D. E. (2002). The Mechanisms of Action of PPARs. *Annual Review of Medicine*. <https://doi.org/10.1146/annurev.med.53.082901.104018>
- Bharatam, P., Patel, D., Adane, L., Mittal, A., & Sundriyal, S. (2007). Modeling and Informatics in Designing Anti-Diabetic Agents. *Current Pharmaceutical Design*. <https://doi.org/10.2174/138161207782794239>
- Bibi, N., Parveen, Z., & Rashid, S. (2013). Identification of Potential Plk1 Targets in a Cell-Cycle Specific Proteome through Structural Dynamics of Kinase and Polo Box-Mediated Interactions. *PLoS ONE*, 8(8). <https://doi.org/10.1371/journal.pone.0070843>
- Blitek, A., & Szymanska, M. (2019). Expression and role of peroxisome proliferator-activated receptors in the porcine early placenta trophoblast. *Domestic Animal Endocrinology*. <https://doi.org/10.1016/j.domaniend.2018.12.001>
- Center for Substance Abuse Treatment. (2012). Medication-Assisted Treatment For Opioid Addiction in Opioid Treatment Programs. In *Treatment Improvement Protocol (TIP) 43. HHS Publication No. (SMA) 12-4214*.
- Colmenarejo, G., Alvarez-Pedraglio, A., & Lavandera, J. L. (2001). Cheminformatic models to predict binding affinities to human serum albumin. *Journal of Medicinal Chemistry*. <https://doi.org/10.1021/jm010960b>
- Cronet, P., Petersen, J. F. W., Folmer, R., Blomberg, N., Sjöblom, K., Karlsson, U., ... Bamberg, K. (2001). Structure of the PPAR α and γ ligand binding domain in complex with AZ 242; ligand selectivity and agonist activation in the PPAR family. *Structure*. [https://doi.org/10.1016/S0969-2126\(01\)00634-7](https://doi.org/10.1016/S0969-2126(01)00634-7)
- Darwish, K. M., Salama, I., Mostafa, S., Gomaa, M. S., & Helal, M. A. (2016). Design, synthesis, and biological evaluation of novel thiazolidinediones as PPAR3/FFAR1 dual agonists. *European Journal of Medicinal Chemistry*. <https://doi.org/10.1016/j.ejmech.2015.12.049>
- Das, D., Sahu, N., Mondal, S., Roy, S., Dutta, P., Gupta, S., ... Sinha, C. (2015). Structures,

- antimicrobial activity, DNA interaction and molecular docking studies of sulfamethoxazolyl-azo-acetylacetone and its nickel(II) complex. *Polyhedron*. <https://doi.org/10.1016/j.poly.2015.06.027>
- DeFronzo, R. A., & Abdul-Ghani, M. (2011). Type 2 diabetes can be prevented with early pharmacological intervention. *Diabetes Care*. <https://doi.org/10.2337/dc11-s221>
- Diradourian, C., Girard, J., & Pégorier, J. P. (2005). Phosphorylation of PPARs: From molecular characterization to physiological relevance. *Biochimie*. <https://doi.org/10.1016/j.biochi.2004.11.010>
- Esiyok, B., Çakar, M., & Kurtuluşoğlu, F. B. (2017). The effect of cultural distance on medical tourism. *Journal of Destination Marketing and Management*. <https://doi.org/10.1016/j.jdmm.2016.03.001>
- Feng, X. Y., Jia, W. Q., Liu, X., Jing, Z., Liu, Y. Y., Xu, W. R., & Cheng, X. C. (2019). Identification of novel PPAR α/γ dual agonists by pharmacophore screening, docking analysis, ADMET prediction and molecular dynamics simulations. *Computational Biology and Chemistry*. <https://doi.org/10.1016/j.compbiolchem.2018.11.023>
- Ferreira, L. G., Dos Santos, R. N., Oliva, G., & Andricopulo, A. D. (2015). Molecular docking and structure-based drug design strategies. *Molecules*. <https://doi.org/10.3390/molecules200713384>
- Francis, G. A., Fayard, E., Picard, F., & Auwerx, J. (2003). Nuclear Receptors and the Control of Metabolism. *Annual Review of Physiology*. <https://doi.org/10.1146/annurev.physiol.65.092101.142528>
- G, C., & S, B. (2017). Breakthroughs in Computational Approaches for Drug Discovery. *Journal of Drug Research and Development*. <https://doi.org/10.16966/2470-1009.129>
- Garcia-Vallvé, S., & Palau, J. (1998). Nuclear receptors, nuclear-receptor factors, and nuclear-receptor-like orphans form a large paralog cluster in Homo sapiens. *Molecular Biology and Evolution*. <https://doi.org/10.1093/oxfordjournals.molbev.a025970>
- Garten, A., Petzold, S., Schuster, S., Körner, A., Kratzsch, J., Kiess, W., & Antje, K. (2011). Diabetes - Perspectives in Drug Therapy. In *Handbook of experimental pharmacology*. <https://doi.org/10.1007/978-3-642-17214-4>
- Gaurav, A., & Gautam, V. (2014). Structure-based three-dimensional pharmacophores as an alternative to traditional methodologies. *Journal of Receptor, Ligand and Channel Research*. <https://doi.org/10.2147/JRLCR.S46845>
- Hasan, A. M., Mazumder, H. M. H., Chowdhury, S. A., Datta, A., & Khan, A. M. (2015). Molecular-docking study of malaria drug target enzyme transketolase in Plasmodium falciparum 3D7 portends the novel approach to its treatment. *Source Code for Biology and Medicine*. <https://doi.org/10.1186/s13029-015-0037-3>
- Holt, P. (2011). Taking hypoglycaemia seriously: Diabetes, dementia and heart disease. *British Journal of Community Nursing*. <https://doi.org/10.12968/bjcn.2011.16.5.246>
- Hossain, M. U., Khan, M. A., Rakib-Uz-Zaman, S. M., Ali, M. T., Islam, M. S., Keya, C. A., & Salimullah, M. (2016). Treating diabetes mellitus: Pharmacophore based designing of potential drugs from gymnema sylvestre against insulin receptor protein. *BioMed Research International*. <https://doi.org/10.1155/2016/3187647>
- International Diabetes Federation. (2011). Global Diabetes Plan 2011-2021. *Vasa*. <https://doi.org/10.1017/CBO9781107415324.004>
- Jani, R. H., Kansagra, K., Jain, M. R., & Patel, H. (2013). Pharmacokinetics, safety, and tolerability of saroglitazar (ZYL1), a predominantly PPAR α Agonist with Moderate PPAR γ Agonist activity in healthy human subjects. *Clinical Drug Investigation*. <https://doi.org/10.1007/s40261-013-0128-3>
- Jones, G., Willett, P., Glen, R. C., Leach, A. R., & Taylor, R. (1997). Development and validation of a genetic algorithm for flexible docking. *Journal of Molecular Biology*.

- <https://doi.org/10.1006/jmbi.1996.0897>
- Kalathiya, U., Padariya, M., & Baginski, M. (2016). Identification of 1H-indene-(1,3,5,6)-tetrol derivatives as potent pancreatic lipase inhibitors using molecular docking and molecular dynamics approach. *Biotechnology and Applied Biochemistry*. <https://doi.org/10.1002/bab.1432>
- Karpuz, A., Kockar, H., & Esiyok, M. (2014). Sputtered FeCl/Cu multilayer thin films: Effect of different thicknesses of Cu layer. *Optoelectronics and Advanced Materials, Rapid Communications*.
- Kausar, S., Asif, M., Bibi, N., & Rashid, S. (2013). Comparative Molecular Docking Analysis of Cytoplasmic Dynein Light Chain DYNLL1 with Pilin to Explore the Molecular Mechanism of Pathogenesis Caused by Pseudomonas aeruginosa PAO. *PLoS ONE*, 8(10). <https://doi.org/10.1371/journal.pone.0076730>
- Kemmish, H., Fasnacht, M., & Yan, L. (2017). Fully automated antibody structure prediction using BIOVIA tools: Validation study. *PLoS ONE*. <https://doi.org/10.1371/journal.pone.0177923>
- Lee, J., Cheng, X., Swails, J. M., Yeom, M. S., Eastman, P. K., Lemkul, J. A., ... Im, W. (2016). CHARMM-GUI Input Generator for NAMD, GROMACS, AMBER, OpenMM, and CHARMM/OpenMM Simulations Using the CHARMM36 Additive Force Field. *Journal of Chemical Theory and Computation*, 12(1), 405–413. <https://doi.org/10.1021/acs.jctc.5b00935>
- Li, R. J., Wang, Y. L., Wang, Q. H., Wang, J., & Cheng, M. S. (2015). In silico design of human IMPDH inhibitors using pharmacophore mapping and molecular docking approaches. *Computational and Mathematical Methods in Medicine*. <https://doi.org/10.1155/2015/418767>
- Lionta, E., Spyrou, G., Vassilatis, D. K., & Cournia, Z. (2014). Structure-based virtual screening for drug discovery: principles, applications and recent advances. *Current Topics in Medicinal Chemistry*.
- Liu, L., Ma, Y., Wang, R. L., Xu, W. R., Wang, S. Q., & Chou, K. C. (2013). Find novel dual-agonist drugs for treating type 2 diabetes by means of cheminformatics. *Drug Design, Development and Therapy*. <https://doi.org/10.2147/DDDT.S42113>
- Lobanov, M. I., Bogatyreva, N. S., & Galzitskaia, O. V. (2008). Radius of gyration is indicator of compactness of protein structure. *Molekuliarnaia Biologiia*.
- Lobanov, M. Y., Bogatyreva, N. S., & Galzitskaya, O. V. (2008). Radius of gyration as an indicator of protein structure compactness. *Molecular Biology*. <https://doi.org/10.1134/S0026893308040195>
- Marchetti, P., Lupi, R., Del Guerra, S., Bugliani, M., D'Aleo, V., Occhipinti, M., ... Masini, M. (2009). Goals of treatment for type 2 diabetes: beta-cell preservation for glycemic control. *Diabetes Care*. <https://doi.org/10.2337/dc09-s306>
- Maruthanila, V. L., Elancheran, R., Roy, N. K., Bhattacharya, A., Kunnumakkara, A. B., Kabilan, S., & Kotoky, J. (2018). In silico Molecular Modelling of Selected Natural Ligands and their Binding Features with Estrogen Receptor Alpha. *Current Computer-Aided Drug Design*. <https://doi.org/10.2174/1573409914666181008165356>
- Meetoo, D., McGovern, P., & Safadi, R. (2007). An epidemiological overview of diabetes across the world. *British Journal of Nursing (Mark Allen Publishing)*. <https://doi.org/10.12968/bjon.2007.16.16.27079>
- Mottin, M., Borba, J. V. V. B., Melo-Filho, C. C., Neves, B. J., Muratov, E., Torres, P. H. M., ... Andrade, C. H. (2018). Computational drug discovery for the Zika virus. *Brazilian Journal of Pharmaceutical Sciences*. <https://doi.org/10.1590/s2175-97902018000001002>
- Nevin, D. K., Peters, M. B., Carta, G., Fayne, D., & Lloyd, D. G. (2012). Integrated virtual screening for the identification of novel and selective peroxisome proliferator-activated

- receptor (PPAR) scaffolds. *Journal of Medicinal Chemistry*. <https://doi.org/10.1021/jm300068n>
- Novac, N., & Heinzl, T. (2004). Nuclear receptors: Overview and classification. *Current Drug Targets: Inflammation and Allergy*. <https://doi.org/10.2174/1568010042634541>
- Pagadala, N. S., Syed, K., & Tuszynski, J. (2017). Software for molecular docking: a review. *Biophysical Reviews*. <https://doi.org/10.1007/s12551-016-0247-1>
- Phillips, J. C., Braun, R., Wang, W., Gumbart, J., Tajkhorshid, E., Villa, E., ... Schulten, K. (2005). Scalable molecular dynamics with NAMD. *Journal of Computational Chemistry*, Vol. 26, pp. 1781–1802. <https://doi.org/10.1002/jcc.20289>
- Priyadarshini, V., Pradhan, D., Munikumar, M., Swargam, S., Umamaheswari, A., & Rajasekhar, D. (2014). Genome-based approaches to develop epitope-driven subunit vaccines against pathogens of infective endocarditis. *Journal of Biomolecular Structure and Dynamics*. <https://doi.org/10.1080/07391102.2013.795871>
- Protein Data Bank. (2019). RCSB PDB: Homepage.
- Puratchikody, A., Umamaheswari, A., Irfan, N., & Sriram, D. (2018). Molecular dynamics studies on COX-2 protein-tyrosine analogue complex and ligand-based computational analysis of halo-substituted tyrosine analogues. *Letters in Drug Design & Discovery*. <https://doi.org/10.2174/1570180815666180627123445>
- Rajapaksha, H., Bhatia, H., Wegener, K., Petrovsky, N., & Bruning, J. B. (2017). X-ray crystal structure of rivoglitazone bound to PPAR γ and PPAR subtype selectivity of TZDs. *Biochimica et Biophysica Acta - General Subjects*. <https://doi.org/10.1016/j.bbagen.2017.05.008>
- Renaud, J. P., & Moras, D. (2000). Structural studies on nuclear receptors. *Cellular and Molecular Life Sciences*. <https://doi.org/10.1007/PL00000656>
- Ritz, E. (2011). Limitations and future treatment options in type 2 diabetes with renal impairment. *Diabetes Care*. <https://doi.org/10.2337/dc11-s242>
- Rose, P. W., Bi, C., Bluhm, W. F., Christie, C. H., Dimitropoulos, D., Dutta, S., ... Bourne, P. E. (2013). The RCSB Protein Data Bank: New resources for research and education. *Nucleic Acids Research*. <https://doi.org/10.1093/nar/gks1200>
- Ruiz-Carmona, S., Alvarez-Garcia, D., Foloppe, N., Garmendia-Doval, A. B., Juhos, S., Schmidtke, P., ... Morley, S. D. (2014). rDock: A Fast, Versatile and Open Source Program for Docking Ligands to Proteins and Nucleic Acids. *PLoS Computational Biology*. <https://doi.org/10.1371/journal.pcbi.1003571>
- Shearer, B. G., & Billin, A. N. (2007). The next generation of PPAR drugs: Do we have the tools to find them? *Biochimica et Biophysica Acta - Molecular and Cell Biology of Lipids*. <https://doi.org/10.1016/j.bbailip.2007.05.005>
- Shore, H. C. (2012). *Computer Aided Drug Design & QSAR*. 012072, 2012.
- Shu, M., Lin, Z., Zhang, Y., Wu, Y., Mei, H., & Jiang, Y. (2011). Molecular dynamics simulation of oseltamivir resistance in neuraminidase of avian influenza H5N1 virus. *Journal of Molecular Modeling*. <https://doi.org/10.1007/s00894-010-0757-x>
- Simmons, K. J., Chopra, I., & Fishwick, C. W. G. (2010). Structure-based discovery of antibacterial drugs. *Nature Reviews Microbiology*. <https://doi.org/10.1038/nrmicro2349>
- Singh, J., Kumar, M., Mansuri, R., Sahoo, G. C., & Deep, A. (2016). Inhibitor designing, virtual screening, and docking studies for methyltransferase: A potential target against dengue virus. *Journal of Pharmacy and Bioallied Sciences*. <https://doi.org/10.4103/0975-7406.171682>
- Sterling, T., & Irwin, J. J. (2015). ZINC 15 - Ligand Discovery for Everyone. *Journal of Chemical Information and Modeling*. <https://doi.org/10.1021/acs.jcim.5b00559>
- Thangapandian, S., John, S., Lee, Y., Kim, S., & Lee, K. W. (2011). Dynamic structure-based pharmacophore model development: A new and effective addition in the Histone

- deacetylase 8 (HDAC8) inhibitor discovery. *International Journal of Molecular Sciences*.
<https://doi.org/10.3390/ijms12129440>
- Tuma, J. M., & Pratt, J. M. (1982). Clinical child psychology practice and training: A survey. *Journal of Clinical Child & Adolescent Psychology*, 137(August 2012), 37–41. <http://doi.org/10.1037/a0022390>, Gobry, F. (1999). This is a title. *My Journal*, 1, 120–130., Osment, S. E. (1980). T. A. of R. 1250-1550. ... and R. H. of L. M. and R. ... R. from <http://scholar.google.com/scholar?hl=en&btnG=Search&q=intitle:THE+AGE+OF+REFORM+125.-1550#2%5Cnhttp://scholar.google.com/scholar?hl=en&btnG=S.>, Caprara, G., & Fida, R. (2008). Longitudinal analysis of the role of perceived self-efficacy for self-regulated learning in academic continuance and achievement. ... of Educational ..., 100(3), 525–534. <http://doi.org/10.1037/0022-0663.100.3.525>, Shanker, S. (2003). Philosophy of science, logic and mathematics in the twentieth century. ... P. L. and N. Y. R. <http://doi.org/10.4324/978020302947.>, Marenbon, J. (1998). R. H. of P. I. ... P. L. and N. Y. R. <http://doi.org/10.4324/978020306227.>, ... Keshav, S. (2007). How to Read a Paper. *Work*, 37(3), 83–84. <http://doi.org/10.1145/1273445.1273458>. (1989). Language and Power. *Language in Social Life Series*.
- van Marrewijk, A., Ybema, S., Smits, K., Clegg, S., & Pitsis, T. (2016). Clash of the Titans: Temporal Organizing and Collaborative Dynamics in the Panama Canal Megaproject. *Organization Studies*. <https://doi.org/10.1177/0170840616655489>
- Viljoen, A., & Sinclair, A. J. (2011). Diabetes and Insulin Resistance in Older People. *Medical Clinics of North America*. <https://doi.org/10.1016/j.mcna.2011.02.003>
- Voors, A. A., & Van Der Horst, I. C. C. (2011). Diabetes: A driver for heart failure. *Heart*. <https://doi.org/10.1136/hrt.2009.183624>
- Wang, X. J., Zhang, J., Wang, S. Q., Xu, W. R., Cheng, X. C., & Wang, R. L. (2014). Identification of novel multitargeted PPAR $\alpha/\gamma/\delta$ pan agonists by core hopping of rosiglitazone. *Drug Design, Development and Therapy*. <https://doi.org/10.2147/DDDT.S70383>
- Wieder, M., Perricone, U., Boresch, S., Seidel, T., & Langer, T. (2016). Evaluating the stability of pharmacophore features using molecular dynamics simulations. *Biochemical and Biophysical Research Communications*. <https://doi.org/10.1016/j.bbrc.2016.01.081>
- Wild, S., Roglic, G., Green, A., Sicree, R., & King, H. (2004). Global Prevalence of Diabetes. *Diabetes Care*.
- Wu, G., Robertson, D. H., Brooks, C. L., & Vieth, M. (2003). Detailed analysis of grid-based molecular docking: A case study of CDOCKER - A CHARMM-based MD docking algorithm. *Journal of Computational Chemistry*. <https://doi.org/10.1002/jcc.10306>
- Yang, Y., Zhan, J., & Zhou, Y. (2016). SPOT-Ligand: Fast and effective structure-based virtual screening by binding homology search according to ligand and receptor similarity. *Journal of Computational Chemistry*. <https://doi.org/10.1002/jcc.24380>
- Zhang, D., & Lazim, R. (2017). Application of conventional molecular dynamics simulation in evaluating the stability of apomyoglobin in urea solution. *Scientific Reports*. <https://doi.org/10.1038/srep44651>
- Zhang, L. (2017). Different dynamics and pathway of disulfide bonds reduction of two human defensins, a molecular dynamics simulation study. *Proteins: Structure, Function and Bioinformatics*. <https://doi.org/10.1002/prot.25247>
- Zhao, H., & Caflich, A. (2013). Discovery of ZAP70 inhibitors by high-throughput docking into a conformation of its kinase domain generated by molecular dynamics. *Bioorganic and Medicinal Chemistry Letters*. <https://doi.org/10.1016/j.bmcl.2013.08.009>